Dissertation

submitted to the

Combined Faculties for the Natural Sciences and for Mathematics

of the Ruperto-Carola University of Heidelberg, Germany

for the Degree of

Doctor of Natural Sciences

Presented by

Rozina Kardakaris

Born in Vancouver, Canada

Oral Examination Date: Thursday, October 29th, 2009

Macrophage and Endothelial-Specific Role of p38α MAPK in Atherosclerosis

Referees: Dr. Matthias Treier
Dr. Matthias Mayer

Acknowledgements

During my four years as a member of the EMBL community, but also as part of the group of Pr. Manolis Pasparakis, I have acquired a vast range of experiences and knowledge, not only in a scientific manner, but also personaly. These experiences have allowed me to grow and become more mature in both aspects of my life. For this reason, I would like to thank all the people from and outside of EMBL that contributed in making these four years a life changing experience.

Most of all, I would like to thank Manolis, who gave me the opportunity to carry out my PhD work in his laboratory. The research performed in this laboratory is very demanding and requires a high level of commitment, but at the same time rewarding and permitting the acquisition of a vast range of knowledge and skills through the many resources available. I strongly believe that during my time in this laboratory I have learned what it really means to be a scientist performing basic research.

Furthermore, I would like to thank Dr. Ralph Gareus who, through excellent supervision at the beginning but also throughout the duration of my PhD, guided me in the right direction concerning my research project. I would also like to thank him for his personal support during this time.

In addition, I would like to thank all the members of the laboratory, especially Dr. Sofia Xanthoulea for her help in staining for and analyzing various markers of atherosclerosis and Jan Heinrichsdorff for showing me how to isolate and culture hepatocytes. Moreover, I would like to thank all the technicians for their great technical assistance especially in preparing the hundreds of heart sections I required for my project but also for their assistance in performing FACS analysis. I would also like to thank the transgenics facility at the University of Cologne for the ES cell injections.

A special thanks to all my Thesis Advisory Committee members, Walter Witke, Carl Neumann and Matthias Mayer, for their helpful suggestions on how to proceed with my project.

Finally, I would like to dedicate this thesis to my family who has always been supportive of my decisions and encouraged me to follow my dreams, but also to Dr. Nikos Oikonomakos who has now passed away but was the person who gave me the final push in the direction of going through the process of a PhD when I was still indecisive.

Macrophage and Endothelial-Specific Role of p38α MAPK in Atherosclerosis

Rozina Kardakaris, University of Cologne, Cologne, Germany

The aim of my PhD project was to investigate the macrophage and endothelial-specific role of the p38α MAPK signaling pathway in the development of Atherosclerosis.

There are four p38 MAP kinases in mammals: α, β, γ and δ. Among all p38 MAPK isoforms, p38α is the best characterised, is expressed in most cell types and is the predominant form of p38 expressed in inflammatory cells. p38 MAPKs are strongly activated *in vivo* by environmental stresses and inflammatory cytokines. The canonical activation of p38 MAPKs occurs via dual phosphorylation of their Thr-Gly-Tyr motif in the activation loop, by MKK3 and MKK6. But it can also occur by an MKK independent mechanism through the adaptor protein TAB1 and by a TCR mediated mechanism by phosphorylation of Tyr323, in T cells. Activation of p38 MAPKs can lead to a variety of responses through phosphorylation of downstream kinases like MK2 or transcription factors like ATF2.

Atherosclerosis, a progressive inflammatory disease of the medium and large arteries characterized by intense immunological activity, comprises the primary underlying cause of about 50% of cardiovascular disease related deaths in the western world today. p38α MAPK, which was first identified in studies on inflammation, is activated in response to various stress factors, including inflammatory cytokines and oxLDL, a major factor contributing to the onset of atherosclerosis. Here I addressed the role of p38α MAPK, the most physiologically relevant p38 MAPK, in macrophages and endothelial cells in the pathogenesis of atherosclerosis in *vivo*. Both macrophage and endothelial cell-ablation of p38α MAPK, achieved by taking advantage of the Cre-loxP recombination system, did not lead to any significant reduction or aggravation of atherosclerosis plaque formation compared to $ApoE^{-/-}$ mice fed with a cholesterol-rich 'western diet' for 10 weeks. This result is contradictory to studies carried out *in vitro* thus far with p38 small molecule inhibitors, but also recently *in vivo* where p38α MAPK ablation in macrophages led to plaques with decreased collagen content and increased necrotic core formation. Thus, macrophage and endothelial cell-specific signaling of p38α MAPK, contrary to general belief, does not appear to either promote or reduce the pathogenesis of atherosclerosis.

In parallel, I also generated two new mouse models of p38α MAPK, p38αCA and p38αKD, by homologous recombination. In the p38αCA model, that expresses a constitutively active form of p38α MAPK, we took advantage of the ROSA26 locus that allows ubiquitous expression of a protein, to target a mutant form of p38α under the control of Cre recombinase. p38αKD, expressing a kinase dead form of p38α MAPK also under the control of Cre recombinase, was generated by targeting exon 2 of the p38α locus with a mutated exon 2, rendering it catalytically inactive. Both of these models, which preliminary results suggest are functional, are very useful genetic tools for the further elucidation of the p38α MAPK pathway with respect to many disease models, like cancer, cardiovascular and other diseases.

Die Makrophagen- und Endothelspezifische Rolle der p38α MAPK in der Arteriosklerose

Rozina Kardakaris, University of Cologne, Cologne, Germany

Das Ziel meiner Dissertation war es, die makrophagen- und endothelspezifische Rolle des p38α MAPK Signaltransduktionsweges während der Entwicklung der Arteriosklerose zu untersuchen.

In Säugern gibt es vier p38 MAP-Kinasen: a, b, g und d. Von allen p38 MAPK Isoformen ist p38α die am besten charakterisierte, die in den meisten Zelltypen exprimierte und die hauptsächliche Form von p38 in Zellen, die an einer Entzündung beteiligt sind. p38 MAP-Kinasen werden *in vivo* stark durch entzündliche Zytokine und Stress durch Umwelteinflüsse aktiviert. Die kanonische Aktivierung von p38 MAP-Kinasen erfolgt durch Doppelphosphorylierung ihres Thr-Gly-Tyr-Motivs in der Aktivierungsschleife durch MKK3 und MKK6. Aber sie kann auch auf MKK-unabhängige Weise über das Adaptorprotein TAB1 und einen TCR-abhängigen Mechanismus durch Phosphorylierung von Tyr323 in T-Zellen erfolgen. Aktivierung von p38 MAP-Kinasen kann zu einer ganzen Reihe von Reaktionen durch Phosphorylierung nachgeschalteter Kinasen, wie z.B. MK2 oder Transkriptionsfaktoren, wie etwa ATF2 führen.

Arteriosklerose, eine fortschreitende entzündliche Krankheit der mittleren und grossen Arterien, die durch starke immunologische Aktivität gekennzeichnet ist, ist die zugrundeliegende Hauptursache für etwa die Hälfte aller Todesfälle, die heutzutage von Herz-Kreislauferkrankungen in der westlichen Welt herrühren. p38a MAPK, die zuerst in Studien über Entzündung identifiziert wurde, wird durch verschiedenste Umweltfaktoren aktiviert, u.a. entzündliche Zytokine und oxLDL, einem Hauptfaktor für Arteriosklerose. In dieser Arbeit behandelte ich die Rolle von p38α MAPK, der physiologisch relevantesten p38 MAPK, in Makrophagen und Endothelzellen für die Pathogenese der Arteriosklerose *in vivo*. Weder die makrophagen- noch die endothelzellspezifische Ablation von p38α MAPK, herbeigeführt durch das Cre-loxP-System, führte zu einer signifikanten Reduktion oder Vermehrung von arteriosklerotischen Plaques im Vergleich zu ApoE-/- Mäusen auf cholesterinreicher „westlicher Diät“ für 10 Wochen. Dieses Ergebnis widerspricht *in vitro*-Studien mit p38-spezifischen Inhibitoren, aber auch neueren *in vivo*-Resultaten, in denen p38α-Ablation zu kleineren Plaques mit weniger Collagengehalt und Bildung von grösseren nekrotischen Kernen führte. Makrophagen- und endothelspezifische p38α-Signaltransduktion scheint daher die Pathogenese der Arteriosklerose weder zu fördern noch zu reduzieren.

Parallel dazu generierte ich zwei neue Mausmodelle für die p38α MAP-Kinase durch homologe Rekombination, p38αCA und p38αKD. Für das p38αCa-Modell, welches eine konstitutiv aktive Form der p38α MAPK exprimiert, machten wir uns den ROSA26-Lokus zu Nutze, der ubiquitäre Expression eines Proteins ermöglicht, und in den wir eine mutierte Form der p38α MAPK unter der Kontrolle von Cre-Rekombinase setzten. p38KD, welche eine Kinase-inaktive Form von p38α unter der Kontrolle der Cre-Rekombinase darstellt, wurde durch Einführung eines mutierten Exon 2 in den p38α-Lokus hergestellt, welches die katalytische Funktion der Kinase inaktiviert. Beide Modelle, die ersten Ergebnissen nach funktional sind, stellen äusserst nützliche genetische Werkzeuge dar, um den p38α MAPK-Signaltransduktionsweg weiter zu untersuchen, vor allem im Hinblick auf zahlreiche Krankheitsmodelle, wie Krebs, Herz-Kreislauf- und andere Erkrankungen.

Table of Contents

Abbreviations

Alb	Albumin
Alfp	Albumin Foetal Protein
AP-1	Activator Protein-1
APO	Apolipoprotein
ASK1	Apoptosis Signal-Regulating Kinase 1
ATP	Adenosine Triphosphate
ATF	Activating Transcription Factor
BAC	Bacterial Artificial Chromosome
B-CLL	B-Cell Chronic Lymphopathic Leukemia
BMDMs	Bone Marrow Derived Macrophages
BSA	Bovine Serum Albumin
CA	Constitutively Active
$CaCl_2$	Calcium Chloride
CCR2	Chemokine (C-C Motif) Receptor 2
CD	Cluster of Differentiation
cDNA	Complementary DNA
C/EBPβ	CCAAT Enhancer Binding Protein Beta
CETP	Cholesteryl Ester Transfer Protein
CHOP	CCAAT/Enhancer-Binding Protein Homologous Protein
cPLA2	Cytosolic Phospholipase 2
CREB	cAMP Response Element Binding
CO_2	Carbon Dioxide
COX2	Cyclooxygenase 2
CXCL	CXC Chemokine Ligand
DDIT3	DNA Damage Inducible Transcript 3
DiI	1,1'-Dioctadecyl 3,3,3',3'-Tetramethylindocarbocyanine Perchlorate
DMEM	Dulbecco's Modified Eagle Medium
DMSO	Dimethyl Sulfoxide
DNA	Deoxyribonucleic Acid
DTA	Diptheria Toxin
DTT	Dithiothreitol
DUSP	Dual Specificity Phosphatase
EC	Endothelial Cell
EPC	Endothelial Progenitor Cell
EDTA	Ethylene Diamine Tetraacetate
eGFP	Enhanced Green Fluorescent Protein

EGTA	Ethyleneglycol-bis [β-aminoethyl ether]-N, N, N', N'-Tetraacetate
eIF-4E	Eukaryotic Initiation Factor-4e
ELK1	Ets Like Gene 1
Epo	Erythropoietin
ERK	Extracellular Signal-Regulated Protein Kinase
ES cells	Embryonic Stem cells
EtOH	Ethanol
FACS	Fluorescence Activated Cell Scanning
FCS	Fetal Calf Serum
FL	Floxed
GADD153	Growth Arrest and DNA Damage Inducible gene 153
GAL	Galactosidase
GFP	Green Fluorescent Protein
Glu	Glutamic Acid
GST	Glutathione-S-Transferase
H2B	Histone 2B
HBP1	HMG-Box Transcription Factor 1
HDL	High Density Lipoprotein
HEK	Human Embyonic Kidney
HEPES	N-2-Hydroxyethylpiperazine-N'-2-Ethane Sulfonic Acid
Hog	High Osmolarity Glycerol
Hrs	Hours
HRP	Horseradish Peroxidase
HSP	Heat Shock Protein
HSV	Herpes Simplex Virus
HTNC	His-TAT-NLS-Cre
ICAM-1	Intercellular Adhesion Molecule-1
IDL	Intermediate Density Lipoprotein
IFN	Interferon
IgG	Immunoglobulin G
IL	Interleukin
IP-10	Interferon Inducible Protein-10
IRES	Internal Ribosomal Entry Site
JNK	c-Jun-N-Terminal Kinase
kDa	Kilo Dalton
KD	Kinase Dead
KCL	Potassium Chloride
KO	Knockout
LAH	Left Arm of Homology

LCAT	Lecithin Cholesterol Acyltransferase
LDL	Low Density Lipoprotein
LIF	Leukemia Inhibitory Factor
LPC-KO	Liver Parenchymal Cell Knockout
LPS	Lipopolysaccharide
LSP1	Lymphocyte Specific Protein 1
LUC	Luciferase
LysM	Lysozyme
LysoPC	LysoPhosphatidylCholine
MAPK	Mitogen-Activated Protein Kinase
MAPKAPK (MK)	MAPK Activated Protein Kinase
MAPKK	MAPK Kinase
MAPKKK	MAPK Kinase Kinase
MCP-1	Monocyte Chemoattractant Protein-1
M-CSF	Macrophage-Colony Stimulating Factor
MEF	Myocyte Enhancer Factor
MEK	MAPK/ERK Kinase
MITF1	Microphthalmia Associated Transcription Factor
MOMA	Metallophilic Macrophages
MKK	MAPK Kinase Kinase
Mins	Minutes
MIP-2α	Macrophage Inflammatory Protein-2 alpha
MMP	Matrix metalloprotease
MNK	Menkes
mRNA	Messenger RNA
MSK1	Mitogen and Stress Activated Protein 1
MyD88	Myeloid Differentiation Primary-Response Gene 88
MY-KO	Myeloid Knockout
NaCl	Sodium Chloride
NaF	Sodium Fluoride
$NaVO_3$	Sodium Vanadate
NEO	Neomycin
NFA1	Nalgeria Fowleri 1
NF-κB	Nuclear Factor- kappa B
NHE1	Na+/H+ Exchanger Isoform 1
NLS	Nuclear Localisation Sequence
NO	Nitric Oxide
NP-40	S-Phase Transcription Coactivator
OCA-S	Nonionic Surfactant

PC12	Phospholipid Transfer Protein
PLTP	Pheochromocytoma Cell Line 12
oxLDL	Oxidized LDL
p	Phospho
PA	Plasminogen Activator
PBS	Phosphate-Buffered Saline
PCR	Polymerase Chain Reaction
PFA	Paraformaldehyde
PGK	Phosphoglycerine Kinase
PPAR	Peroxisome Proliferator Activated Receptor
PRAK	P38 Regulated/Activated Kinase
Pro	Proline
RAH	Right Arm of Homology
RIPA	Radio-Immunoprecipitation Assay
RNA	Ribonucleic Acid
RNAi	RNA Interference
ROS	Reactive Oxygen Species
Rpm	Rounds per Minute
RPMI	Reduced Serum Media
RT	Room Temperature
SA	Splice Acceptor
Sap-1	SRF-Accessory Protein
Secs	Seconds
SDS	Sodium Dodecyl Sulfate
SNP	Single Nucleotide Polymorphism
SR	Scavenger Receptor
SRE	Serum Response Element
SRF	Serum Response Factor
TAB1	Transforming Growth Factor Beta1
TAK1	Transforming Growth Factor Beta Activate Protein Kinase 1
TCF	Ternary Complex Factor
TCR	Thymidine Kinase
TK	T-Cell Receptor
TLR	Toll-Like Receptor
Tm	Melting Temperature
TNF	Tumor Necrosis Factor
TRAIL	Tristetrapolin
TTP	TNF-Related Apoptosis-Inducing Ligand
TUNEL	Terminal Deoxynucleotidyl Transferase Mediated dNTP Nick End Labelling

UPR	Unfolded Protein Response
UV	Ultraviolet
VSMC	Vascular Smooth Muscle Cell
VCAM-1	Vascular Adhesion Molecule-1
VEGF	Vascular Endothelial Growth Factor
VLDL	Very Low Density Lipoprotein
WB	Western Blot
WT	Wild-Type

1. Introduction

1.1 Mitogen-Activated Protein Kinases (MAPKs)

Cellular behavior in response to extracellular stimuli is mediated through intracellular signaling pathways such as mitogen-activated protein kinase (MAPKs) pathways [1]. MAPKs are evolutionary conserved enzymes connecting cell-surface receptors to critical regulatory targets within cells. They respond to chemical and physical stresses, thereby controlling cell-survival and adaptation [2]. There are 14 MAPKs in mammalian cells that can be divided into four distinct subgroups, and are 60-70% identical to each other [3]: (1) extracellular signal-regulated kinases (ERKs 1 & 2) which were the first to be discovered, (2) c-jun N-terminal or stress-activated protein kinases (JKNK/SAPK), (3) the p38 group of protein kinases and (4) atypical MAPKs such as ERK3, ERK5 and ERK8 [4,5]. Each MAPK pathway can be activated by different stimuli, and lead to different responses. In general, the ERKs are activated by mitogenic and proliferative stimuli, whereas the JNKs and p38 MAPKs respond to environmental stress, including ultraviolet light, heat, osmotic shock and inflammatory cytokines [6]. Cellular responses for ERKs include cell proliferation, transformation and differentiation, whereas the activation of JNKs and p38 MAPKs can lead to apoptosis, stress responses and inflammation [7] (Fig. 1).

1.1.1 MAPK Signal Transduction

MAPK activity is regulated through three-tiered cascades composed of a MAPK, MAPK kinase (MAPKK, MKK or MEK) and a MAPKK kinase or MEK kinase (MAPKKK or MEKK) [8] (Fig. 1). Activation of MAPKs occurs through phosphorylation. A common feature of all MAPK isoforms is the phosphorylation of both threonine (Thr) and tyrosine (Tyr) residues by a dual-specificity serine-threonine MAPK kinase that, in turn, is phosphorylated and activated by an upstream MKK kinase. All MAPKs share the amino acid sequence Thr-Xxx-Tyr in which X differs depending on the MAPK isoform. The amino acid X is glutamic acid (Glu), proline (Pro) and glycine (Gly) for ERK, JNK and p38 MAPK respectively. The Thr-Xxx-Tyr phosphorylation motif is localized in an activation loop near the ATP- and substrate-binding sites. The length of the activation loop also differs between the three MAPK families.

Phosphorylation occurs by an ordered addition of phosphate to the tyrosine then the threonine, with MKK dissociating from MAPK between each step [3,6,7].

Once activated, MAPKs can phosphorylate and activate other kinases or nuclear proteins such as transcription factors in either the cytoplasm or the nucleus. This leads to an increase or decrease in the expression of certain target genes, resulting in a biological response. The variation in specificity within a pathway suggests that different extracellular signals can produce stimulus- and tissue – specific responses by activating one or more MAPK pathways [7].

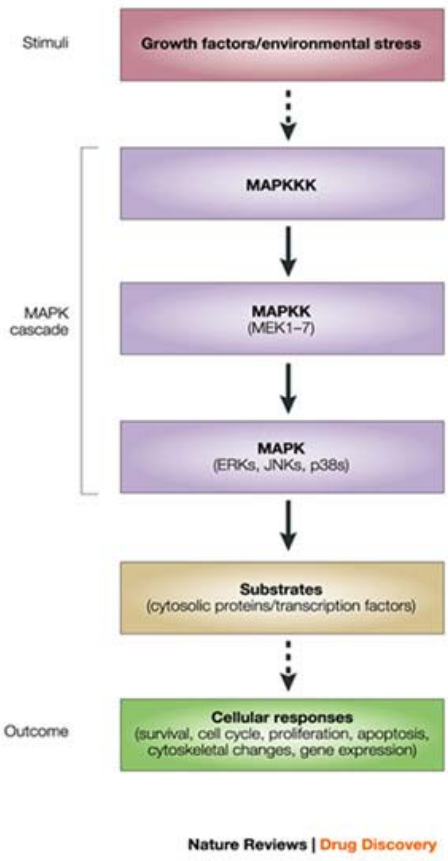

Figure 1. Mitogen-activated protein kinases (MAPKs), which integrate and process various extracellular signals. The MAPK cascade consists of a series of three protein kinases — a MAPK and two upstream components, MAPK kinase (MAPKK or MEK) and MAPKK kinase (MAPKKK). ERK, extracellular signal-regulated kinase; JNK, c-Jun N-terminal kinase. Image taken from Kumar, S. *et al*. 2003, Nature Reviews Drug Discovery.

1.2 p38 MAPK

Mammalian p38 MAPK, a 38 kDa protein, was originally identified as a molecular target of the pyridinyl imidazole class of compounds that were known to inhibit biosynthesis of inflammatory cytokines like interleukin-1 (IL-1) and tumor-necrosis factor (TNF) in lipopolysaccharide (LPS) and IL-1 stimulated human monocytes 1,9-11. Four isoforms of p38 are known to exist in mammals, p38α, p38β, p38γ and p38δ. From these, p38α and p38β are 74% identical and widely expressed [12], whereas p38γ (63% identical to p38α) is predominantly expressed in the skeletal muscle [13] and p38δ (61% identical to p38α) in the testes, pancreas and small intestine, as well as $CD4^+$ T cells [14,15]. They have the same preference for activating downstream targets by phosphorylating serines and/or threonines that precede prolines, e.g. activating transcription factor 2 (ATF2) and MAPK activated protein kinase (MAPKAPK2), but, despite their high overall degree of homology they seem to have different fine specificities for substrates, at least *in vitro* 13-15.

1.2.1 p38 MAPK Activation and Downregulation

p38 MAPK is mainly activated by dual phosphorylation on Thr180 and Tyr182 by the upstream MAPKKs MAP2K6 or otherwise MKK6 and MAP2K3 (MKK3), although the ability of these kinases to phosphorylate the various p38 isoforms varies. This is evidenced by the inability of MKK3 to effectively activate p38β while MKK6 can activate it potently despite 80% homology between these two MKKs [16]. MKK4, an upstream kinase of JNK, has also been shown to aid in the activation of p38α and p38δ in specific cell types [17]. MKKs are activated by several MAPKKKs, like apoptosis signal-regulating kinase-1 (ASK-1) or transforming growth factor β-activated protein kinase 1 (TAK1), which in turn are activated by a wide variety of stimuli [18,19], underscoring the complex nature of these signal transduction pathways, which require the integration of multiple signals from different pathways (Fig. 2).

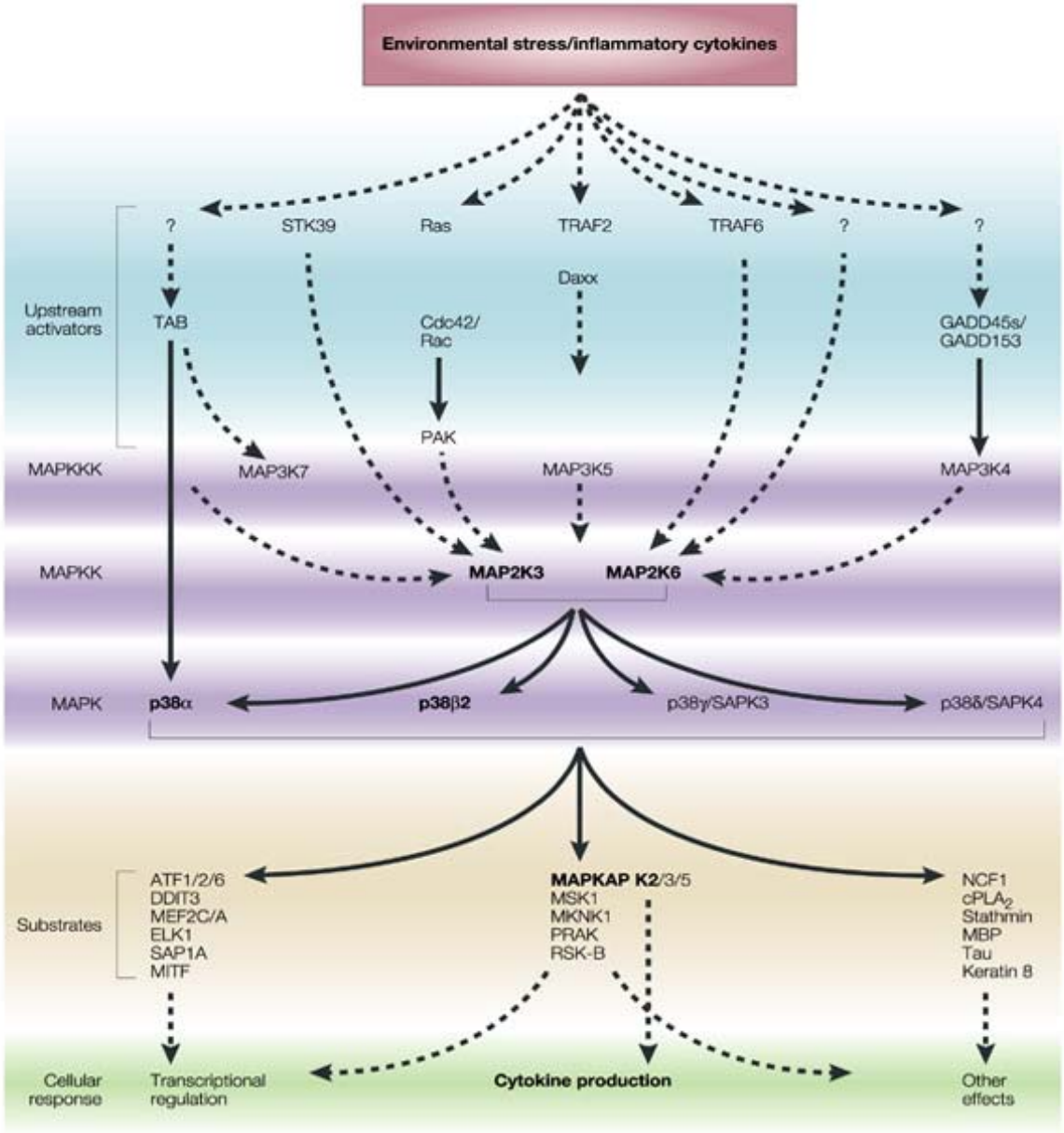

Figure 2. The complex nature of the p38 MAPK signal transduction pathway. Environmental stress and/or inflammatory cytokines activate MAPKKKs through a variety of signaling mechanisms. Activated MAPKKKs subsequently activate MAPKKs, which in turn activate MAPKs. Activated MAPKs then phosphorylate several substrates, such as transcription factors, other kinases and cytosolic proteins. These effector molecules are essential for cellular responses that include cytokine production and transcriptional regulation. In this figure, dotted lines represent indirect effects, and solid lines represent a direct effect. Image taken from Kumar, S. *et al*. 2003, Nature Reviews Drug Discovery.

Recently, a MAPKK-independent mechanism of p38α MAPK activation has been described. This involves association of the protein TAK1-binding protein 1 (TAB1), and intramolecular autophosphorylation of p38, independent of MAPKKs. This activation of p38 appears to be as efficient as activation by MAPKKs, like MKK6 [20]. Another MKK-independent mechanism of activation for p38α MAPK has been observed in T cells stimulated through the T-cell antigen receptor. In this system, p38α MAPK is activated by an alternative mechanism in which TCR-mediated stimulation activates proximal tyrosine kinases that results in the phosphorylation of p38α MAPK on a noncanonical activating residue, Tyr323. This phosphorylation activates p38α MAPK, probably by causing changes in its structural conformation, to phosphorylate third party substrates as well as its own Thr-Gly-Tyr motif [21, 22, 23].
When p38 MAPKs are activated under physiological conditions, their activity is often transient despite the unchanging levels of protein throughout the stimulation. This means that activation is only dependant on phosphorylation, and thus dephosphorylation of p38, but also other MAPKs, plays an important role in their downregulation. The activity of p38 specifically has been shown to be downregulated by various protein phosphatases, such as protein phosphatase 2A [24]. *In vitro* studies have also shown that it can be dephosphorylated by the dual –specificity phosphatases 16 (DUSP16) [25,26], and to a lesser extent by DUSP10 [27]. Recently, specifically for p38α, it was also shown to be dephosphorylated by DUSP1 [28].

1.2.2 p38 MAPK Downstream Targets

The identification of downstream targets for p38 MAPKs has been assisted by the utilization of relatively specific pyridinyl imidazole inhibitors such as SB203580 and SB202190 [29, 30]. These compounds, which are mostly specific for p38α and p38β MAPKs, have been very important tools in the delineation of pathways in which these MAPKs are involved. Many p38 MAPK targets have been described, both in the cytoplasm and the nucleus, the vast majority of which fall into two categories, transcription factors and protein kinases, although some other proteins have also been described as p38 MAPK substrates (Fig. 1 and 2). Activation (or inhibition) of these substrates occurs via p38 MAPK. This phosphorylation is known to take place

in the cytoplasm where p38 MAPKs are located, although some evidence suggests that upon cell stimulation p38α MAPK translocates into the nucleus [31].

1.2.2.1 Protein Kinase Substrates of p38 MAPKs

The first p38α substrate identified was MAPKAPK2 (or MK2) [1,11,32]. This substrate, along with its closely related family member MK3, were both shown to activate various substrates including small heat shock protein 27 (HSP27) [33], lymphocyte-specific protein 1 (LSP1) [34], cAMP response element-binding protein (CREB) [35], transcription factor ATF1 [35], SRF [36], and tyrosine hydroxylase [37]. More recently, MK2 has been found to phosophorylate tristetrapolin (TTP), a protein that is known to destabilize mRNA hinting at a role for p38 in mRNA stability [38]. MNK1 is another substrate of p38 whose function is thought to reside in translational initiation due to the observation that MNK1 and MNK2 can phosphorylate eukaryotic initiation factor-4e (eIF-4E) [39,40]. p38 regulated/activated kinase (PRAK) is a p38α and/or p38β activated kinase that shares 20-30% sequence identity to MK2 and is thought to regulate HSP27 [41]. Mitogen- and stress-activated protein kinase-1 (MSK1) can be directly activated by p38 and ERK, and may mediate activation of CREB 42-44. p38 is also thought to regulate S phase activation of histone 2B (H2B) promoter through OCA-S, a component of p38 [45].

1.2.2.2 Transcription Factor Substrates of p38 MAPKs

p38 MAPK is also capable of modulating gene expression by phosphorylating transcription factors directly and by activating other protein kinases (e.g. MNKs as described above) which then phosphorylate proteins involved in gene expression. Many transcription factors encompassing a broad range of action have been shown to be phosphorylated and subsequently activated by p38. Examples include ATF-1, 2 and 6, SRF accessory protein (Sap1), CHOP, growth arrest and DNA damage inducible gene 153 (GADD153), p53, C/EBPβ, myocyte enhance factor 2C (MEF2C), MEF2A, MITF1, DDIT3, ELK1, NFAT, and high mobility group-box protein 1 (HBP1) [31,35,46-56]. An important *cis*-element, the activator protein-1 (AP-1) binding site appears to be influenced by p38 through several different mechanisms. ATF-2 is known to form heterodimers with Jun family transcription factors thereby directly associating with the AP-1 binding site [51]. Another possible mechanism comes from the observation that a component of AP-1 is c-fos. C-fos is known to be SRE dependant and SRE is able to bind Ternary Complex Factor (TCF). Ternary Complex Factor is comprised of Sap-1a, a protein that is phosphorylated by p38. Thus, p38 indirectly regulates AP-1 activity. ERK and JNK can also mediate another component of the TCF called Elk-1 [57]. It is thought then that there is coordinated participation of the three MAP kinases in regulation of c-fos expression. Recently, the HBP1 transcription factor has been identified as a substrate for p38. HBP1 has been linked to G1 cell cycle arrest and inhibition of p38 has been shown to decrease HBP1 protein levels [53].

1.2.2.3 Other Substrates of p38 MAPKs

Other substrates of p38 MAPKs include metabolic enzymes like glycogen synthase or cytosolic phospholipase A2 (cPLA2) [58, 19, 59]. Na+/H+ exchanger isoform 1 (NHE-1), tau and keratin 8 have also been reported to be substrates of p38α MAPK, just like stathmin. Taken together, this vast collection of substrates suggests that the p38 pathway is involved in a wide and diverse variety of functions.

1.2.3 Physiological Functions of p38 MAPKs

Taking into consideration the wide range of substrates linked to p38 MAPKs, it is a natural consequence that this kinase should also be involved in a wide and diverse variety of functions. Indeed, roles for p38 MAPKs have been described in processes such as cell differentiation and migration, cell transformation, cell survival, inflammation, angiogenesis, myogenesis and others. Deregulation of p38 MAPK pathways is implicated with the development of several pathological conditions like rheumatoid arthritis, Alzheimer's disease, cardiovascular dysfunction and cancer [23] (Fig. 3). For this reason p38 MAPK comprises one of the major drug targets for pharmaceutical companies in today.

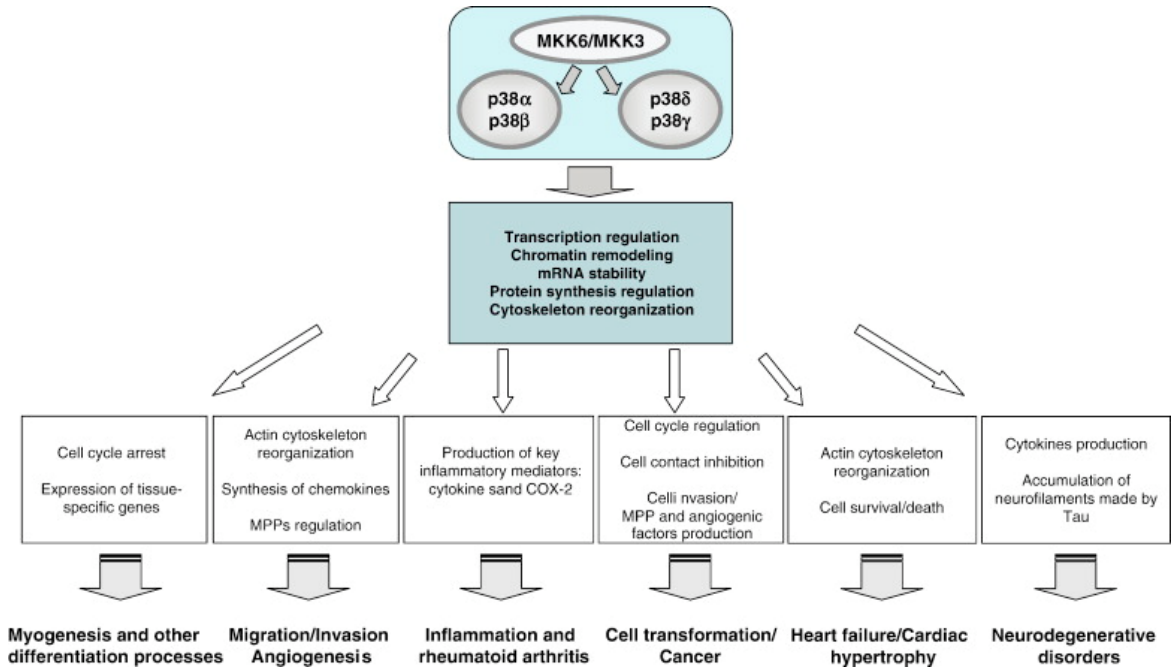

Figure 3. Physiological roles and pathological implications of p38 MAPKs pathways. p38 MAPKs play a central role in the regulation of many biological functions, which contribute to physiological processes. Deregulation of p38 MAPKs pathways lead to the development of several pathological conditions. Image taken from Cuenda, A. *et al.* 2007, Biochimica and Biophysica Acta.

1.3 p38α MAPK

The p38α MAPK is the best characterized of the four p38 MAPK isoforms. Contrary to the other isoforms of p38 MAPK which appear to be more cell-specific, p38α MAPK has been found to be expressed ubiquitously in human and mouse tissues [15, 17]. In particular it is most abundant in inflammatory cells, e.g. those of myeloid origin [15].

1.3.1 p38α MAPK Signaling and Inflammation

p38α MAPK was originally identified as a major modulator of inflammatory responses. It is essential in regulating the expression of cytokines in response to stimulation by LPS or by proinflammatory cytokines [3]. It was also identified as a protein that binds with high affinity to a group of anti-inflammatory compounds such as SB202190 [10,1,9,11]. p38α MAPK mediates inflammatory responses partly through activating a gene expression programme. This activation results in the expression of molecules that participate in inflammation, including proinflammatory cytokines, chemokines and adhesion molecules. Transcriptional profiling of p38α MAPK in endothelial cells in response to TNF stimulation, has revealed a list of genes involved in inflammation that are regulated by this protein, including IL-8 [60], vascular adhesion molecule-1 (VCAM-1) [61] and cyclooxygenase-2 (COX-2) [62, 63]. In macrophages where p38α MAPK was deleted, stimulation with LPS also resulted in the downregulation of genes involved in inflammation, like IL-10, matrix metalloprotease 13 (MMP-13), CXC chemokine ligand 1 and 2 (CXCL1 and CXCL2) and again VCAM-1 [28]. The fact that only p38α and p38β are sensitive to inhibition by anti-inflammatory compounds like SB202190 and its derivates [64, 14] and knockout of p38β in mice did not have any effect on T-cell development, LPS-induced cytokine responses, rheumatoid arthritis or bowel disease progression, only served to highlight the importance of p38α MAPK in inflammation [5].

1.3.2 p38α MAPK Knockout Mice

Several attempts have been made to determine how p38α MAPK contributes to immunity and inflammation. Initially these attempts were performed with the use of

p38 MAPK inhibitors. Although these attempts have provided us with hints concerning the function of p38α MAPK in inflammation, however, they are hampered by the fact that p38 MAPK inhibitors have limited target specificity [65, 66]. In fact, they have even been known to act on other kinases, e.g. JNK, when administered in higher concentrations [30]. For this reason, the generation and use of p38α specific knockout mice was considered to be an important genetic tool in the elucidation of the role of this molecule in inflammation. Four groups have reported the generation of these mice [67,68,69,70]. However, in all cases, loss of p38α MAPK resulted in death starting from embryonic day 10.5 (E10.5) and persisting for variable times afterwards. Insufficient vascularization during placental development was described as a possible cause of death. Mudget et al. found that in addition to the placental defect, angiogenesis was also abnormal in the yolk sac and the embryo itself [67]. Also, Adams et al. reported massive reduction of the myocardium and malformation of blood vessels in the head region [68]. However this defect appears to be secondary to insufficient oxygen and nutrient transfer across the placenta. Finally, fetuses surviving to relatively late stages of development are anemic and have a deficiency of erythropoietin (Epo) mRNA expression in their livers [69]. Rescue of the placental defect in these mice allowed the mice to develop to term and they were normal in their appearance, indicating that p38α MAPK is required for placental organogenesis but not essential for other aspects of mammalian embryonic development [68,71]. Gene disruption methods used to ablate p38α MAPK alleles in embryonic but not placental tissues [71] or at postnatal stages in a drug-inducible fashion [72] permitted survival of these mice. However, these p38α MAPK –null animals were found to develop spontaneous anomalies in homeostasis of pulmonary epithelial and fetal hematopoietic tissues, thus precluding further characterization of their response in experimentally induced diseases.

1.3.3 Generation of p38α MAPK Conditional Mouse Models

Since it was not possible to use complete p38α knockout mice to study the role of p38α MAPK *in vivo*, due to the lethality of this model and other complications described above, it was necessary to create a new model for this purpose. For this reason, our laboratory has generated a p38α MAPK mouse model where expression

of this protein can be controlled spatially and temporally. This was done by taking advantage of the Cre/loxP recombination system, which allows tissue or cell-specific deletion of a target gene at a given timepoint. This system is based on the specific activity of the bacteriophage P1-derived Cre recombinase, which recognizes and mediates site-specific recombination between 34 bp recognition sequences referred to as loxP sites. When the Cre recombinase finds two loxP sites in the same orientation, it deletes the sequence in between with high efficiency [73]. The Cre recombinase can be placed under the control of cell or tissue specific promoters, thus allowing recombination to occur only in these specific sites. Activation of the Cre at a certain timepoint, i.e. an inducible Cre, has also been achieved. For example, the endothelial specific Cre recombinase, placed under the control of the Tie2 promoter, was fused to a mutated estrogen receptor-ligand binding domain known as ER^{T2}. This functionally inactive Cre mainly resides in the nucleus in a chaperone complex, which it can dissociate from and become activated in the presence of a ligand like tamoxifen [74]. In our p38α mouse model, exons 2 and 3 that include the ATP-binding site of the kinase domain, are flanked by loxP sites [75]. So, in the presence of the Cre recombinase, these loxP flanked exons are deleted, leading to ablation of the protein in the given cell or tissue.

1.4 Atherosclerosis

1.4.1 Atherosclerosis, a Disease of the Arteries

Atherosclerosis is a progressive disease of the large arteries that occurs as a response to acute or chronic endothelial wall injury 76-78. In westernized societies, it is the underlying cause of about 50% of all deaths [79]. The term atherosclerosis is derived from two Greek words –'*sclerosis'* (hardness) and *'athere'* (gruel or porridge), and refers to the consistency of the lesions that are formed in this disease. It is characterized by lesions in the intima of the arterial wall called *atheromas* (also called *atheromatous* or *atherosclerotic plaques*) that protrude into the vascular lumina of the large arteries, and consist of accumulated lipids and fibrous materials 78-80. The earliest morphologically identifiable atherosclerotic lesion is the 'fatty streak', which is made up of lipid-filled foam cells [80] but are not significantly raised and thus do not cause any disturbance in blood flow. In humans, they begin as multiple minute yellow, flat spots that can coalesce into elongated streaks, 1 cm long or longer (Fig. 4).

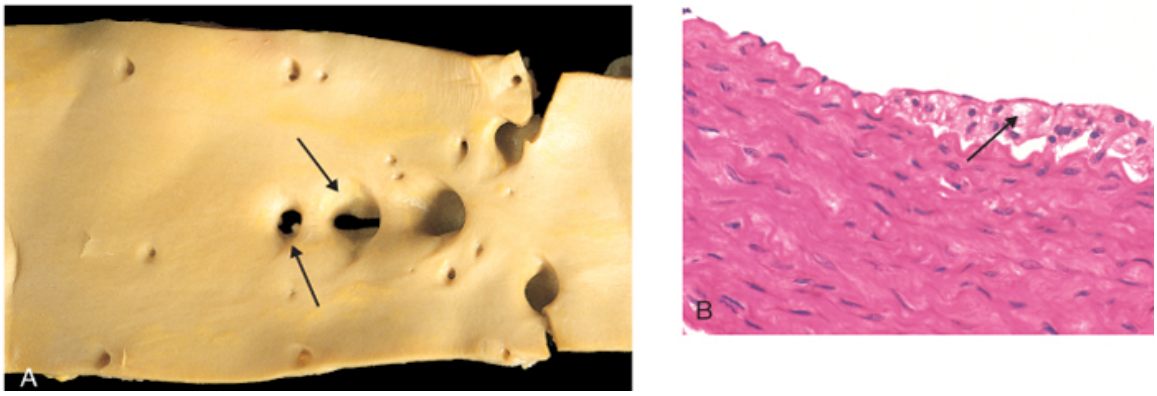

Figure 4. Fatty streak formation characterised by a collection of foam cells in the arterial intima. (A) Aorta with fatty streaks (*arrows*), associated largely with the ostia of branch vessels. (B) Photomicrograph of fatty streak in an experimental hypercholesterolemic rabbit, demonstrating intimal, macrophage-derived foam cells (*arrow*). (Courtesy of Dr. Myron I. Cybulsky, University of Toronto, Ontario, Canada.)

The fully developed, or 'mature' atherosclerotic plaque has a more complex structure, consisting of foam cells and extracellular lipid droplets in the centre of the plaque to form a 'core' region surrounded by a cap of smooth muscle cells and a collagen rich matrix that stabilizes it. Other cell types present in plaques include dendritic cells, mast cells, a few B cells and probably natural killer T cells [80] (Fig. 5).

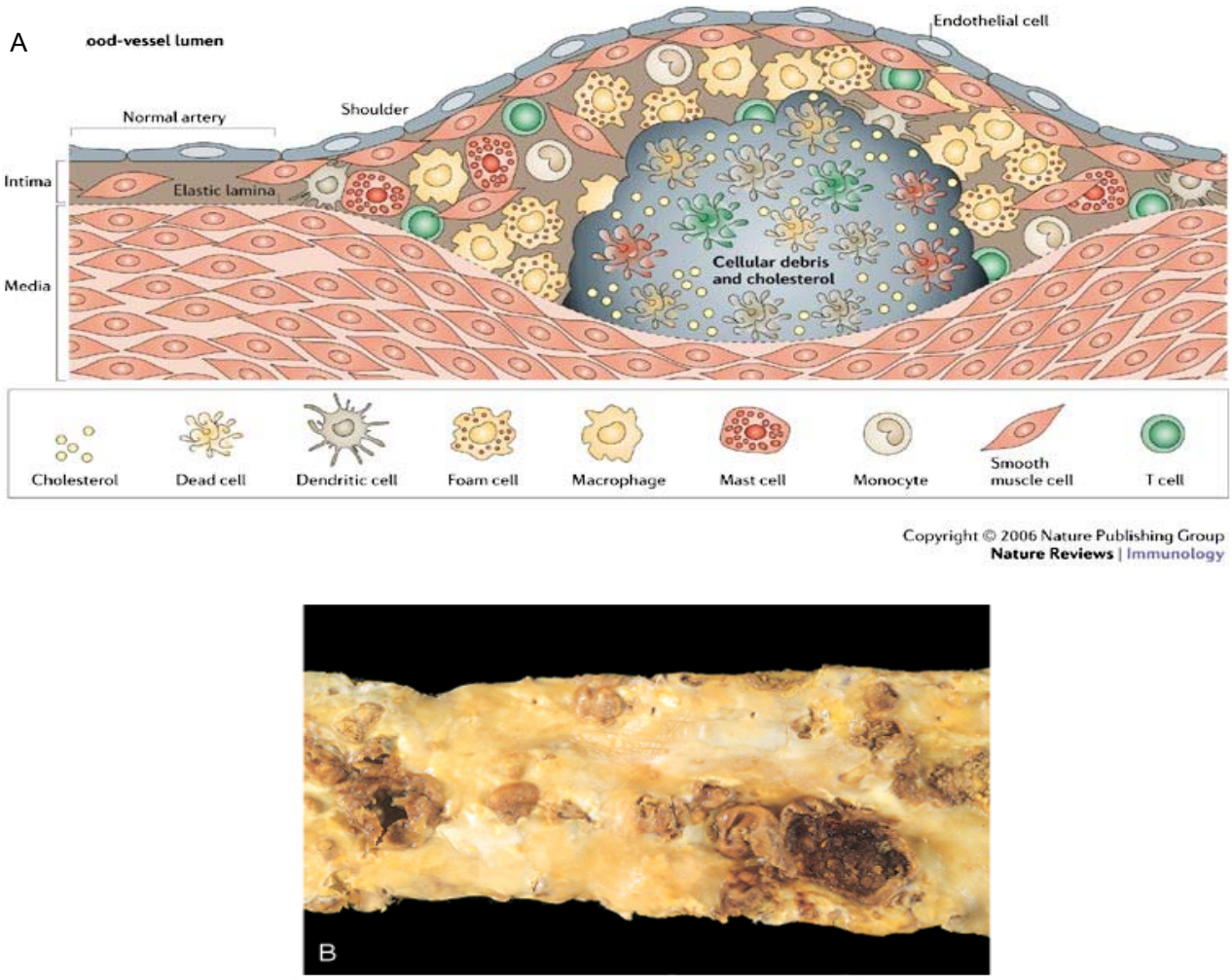

Figure 5. **Fully developed atherosclerotic plaque**. (A) The mature atherosclerotic plaque has a core containing lipids and debris from dead cells. Surrounding it and stabilizing it is a fibrous cap made up of smooth muscle cells and collagen fibers. Image taken from Hansson, G. K. *et al.* 2006, Nature Reviews Immunology (B) Severe disease with diffuse and complicated lesions, some of which have coalesced, in human aorta.

1.4.2 Major Risk Factors of Atherosclerosis

Atherosclerosis development is influenced by various factors, the major ones of which are described below:

Age

Atherosclerosis and age are intimately linked, atherosclerosis being the best example of an age-related disease. Although the accumulation of atherosclerotic plaque is typically a progressive process, it does not usually become clinically manifest until lesions reach a critical threshold and begin to precipitate organ injury in middle age or later. Thus, between ages 40 and 60, the incidence of myocardial infarction in men increases fivefold, even though the underlying arterial lesions were probably evolving before that. The prevalence of these diseases in advanced age has been attributed to the increase in arterial stiffness that occurs with age because of structural changes of the arterial walls as well as endothelial dysfunction. However, convincing molecular mechanisms have not yet been reported for these age-associated alterations of the vascular wall. Recently, the idea of vascular cellular senescence has become attractive as a molecular mechanism linking ageing and atherogenesis [81,82].

Sex

Premenopausal women are relatively protected against atherosclerosis and its consequences compared with age-matched men. Thus, myocardial infarction and other complications of atherosclerosis are uncommon in premenopausal women unless they are otherwise predisposed by diabetes, hyperlipidemia, or severe hypertension. After menopause, however, the incidence of atherosclerosis-related diseases increases and with greater age eventually exceeds that of men. The presumed protective effects of estrogens in women have been widely investigated with a series of large observational studies tending to support this notion [83,84]. However, clinical trials designed to assess the effect of female hormone replacement have failed to report any benefit [85] or harm. Indeed, postmenopausal estrogen replacement probably is associated with increased cardiovascular risk and is no longer recommended for preventing heart disease in women [86].

Hypertension

Hypertension is known to act on the arterial wall to promote both vascular remodeling, and atherosclerosis resulting in diminished arterial wall compliance and elevated stiffness [87]. Clinical and experimental investigations have shown that increased blood pressure is associated with exaggerated atherosclerosis. In humans, measurement of carotid-artery intima-media thickness is highly correlated with blood pressure levels and well-reflects atherosclerosis and tracks its progression [88]. In animal models, including rabbits [89], monkeys [90] and mouse models of atherosclerosis [91], it has been demonstrated that hypertension increases the rate of atherosclerotic plaque development. Mechanisms that could account for the effect of hypertension on atherosclerosis include increased endothelial permeability to LDL due to pressure-induced stretch [92], endothelial dysfunction [93], enhanced monocyte adhesion [94] and inflammation [95].

Genetics

As a complex disease process that results from the interaction between an individual's genetic makeup and environmental risk factors 96-98, the genetic component of atherosclerosis has been elusive to characterize. Over the past three decades, a great deal of research has focused on defining the genetic component of this disease with the hopes that detailed knowledge of the genes and gene variants will lead to improvements in the diagnosis and treatment [99]. There are rare Mendelian disorders in which single gene changes lead to accelerated atherosclerosis such as familial hypercholesterolemia. In common 'garden variety' atherosclerosis however, multiple genes probably influence the disease process by enhancing disease susceptibility or by modifying the impact of environmental risk factors. The genetic component is likely to be a collection of gene variants in the form of single nucleotide polymorphisms (SNPs). Each SNP individually may have a mild - to - moderate affect on the resulting protein by modifying the quantity, function or posttranslational changes. A combination of many SNPs however, may have a major effect. These gene variants and their resulting proteins could serve as disease biomarkers for diagnosis and prognosis, functional biomarkers to assess treatment response or as targets for novel treatment strategies. This is why much effort is being put into elucidating further the genetic component of atherosclerosis [99].

Cigarette smoking

Cigarette smoking is a well-established risk factor in men, and an increase in the number of women who smoke probably accounts for the increasing incidence and severity of atherosclerosis in women. Prolonged smoking of one pack of cigarettes or more daily increases the death rate from coronary artery disease, and it appears that cessation of smoking does not reverse this effect [100]. The precise nature for this effect of smoking on atherosclerosis was unclear up to now, but recently in a study by Wang, Z. *et al.,* 2007 it was reported that oxidation of thiocyanate, which is elevated in the plasma of smokers, may lead to carbamylation of low-density lipoproteins (LDL) and facilitate in the progression of atherosclerosis [101].

Diabetes mellitus

Atherosclerosis is accelerated both in type 1 and type 2 diabetes. The underlying cause of this effect, which is common in both types of diabetes, appears to be hypercholesterolemia [102]. Strong epidemiological evidence exists to support an association of glycaemic control and cardiovascular disease risk [103]. Together with other factors like abnormal levels of blood pressure, lipids and markers of inflammation but also oxidative stress, it has a detrimental impact on the artery wall and the ability of organs to tolerate ischemic injury. Although it has been demonstrated that intensive glucose control had a beneficial effect on macrovascular complications in type 1 diabetes patients, the effect was not the same for type 2 patients. Therapeutic strategies that have the greatest cardiovascular benefit for diabetes patients appear to be those focusing on lowering of LDL-cholesterol and blood pressure, rather than glucose-lowering specifically [104].

Lipid metabolism

Elevated cholesterol and/or triglyceride levels in the plasma consist one of the main risk factors of atherosclerosis. Both these molecules are important for many different cellular processes. The synthesis of cellular membranes, steroid hormones and bile are some of the processes cholesterol is involved in. Triglycerides, which are the major source of energy for the body, can be used either directly or indirectly by the muscle and other organs or stored as fat in adipose tissues. Transportation of cholesterol and triglycerides is achieved by packaging into water-soluble lipoprotein

particles. These lipoproteins consist of a core of apolar lipids, mainly cholesteryl esters and triglycerides, covered by a surface of polar molecules, primarily free cholesterol, phospholipids and apolipoproteins.

Plasma lipoproteins have been divided in different classes according to their density: chylomicrons, very low density lipoproteins (VLDL), low density lipoproteins (LDL) and high density lipoproteins (HDL). Furthermore, several derivatives have been described, such as the chylomicron and VLDL remnants and intermediate density proteins (IDL). These different classes of lipoproteins not only differ in their density, but also in size, electrophoretic mobility, lipid content and apolipoprotein composition.

Lipid metabolism can be divided into three main pathways. The exogenous pathway that mediates the uptake of dietary lipids by the body, the endogenous pathway that delivers lipids from the liver throughout the body and the reverse cholesterol pathway that mediates the redirection of cholesterol from the periphery to the liver [105] [106] [107] [108].

Elevated levels of plasma LDL, which has an essential role in the uptake and transfer of lipids throughout the body, is considered to be unfavorable and predispose to the development of atherosclerosis. They can accumulate in the vascular wall where they become modified. Modifications that can occur include oxidation, lipolysis, proteolysis and aggregation [79]. One of the modifications that is considered most significant especially for early lesion formation is lipid oxidation as a result of exposure to the oxidative waste of vascular cells. Such modifications initially give rise to ‘minimally oxidized’ LDL species that have proinflammatory activity but may not be sufficiently modified to be recognized by macrophage scavenger receptors. Mice lacking 12/15 lipoxygenase have considerably diminished atherosclerosis, suggesting that this enzyme may be an important source of reactive oxygen species in LDL oxidation [109].

On the other hand, HDL also known as ‘good cholesterol’ appears to have a strongly protective role against atherosclerosis. The underlying cause for this protective mechanism is its role in the reverse cholesterol pathway, where it is involved in the removal of excess cholesterol from peripheral tissues. In addition, it also protects by inhibiting lipoprotein oxidation. This last property of HDL is due in part to the fact that

it carries serum paraoxonase, an esterase that can degrade certain biologically active oxidized phospholipids [110, 111] (Fig. 6).

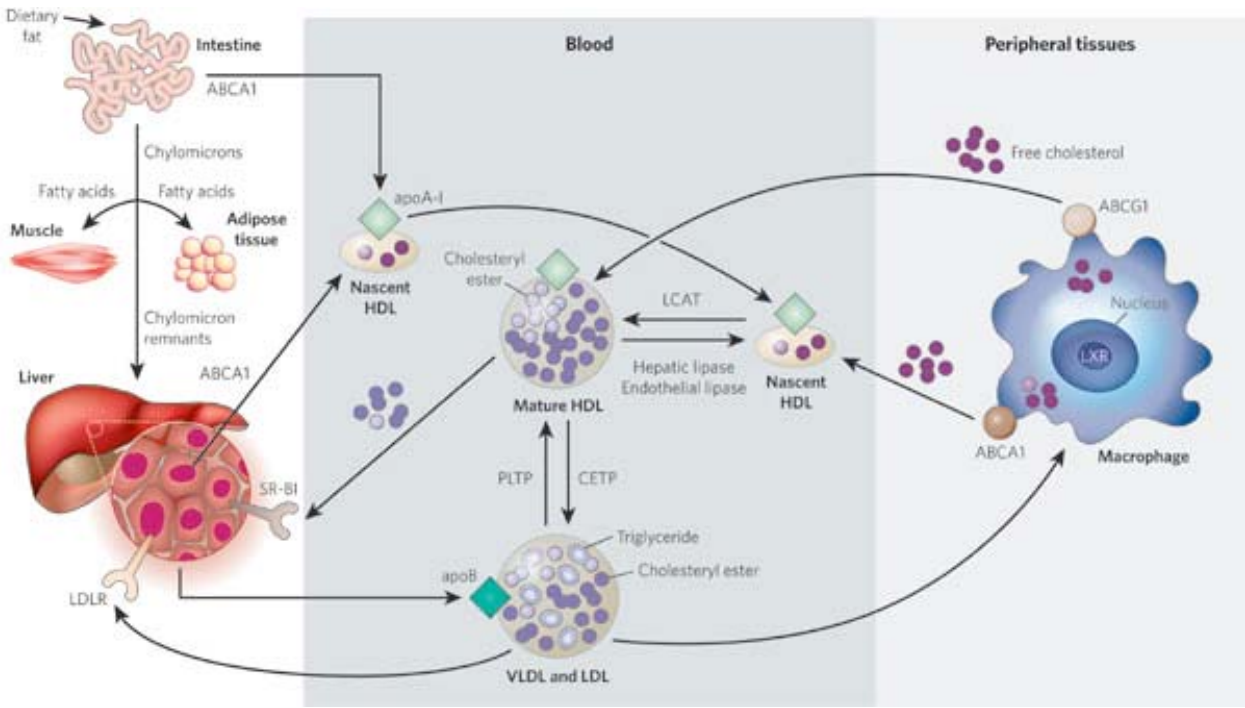

Figure 6. **Lipid metabolism in atherosclerosis.** It involves the transport of lipids, particularly cholesterol and triglycerides, in the blood. The intestine absorbs dietary fat and packages it into chylomicrons (large triglyceride-rich lipoproteins), which are transported to peripheral tissues through the blood. In muscle and adipose tissues, the enzyme lipoprotein lipase breaks down chylomicrons, and fatty acids enter these tissues. The chylomicron remnants are subsequently taken up by the liver. The liver loads lipids onto apoB and secretes very-low-density lipoproteins (VLDLs), which undergo lipolysis by lipoprotein lipase to form low-density lipoproteins (LDLs). LDLs are then taken up by the liver through binding to the LDL receptor (LDLR), as well as through other pathways. By contrast, high-density lipoproteins (HDLs) are generated by the intestine and the liver through the secretion of lipid-free apoA-I. ApoA-I then recruits cholesterol from these organs through the actions of the transporter ABCA1, forming nascent HDLs, and this protects apoA-I from being rapidly degraded in the kidneys. In the peripheral tissues, nascent HDLs promote the efflux of cholesterol from tissues, including from macrophages, through the actions of ABCA1. Mature HDLs also promote this efflux but through the actions of ABCG1. (In macrophages, the nuclear receptor LXR upregulates the production of both ABCA1 and ABCG1.) The free (unesterified) cholesterol in nascent HDLs is esterified to cholesteryl ester by the enzyme lecithin cholesterol acyltransferase (LCAT), creating mature HDLs. The cholesterol in HDLs is returned to the liver both directly, through uptake by the receptor SR-BI, and indirectly, by transfer to LDLs and VLDLs through the cholesteryl ester transfer protein (CETP). The lipid content of HDLs is altered by the enzymes hepatic lipase and endothelial lipase and by the transfer proteins CETP and phospholipid transfer protein (PLTP), affecting HDL catabolism. Image taken from Rader, D. J. *et. al.,* 2008, Nature.

1.4.3 Atherosclerosis Development and Progression

The set of processes believed to be involved in atherogenesis and its progression includes the following:

1) Accumulation of low density lipoprotein within the arterial intima

The endothelium, with its tight junctional complexes, functions as a selectively permeable barrier between blood and tissues. Endothelial cell morphology is affected by physical forces such as fluid shear stress. In tubular areas of arteries where blood flow is uniform and laminar, endothelial cells are ellipsoid in shape and aligned in the direction of flow. In areas of arterial branching, where blood flow is disturbed, they have polygonal shapes and no particular orientation [79]. In these latter areas, where there is predilection for lesion development [112,113], excess amounts of cholesterol-rich, LDL derived from plasma are deposited by passive diffusion, and retained in the subendothelium matrix via interactions between the LDL constituent apolipoprotein (apoB) and matrix proteoglycans [114].

2) Migration of monocytes and T lymphocytes from the arterial blood into the subendothelial space and 'fatty streak' formation

Once inside the arterial intima, trapped LDL undergoes modifications, including oxidation, lipolysis, proteolysis and aggregation [79], as described above. Such modifications, and in particular lipid oxidation which occurs due to reactive oxygen species production from endothelial cells and macrophages and has been shown to be significant for early lesion formation [115], can activate the endothelium. This in turn can express leukocyte adhesion molecules like VCAM-1. Monocytes and T-cells bind to VCAM-1 expressing endothelial cells and subsequently migrate into the arterial intima in response to locally produced chemokines like MCP-1. These monocytes then differentiate into macrophages in response to local macrophage-colony stimulating factor (M-CSF) produced by endothelial and smooth muscle cells, ingesting large amounts of modified LDL through the expression of scavenger [116] receptors such as SR-A and CD36 [79]. This results in their conversion to 'foam cells' (macrophages with abundant lipid-filled cytoplasm). These first two processes lead to formation of a widely prevalent lesion, the 'fatty streak' [80].

3) Migration of smooth muscle cells from the tunica media into the affected area of the intima

After formation of the 'fatty streak', the nascent atheroma typically evolves into a more complex lesion, which eventually leads to clinical manifestations. Part of this process is characterized by the accumulation of smooth muscle cells in the lesion which occurs due to cytokine and growth factor production by the macrophages and T-cells in the atherosclerotic intima. Migration of smooth muscle cells can also occur due to other risk factors like homocysteine, which appears to injure endothelial cells and to stimulate proliferation of vascular smooth muscle cells [117]. Once in the intima, they divide and synthesize and secrete all the connective tissue components of the plaque cap (collagen-rich connective tissue matrix, the microfibrillar component of elastin, proteoglycans and glycosoaminoglycans).

4) Breakdown of part of the plaque connective tissue, usually at or near the base of the lesion to form advanced lesions

As the lesion progresses, various factors like proteinases, collagenase, gelatinases , stromolysin and cathepsins are produced by the different cells types that are present in the atherosclerotic plaque [79]. These can change the composition and vulnerability of the plaque by promoting the formation of a 'core' or 'pool' which contains large amounts of extracellular lipid and which may be highly deformable (fibrolipid plaque). Besides, smooth muscle cells, macrophages and T cells, other cells that are also present in the plaques and can contribute to this process include dendritic cells [118], mast cells [119], a few B cells [120] and probably nature killer T cells. The stability of atherosclerotic lesions may also be influenced by infection. This may have systemic effects such as induction of acute phase proteins and local effects such as increased expression of tissue factor and decreased expression of plasminogen activator (PA), but also by calcification [121] and revascularization which are both common features of advanced lesions.

5) Injury to the plaque cap that results in plaque rupture and acute thrombus formation

Plaques that have become vulnerable over time may rupture an event that may be clinically silent and lead either to further plaque growth and hence more severe

stenosis of the affected arterial segment or to one of the acute syndromes of coronary heart disease. Inflammatory mediators appear to play a major role in weakening of the fibrous cap and subsequent plaque rupture. For example, the inflammatory mediator interferon gamma (IFN-γ) has been shown to inhibit the synthesis of interstitial collagen, a product of smooth muscle cells in the artery wall that lends strength to the 'fibrous cap'. Also, various proteases produced by macrophages, like interstitial collagenases, gelatinases and stromolysin, can participate in matrix degradation [122].

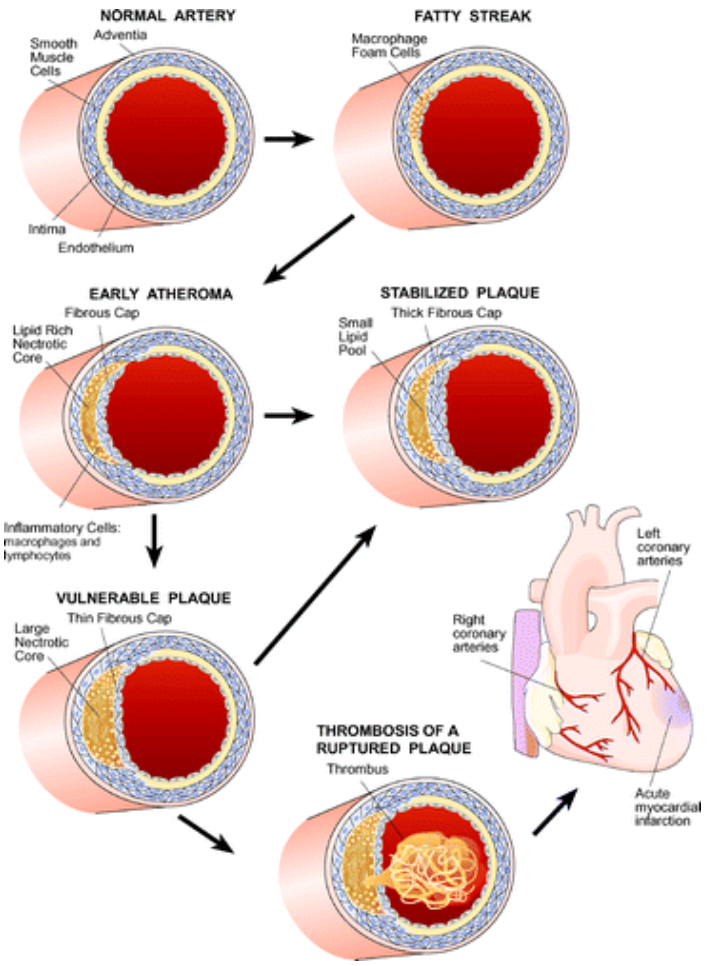

Figure 7. The stages of atherosclerotic lesion formation and progression. Image taken from Lusis, A. J. *et al*., 2004, Annual Review of Genomics and Human Genetics.

1.4.4 Inflammation and Atherosclerosis

95 years ago, Nikolaj N. Anitschkov and Semen S. Chalatov performed the first important experiment in atherosclerosis research. They speculated that the cholesterol deposit in the atherosclerotic lesion is caused by the consumption of fat and tested this hypothesis by feeding rabbits cholesterol. In their classical 1913 paper, they demonstrated that this was the case; cholesterol leads to atherosclerosis. This finding established the link between diet, metabolism, and atherosclerotic and cardiovascular disease and would set the stage for much of cardiovascular research for the rest of the 20th century. Anitschkov recognized, as Virchow before him, that the atherosclerotic plaque contains not only lipids but also several types of cells, among them inflammatory cells. Antischov identified them as smooth muscle cells, macrophages, and lymphocytes. While this discovery of cholesterol as an etiologic agent became historic, his observation of macrophages and lymphocytes in the lesion was forgotten [123].

Today, atherosclerosis is considered to be an inflammatory disease, characterized by the accumulation of a large number of immune cells in the atherosclerotic lesion, in particular macrophages and T-cells which form the first lesions of atherosclerosis since they are recruited to the arterial intima through chemokines and adhesion molecules expressed on the endothelium [124]. As our knowledge of this disease increases, the understanding that immune responses are involved in atherosclerosis development from the initiation through to its thrombotic complications becomes more and more established. This realization is clinically useful because, therapeutic agents can be redirected from lipid lowering, to targeting inflammatory responses. Statins, which have shown striking clinical benefit against atherosclerosis during the past decade, were initially thought to have these effects by lowering cholesterol concentrations in the blood. However, recent data indicate that part of the clinical benefit occurs because of an anti-inflammatory effect that is not related to LDL reduction [80]. Therefore, directing future studies in atherosclerosis on the inflammatory component of this disease appears to be the way forward in its treatment.

1.5 Aim of the Thesis

The aim of this project was to study the macrophage and endothelial-specific role of p38α MAPK in atherosclerosis development, two of the most important cell types involved in the initiation and progression of this disease. At the same time, we wanted to generate two new p38α MAPK mouse models, p38αCA (Constitutively Active) and p38αKD (Kinase Dead), to potentially assist us in our studies, but that could also be used as genetic tools to answer other interesting questions in relation to the function of this molecule.

1.5.1 Investigation of the Macrophage and Endothelial-Specific Role of p38α MAPK in Atherosclerosis

As describe above, inflammation plays a key role in the development and progression of atherosclerosis. Inflammatory triggers include oxidized lipoproteins (oxLDL), hypertension and diabetes. As a molecule involved in inflammation, various roles have been attributed to p38α MAPK with respect to atherogenesis, including the regulation of scavenger receptor expression like CD36 in macrophages and therefore oxLDL uptake [125] and regulation of expression of the monocytic chemokine receptor CXCR2 that is upregulated in response to oxLDL [126]. It has been described as a mediator of vascular smooth muscle cell migration by stimulating vascular endothelial growth factor (VEGF) in response to thrombin-induced ROS production [127]. In endothelial cells, it has been associated with migration and proliferation [128, 129, 130], cell permeability [131], apoptosis [132] and adhesion molecule expression, like VCAM-1 [61, 63]. Finally, it is critical for the production and activity of multiple pro-inflammatory cytokines like TNFα, IL-1β, IL-6 and IL-8 in most of the cell types that participate in atherosclerosis development [133, 134, 135, 136, 28].

Due to this suggestive *in vitro* evidence that p38α MAPK is involved in atherosclerosis development, here we wanted to address the cell-specific *in vivo* role of p38α MAPK signalling in vascular endothelial cells and macrophages. These cell types were selected because of their significant role in the development and progression of this disease. As a reminder, endothelial cells (ECs) are involved in all stages of atherogenesis and their dysfunction is a key early event in plaque formation. The strategic location of the endothelium between blood and tissue and

the constitutive properties of endothelial cells, allow them to monitor the transport of plasma molecules, by employing bidirectional receptor-mediated and receptor-independent transcytosis and endocytosis, and to regulate vascular tone, cellular cholesterol and lipid homeostasis. Heterogeneity of ECs defines lesion-prone areas of increased shear stress [137]. Similarly, monocytes/ macrophages play a key role both in initation and progression of atherosclerosis. They function as a scavenger cell, an immune mediator cell, and a source of chemotactic molecules and cytokines. Recruitment of monocytes, as described earlier is one of the earliest events in atherosclerosis. In the intima, monocytes develop into macrophages, which are important mediators of inflammation and the innate (antigen-independent) immune response in atherosclerosis. Macrophages contribute to the local inflammatory responses through production of cytokines, free radicals, proteases, and complement factors. By serving as antigen-presenting cells, macrophages participate in the acquired immune response. The uptake of modified lipoproteins by macrophages leads to the accumulation of cholesterol esters and formation of macrophage-derived foam cells, the hallmark of the fatty streak. Macrophages also contribute to lesion remodeling and to plaque rupture by secreting matrix metalloproteinases. Thus macrophages contribute to the evolution of atherosclerosis in diverse and significant ways [138].

For this study, we made use of the conditional p38α MAPK mouse model previously generated in our laboratory. Crossing these mice with myeloid (LysMCre) and endothelial (Tie2-Cre^{ERT2}) specific Cre lines allowed us to generate mice with macrophage (p38α^{MY-KO}) and endothelial (p38α^{EC-KO}) specific deficiency of this protein. The well established Apolipoprotein E deficient mouse model of atherosclerosis [139], was then further crossed with these mice, to render them susceptible to atherosclerosis development.

1.5.2 Generation of Two New p38α MAPK Mouse Models: p38αCA and p38αKD

Besides studying the function of p38α MAPK in atherosclerosis by knocking out the protein in macrophages and endothelial cells, we also wanted to create two new models p38αCA and p38αKD, a constitutively active and kinase dead form of the

protein, respectively. These mice are very important, each in a different manner, because they can help better understand the role of p38α MAPK both in atherosclerosis, but also in other pathological processes this protein may be related to.

Previous efforts to obtain active forms of MAPKs have only been partially successful. Several gain-of function mutations that were identified in the *S. cerevisiae FUS3* [140, 141] and in the Rolled MAPK of *Drosophila melanogaster* [142, 143] did not render kinases catalytically active. Also, the use of MAPKK-MAPK hybrids [144, 145], i.e. coupling of MAPKs with their upstream kinases which seemed a more useful approach, did not work *in vivo*, since these two molecules are not colocalized in the cell and are differently controlled. The most successful attempts have been with producing constitutively active upstream kinases, like MKK3 and MKK6 for p38α MAPK. However this system does not allow the isolation of one molecule and its downstream targets, since it activates more than one downstream kinases. Therefore, the generation of a mouse model where only p38α MAPK would be constitutively activated would be very useful in isolating and examining further the components of this specific pathway. In this study we proceeded in the generation of these mice, by taking advantage of three point mutations described previously for the p38 homologous yeast protein, Hog1, that render this protein catalytically and biologically hyperactive [146].

On the other hand, the p38αKD model, which was generated in this study by introducing a mutation in the ATP-binding site of the kinase domain in exon 2 rendering the protein catalytically and biologically inactive, is a useful model because it can assist our studies with this molecule by excluding the possibility of compensation that can occur by other isoforms of p38 when knocking out p38α. It is also a more accurate model to prove or disprove studies carried out with small molecule pharmacological inhibitors, since these molecules act by inhibiting the catalytic activity of the protein. Finally, it will allow the elucidation of any kinase-independent function of p38α MAPK.

2. Results

2.1 Macrophage and Endothelial-Cell Specific Role of p38α MAPK in Atherosclerosis

2.1.1 Macrophage-Cell Specific Role of p38α MAPK in Atherosclerosis

2.1.1.1 Generation of Myeloid-Specific p38α Knockout Mice in an ApoE Deficient Background

In order to address the macrophage-specific *in vivo* role of p38α MAPK in atherosclerosis we generated mice with specific ablation of p38α in myeloid cells by crossing mice with loxP-flanked p38α alleles ($p38\alpha^{FL/FL}$), previously generated in our laboratory [75], with LysMCre mice, expressing Cre under the myeloid-specific M lysozyme promoter ($p38\alpha^{MY\text{-}KO}$)[147] (Fig. 8). $p38\alpha^{MY\text{-}KO}$ mice were then bred into the $ApoE^{-/-}$ genetic background, a mouse model that spontaneously develops atherosclerotic plaques due to elevated levels of cholesterol circulation [148], rendering the mice prone to atherosclerosis.

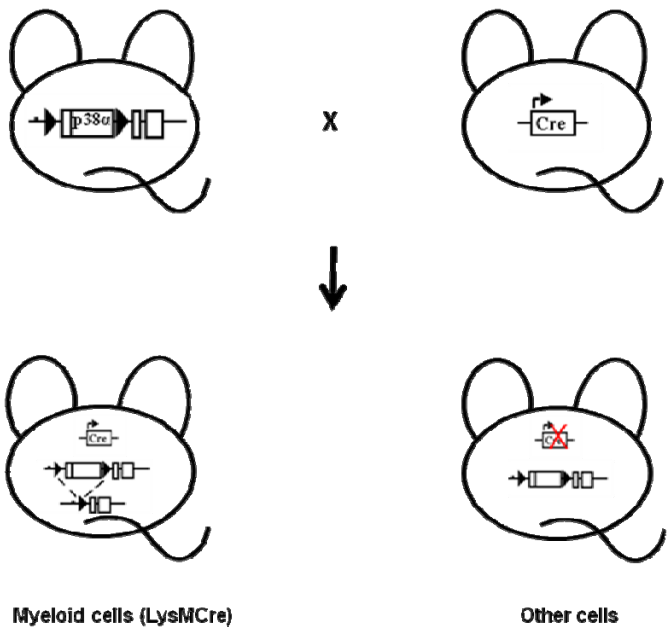

Figure 8. Strategy for the generation of myeloid–specific p38α MAPK knockout mice. Myeloid-specific knockout mice were generated by crossing $p38\alpha^{FL/FL}$ mice with LysMCre mice.

2.1.1.2 Efficient Ablation of p38α MAPK in Macrophages of p38α^{MY-KO}/ ApoE$^{-/-}$ Mice

Immunoblot and southern blot analysis of bone-marrow derived macrophage (BMDM) extracts showed efficient ablation of p38α MAPK in macrophages of p38α^{MY-KO} mice (Fig. 9A and B, respectively). LPS stimulation (1µg/ml) induced p38α MAPK activation in wild-type cells (ApoE$^{-/-}$ in our case)[28], which, as expected, was clearly reduced in p38α^{MY-KO}/ApoE$^{-/-}$ mice (Fig. 9B).

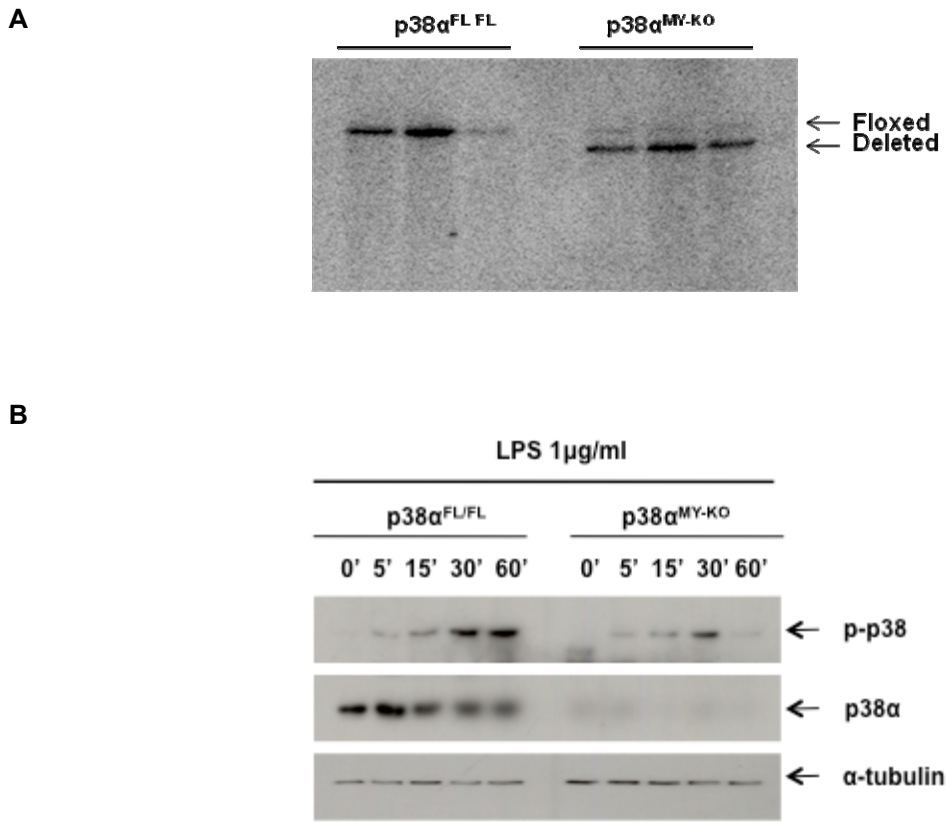

Figure 9. Deletion efficiency of p38α MAPK in macrophages of p38α^{MY-KO} mice.
(A) Analysis of deletion efficiency of p38α MAPK in macrophages by isolation of BMDMs from p38α^{MY-KO} and p38α$^{FL/FL}$ mice and southern blotting to detect the deleted p38α allele after cre recombination. p38α^{MY-KO} mice, n= 3; p38α$^{FL/FL}$ n= 3. (B) LPS (1µg/ml, Sigma) stimulation of BMDMs from p38α^{MY-KO} and p38α$^{FL/FL}$ mice showed a clear reduction in total p38 activation (total p-p38) and ablation p38α MAPK.

2.1.1.3 p38α MAPK Ablation Did not Affect *in vitro* Lipid Uptake and Foam Cell Formation

Given the extensive literature claiming important functions for p38α MAPK in macrophages with respect to atherosclerosis as a result of studies with p38-specific inhibitors [125, 126], and in an attempt to investigate these claims in a more physiological environment without the use of inhibitors, we isolated and cultured thioglycolate-elicited peritoneal macrophages from p38α^{MY-KO}/ApoE$^{-/-}$ and ApoE$^{-/-}$ mice. These macrophages were then stimulated with 50µg/ml oxLDL and uptake was compared in p38α^{MY-KO}/ApoE $^{-/-}$ and ApoE$^{-/-}$ macrophages by FACS analysis (Fig. 10B). Our results showed that there was no significant difference in the uptake of modified lipids.

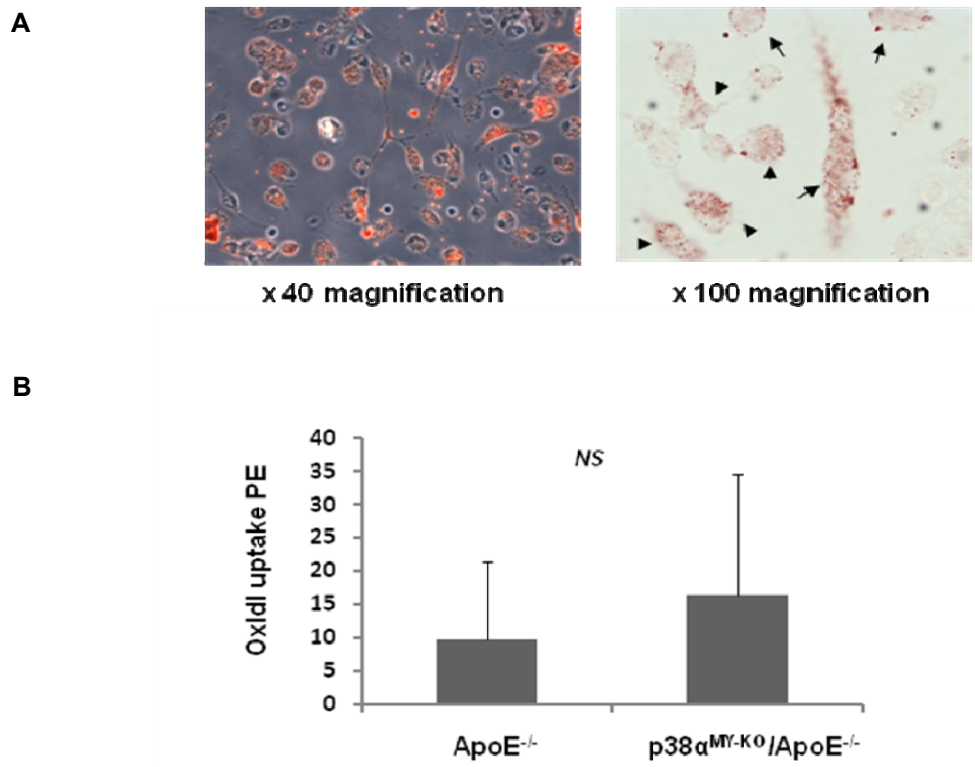

Figure 10. Similar oxLDL uptake in macrophages of p38α^{MY-KO}/ ApoE $^{-/-}$ and ApoE $^{-/-}$ mice stimulated *in vitro* with oxLDL, (A) Staining of oxLDL stimulated macrophages with Oil red O (lipid staining). Foam cells, which are defined as cells with ≥ 10 lipid droplets, are indicated with arrows. (B) Quantification of oxLDL uptake by thioglycolate-elicited peritoneal macrophages after stimulation with 50µg/ml oxLDL for 2.5 hrs. OxLDL was previously labeled with DiI and quantification was performed by FACS analysis. Error bars represent SD. ApoE $^{-/-}$ mice, n= 3; p38α^{MY-KO}/ ApoE $^{-/-}$ n= 3.

However, we did observe a considerable reduction in the expression of the chemokine MIP-2α and the cytokine IL-1β (Fig. 11B, top and bottom respectively), which was previously reported upon LPS stimulation in p38α^{MY-KO} macrophages [28].

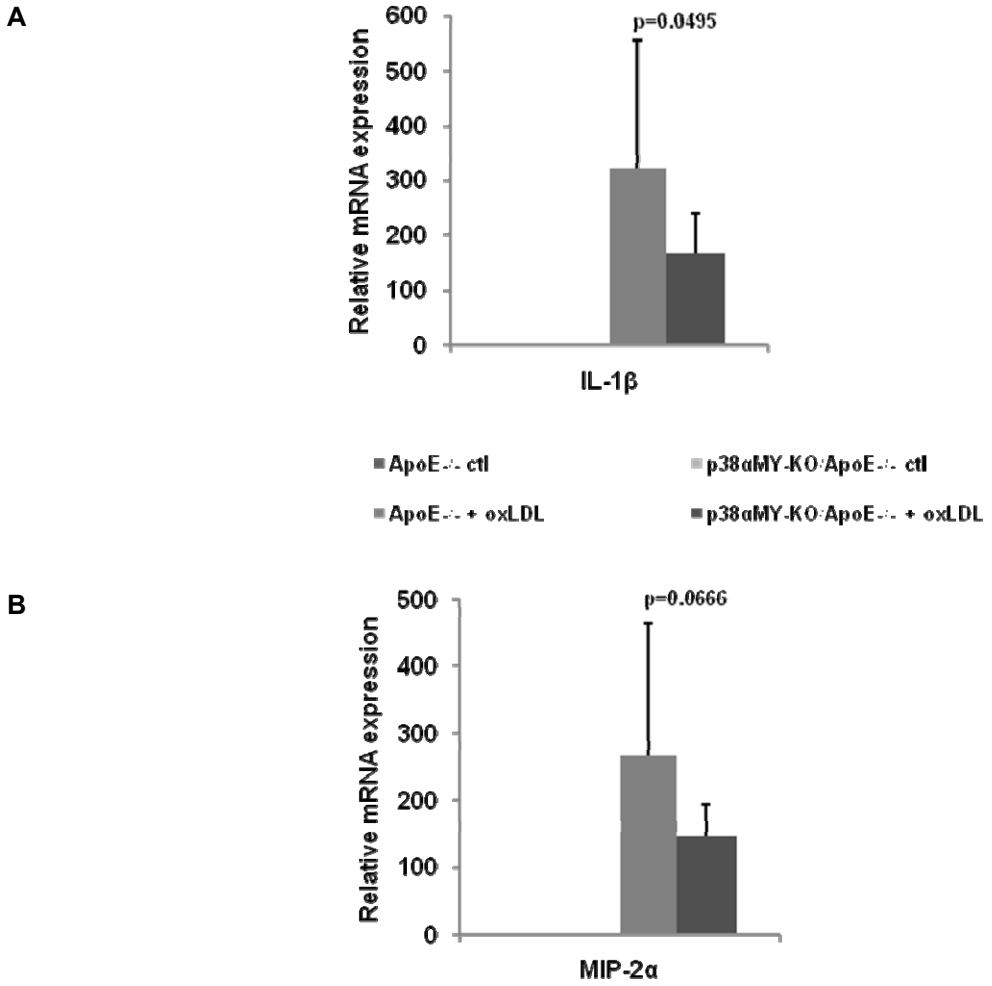

Figure 11. Considerable reduction in MIP-2α and IL-1β in p38α^{MY-KO}/ ApoE$^{-/-}$ macrophages stimulated with oxLDL *in vitro* Relative mRNA expression levels of chemokine MIP-2α (A) and cytokine IL-1β (B) in macrophages isolated from p38α^{MY-KO}/ ApoE$^{-/-}$ and ApoE$^{-/-}$ mice stimulated with 50μg/ml oxidized LDL for 2.5 hrs.Error bars represent SD. ApoE$^{-/-}$ mice, n= 7; p38α^{MY-KO}/ ApoE$^{-/-}$, n= 9.

2.1.1.4 p38α MAPK Ablation in Macrophages Did not Affect Atherosclerosis Development *in vivo*

From our *in vitro* studies in p38α MAPK knockout macrophages it was apparent that, surprisingly and contrary to previous claims, p38α MAPK ablation did not affect oxLDL uptake by macrophages. In order to address the role of p38α in macrophages in the pathogenesis of atherosclerosis *in vivo*, we placed groups of male and female p38α^{MY-KO}/ApoE$^{-/-}$ and their ApoE$^{-/-}$ littermates on a cholesterol-rich 'western diet' for 10 weeks starting from 6-8 weeks of age. Analysis of bodyweight and cholesterol levels before and after the 'western diet' revealed no differences between the two genotypes, although at week 10 cholesterol levels had increased ~ 5-fold in both male and female littermates and both had gained ~ 5gr of weight (Fig. 12).

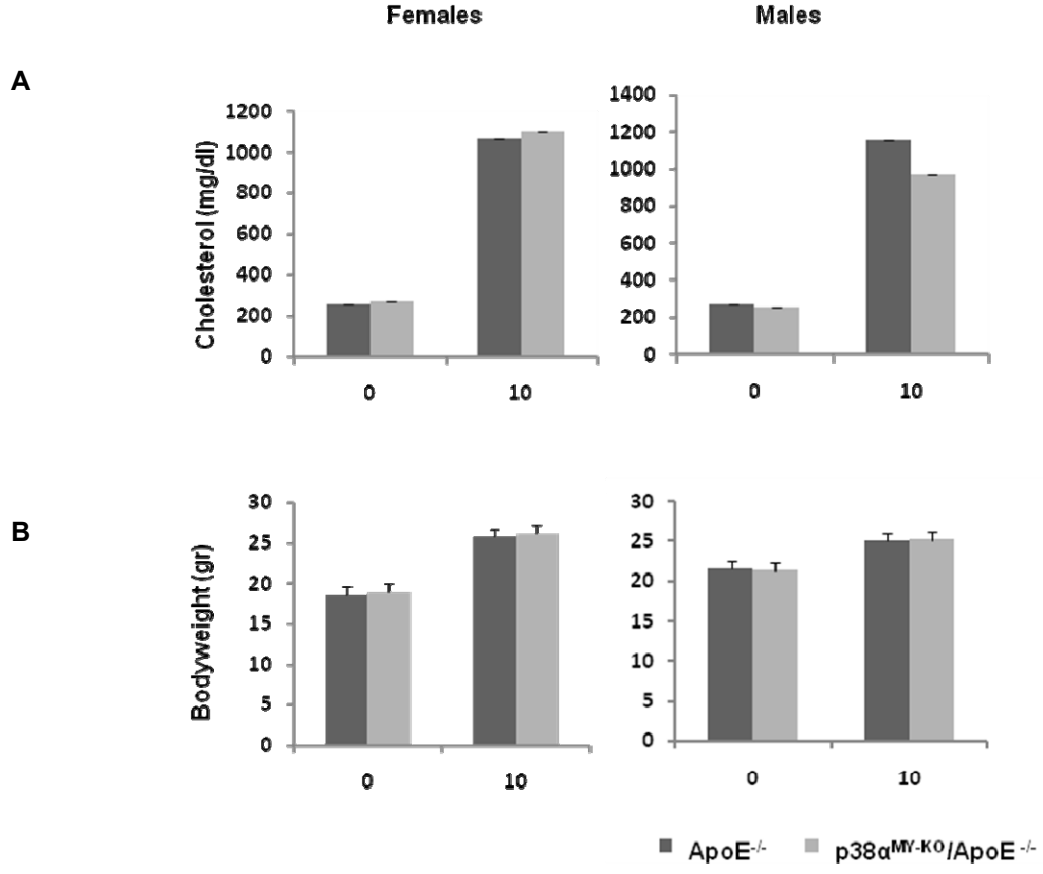

Figure 12. Bodyweight and cholesterol levels of p38α^{MY-KO}/ApoE$^{-/-}$ mice. (A) Cholesterol (mg/dl) and (B) bodyweight (gr) levels of male and female mice before and after 10 weeks of a cholesterol-rich 'western' diet starting from 6-8 weeks. p38α^{MY-KO}/ ApoE $^{-/-}$ males, n= 9; ApoE$^{-/-}$ males, n= 15; p38α^{MY-KO}/ ApoE $^{-/-}$ females, n= 8; ApoE$^{-/-}$ females, n= 9. Error bars represent SD.

After 10 weeks on a western diet, mice were sacrificed, and atherosclerotic lesion development was assessed in the whole aorta by *en face* Sudan IV staining (Fig. 13), but also at the aortic sinus by histological analysis of consecutive sections followed by cross-sectional plaque area quantification (Fig. 14). This analysis did not reveal any differences in lesion size between male and female p38α^{MY-KO}/ApoE$^{-/-}$ and their ApoE$^{-/-}$ littermates, either in the whole aorta or in the aortic sinuses.

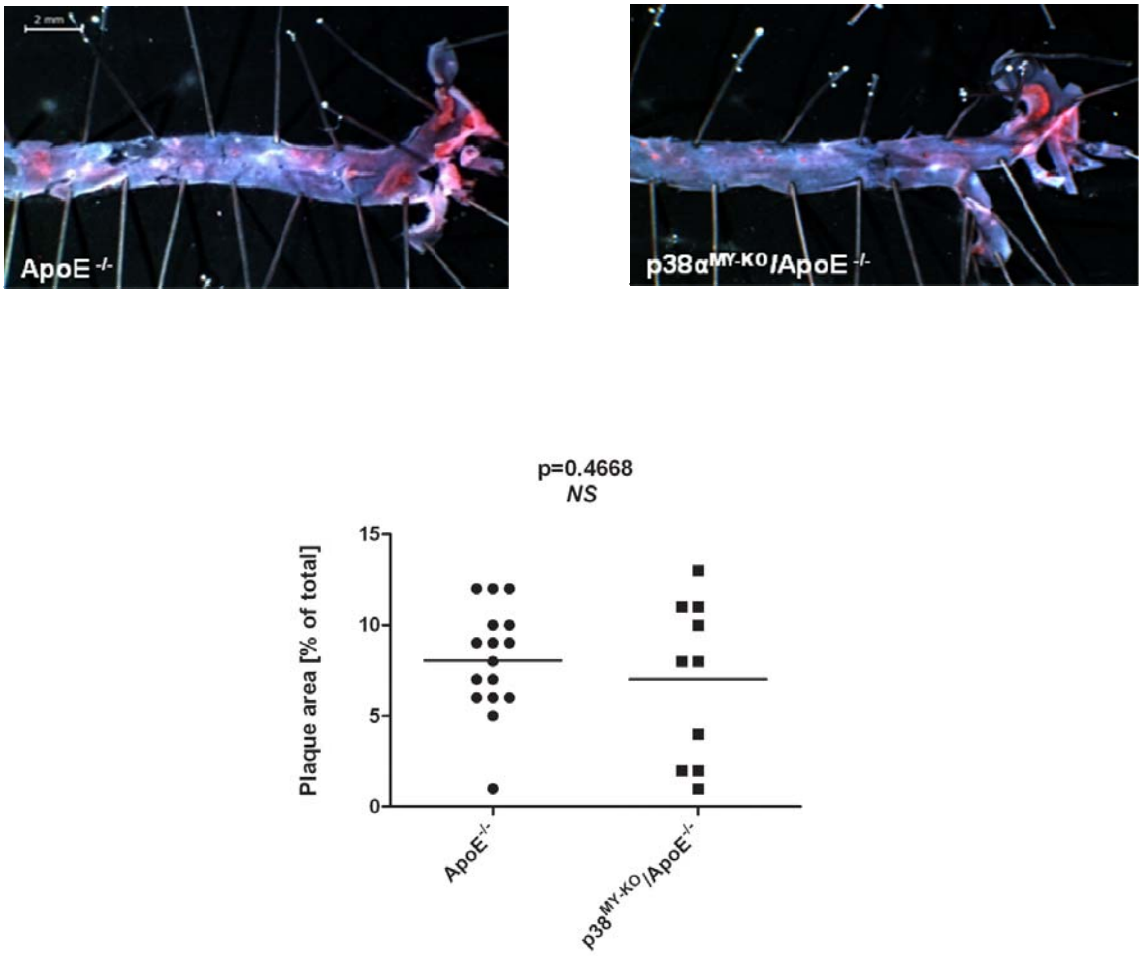

Figure 13. Deficiency of p38α MAPK in macrophages does not affect lesion development in the aorta of p38α^{MY-KO}/ApoE$^{-/-}$ mice. Quantification of atherosclerotic plaque size on whole aorta from male p38α^{MY-KO}/ ApoE$^{-/-}$ and ApoE$^{-/-}$ mice. *En face* Sudan IV staining of lesions. Scale bar 2 mm**.** p38α^{MY-KO}/ ApoE $^{-/-}$ males, n= 9; ApoE$^{-/-}$ males, n= 15. Error bars represent SD.

Females

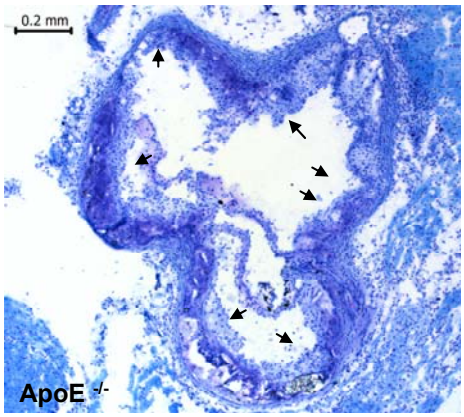

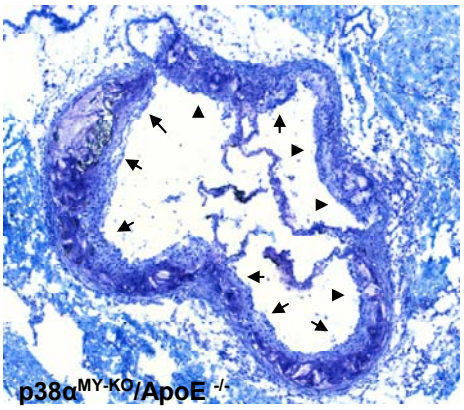

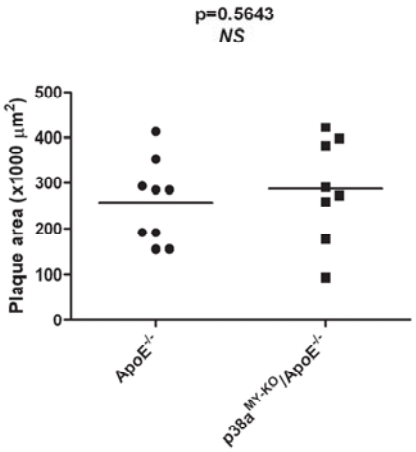

Males

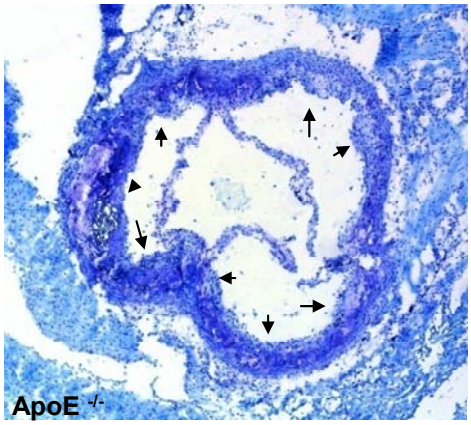

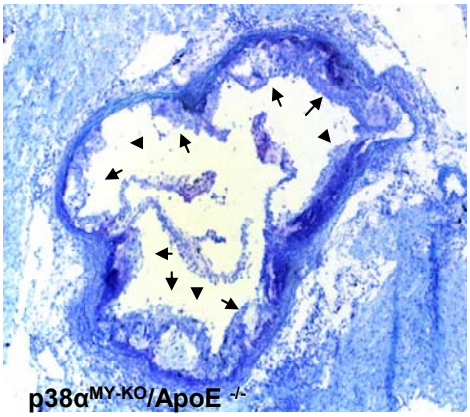

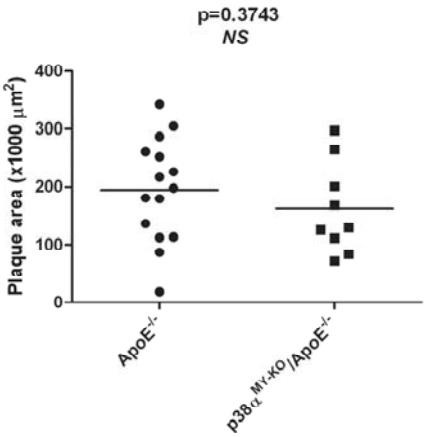

Figure 14. Deficiency of p38α MAPK in macrophages does not affect atherosclerosis development at the aortic sinus of p38α^{MY-KO}/ApoE$^{-/-}$ mice. Quantification of the lesion area of atherosclerotic plaques at the aortic sinus of p38α^{MY-KO}/ApoE$^{-/-}$ and ApoE$^{-/-}$ female (A) and male (B) mice. Plaques are marked by arrows on aortal cross sections at the height of the aortic sinus. p38α^{MY-KO}/ApoE$^{-/-}$ males, n= 9; ApoE$^{-/-}$ males, n= 15; p38α^{MY-KO}/ApoE$^{-/-}$ females, n= 8; ApoE-/- females, n= 9. Error bars represent SD.Scale bar, 0.2 mm.

To further characterize the lesions at the aortic sinus in these mice, we stained and quantified collagen content (Fig. 15A), foam cell content (Fig. 15B) and necrotic core formation (Fig. 15C), since it had previously been observed that atherosclerotic lesions in p38α^{MY-KO}/ApoE$^{-/-}$ mice appear to be more advanced compared to ApoE$^{-/-}$ mice even though plaque size is not altered. More specifically, these mice were characterized by increased lesional necrosis and decreased collagen content compared to ApoE$^{-/-}$ mice [149]. However, in our case, this analysis did not reveal any differences either in collagen content (Fig. 15A) or lesional necrosis (Fig. 15C), after quantification at the aortic sinus. We also did not observe any differences in foam cell content (Fig. 15B), between the two genotypes. Finally, p38α MAPK has been shown to regulate the expression of many genes involved in the initiation and progression of atherosclerotic lesions, including cytokines like TNF and IL-6, chemokines like IL-8 and adhesion molecules like VCAM-1 and ICAM-1[7,61,70,150,151], an effect thought to be mediated via a mechanism involving messenger RNA turnover and protein translation[3,61]. Thus, we tested with real-time PCR (qRT-PCR) the expression of a panel of cytokines chemokines and adhesion molecules on RNA isolated from the aortic arch of p38α^{MY-KO}/ApoE$^{-/-}$ and their ApoE$^{-/-}$ littermates after 10 weeks on a ‘western’ diet. Although we observed a slight upregulation in most of the genes tested, there were no statistically significant differences in any of these genes (Fig. 16). Thus, we can conclude that p38α MAPK signaling in macrophages does not play a significant role in the development of atherosclerosis, in the ApoE deficient mouse model.

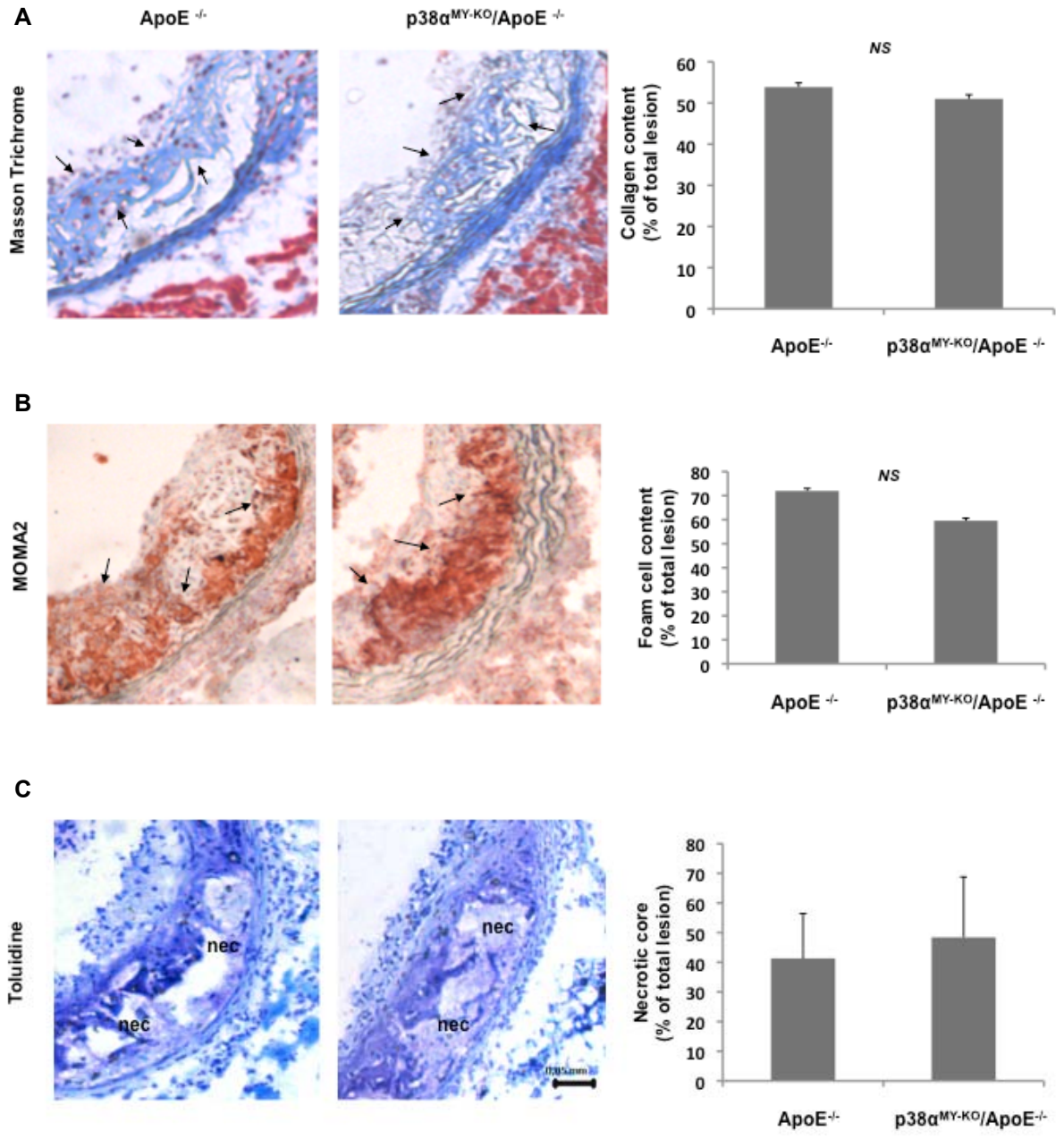

Figure 15. Similar plaque characteristics in p38α^{MY-KO}/ ApoE$^{-/-}$ and ApoE$^{-/-}$ mice

(A) Quantification of collagen content (Masson Trichrome staining) at the aortic sinus of p38α^{MY-KO}/ ApoE$^{-/-}$ and ApoE$^{-/-}$ mice. Collagen fibers (blue) indicated by arrows. p38α^{MY-KO}/ ApoE$^{-/-}$ females, n= 6; ApoE-/- females, n= 6. (B) Quantification of foam cell content (MOMA2 staining) at the aortic sinus of p38α^{MY-KO}/ ApoE$^{-/-}$ and ApoE$^{-/-}$ mice. Foam cells (red) indicated by arrows. p38α^{MY-KO}/ ApoE$^{-/-}$ females, n= 6; ApoE$^{-/-}$ females, n= 6. (C) Quantification of necrotic core formation at the aortic sinus of p38α^{MY-KO}/ ApoE$^{-/-}$ and ApoE$^{-/-}$ mice (nec=necrosis). p38α^{MY-KO}/ ApoE$^{-/-}$ females, n= 8; ApoE$^{-/-}$ females, n= 9. Error bars represent SD.

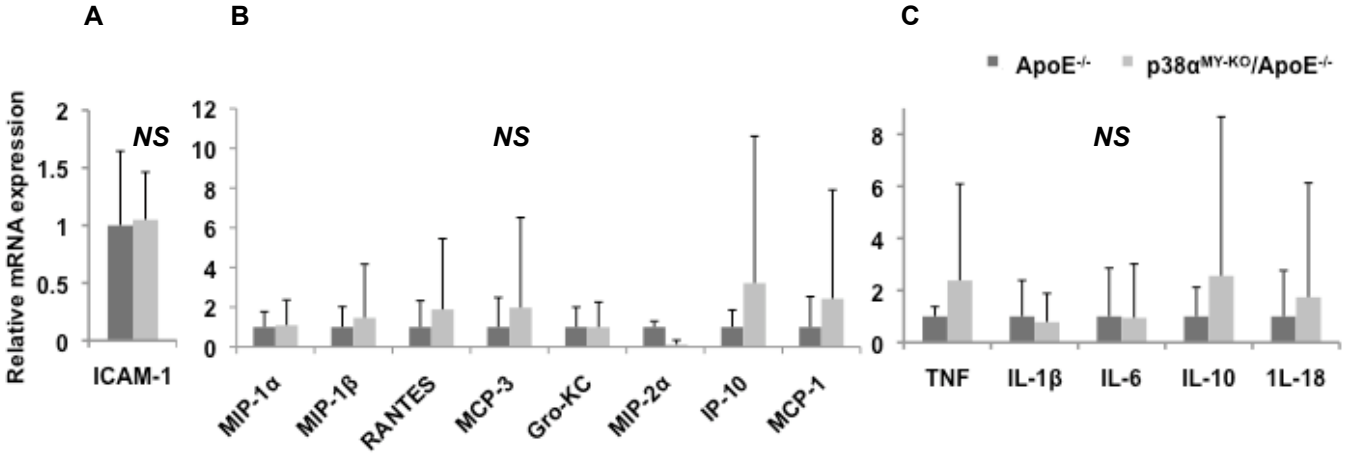

Figure 16. Similar mRNA expression of proinflammatory cytokines, chemokines and adhesion molecules in p38α^{MY-KO}/ ApoE$^{-/-}$ and ApoE$^{-/-}$ mice. Relative mRNA levels of adhesion molecules (A), proinflammatory cytokines (B) and chemokines (C) in aortal arches from p38α^{MY-KO}/ApoE$^{-/-}$ and ApoE$^{-/-}$ mice after 10 weeks on a cholesterol rich 'western' diet. p38α^{MY-KO}/ApoE$^{-/-}$ females, n= 8; ApoE$^{-/-}$ females, n= 9.Error bars represent SD.

2.1.2 Endothelial-Cell Specific Role of p38α MAPK in Atherosclerosis

2.1.2.1 Generation of Endothelial-Specific p38α Knockout Mice in an ApoE Deficient Background

In order to address the endothelial-specific *in vivo* role of p38α MAPK in atherosclerosis, we generated mice with specific ablation of p38α in endothelial cells, in the ApoE-deficient genetic background ($p38\alpha^{EC\text{-}KO}$/ $ApoE^{-/-}$). This was accomplished by crossing $p38\alpha^{FL/FL}$ mice with mice expressing a tamoxifen-inducible Cre transgene fused to a mutated estrogen receptor ligand-binding domain known as ER^{T2} ($Tie2CreER^{T2}$) (Fig. 17). Expression of Cre in this form is inactive and only becomes active upon treatment with tamoxifen [74].

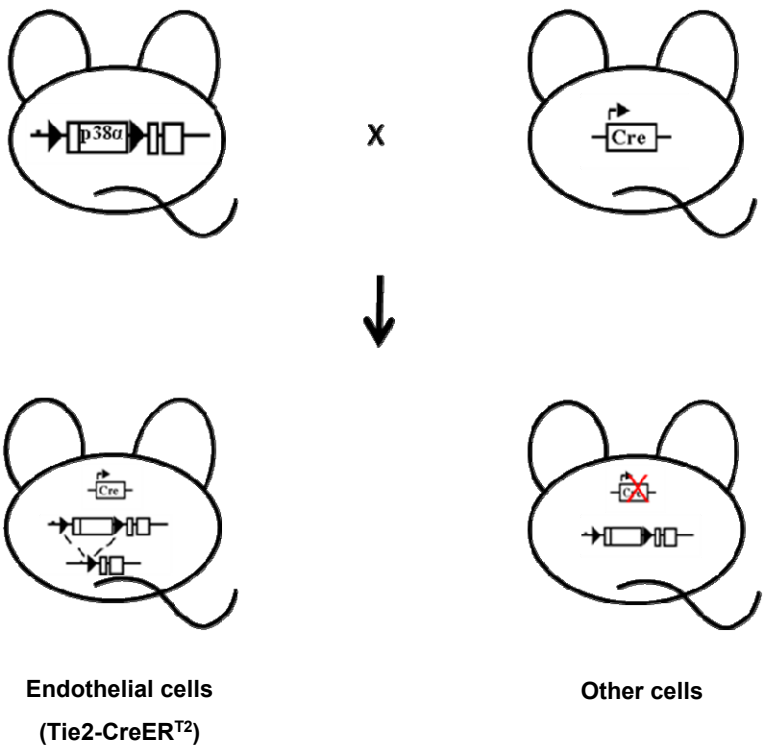

Figure 17. Strategy for the generation of endothelial–specific p38α MAPK knockout mice. Endothelial-specific knockout mice were generated by crossing $p38\alpha^{FL/FL}$ mice with $Tie2CreER^{T2}$ mice.

2.1.2.2 Efficient Ablation and Diminished Activation of p38α MAPK in Endothelial Cells of p38α^{EC-KO}/ ApoE$^{-/-}$ Mice

To assess the efficiency of p38α MAPK ablation we measured expression of this protein in primary lung endothelial cells by immunoblotting. Primary lung endothelial cells were isolated from dissociated lung tissue isolated from groups of 6-8 week old p38α^{EC-KO}/ApoE$^{-/-}$ and their p38α$^{FL/FL}$/ApoE$^{-/-}$ littermates that did not carry the Tie2-CreER^{T2} transgene. These mice had previously been fed a tamoxifen containing diet (400mg/kg tamoxifen citrate, 5% sucrose in phytoestrogen-free chow) for 5 consecutive weeks to induce Cre-mediated excision of the p38α loxP-flanked allele in endothelial cells [152], followed by 10 weeks on a cholesterol rich 'western diet' to promote atherosclerosis development. MACS (Magnetic Cell Sorting) was used to enrich the CD146^{+} endothelial cell fraction. Immunoblot analysis of protein lysates from whole lung, CD146^{+} and CD146^{-} cell fractions showed efficient ablation of p38α MAPK in endothelial cell isolates from p38α^{EC-KO}/ApoE$^{-/-}$ mice taken at the end of the 10 week period of 'western diet' feeding (Fig. 18). In order to study p38α MAPK activation in endothelial cells with p38α deficiency, we isolated lung primary endothelial cells from p38α$^{FL/FL}$/ApoE$^{-/-}$ mice and used His-TAT-NLS-Cre (HTNC), a transducible Cre recombinase that can be used efficiently to mediate recombination of loxP flanked alleles in cultured cells [153,154], to induce cre recombination and thus p38α deletion in these cells. As can be seen from figure 19B, immunobloting for p38α in endothelial cells after HTNC treatment, showed efficient ablation of this protein. Stimulation of lung endothelial cells *in vitro* with 100μg/ml oxLDL, treated (+HTNC) or untreated (-HTNC) with HTNC, showed very low levels of total p38 activation in cells positive for Cre recombination compared to wild-type (untreated) cells (Fig. 19B). Purity of endothelial cell cultures was assessed by FACS analysis after staining with CD146 (Fig. 19A). Taken together, these results indicate that the mouse models generated were sufficient for the purpose of this study.

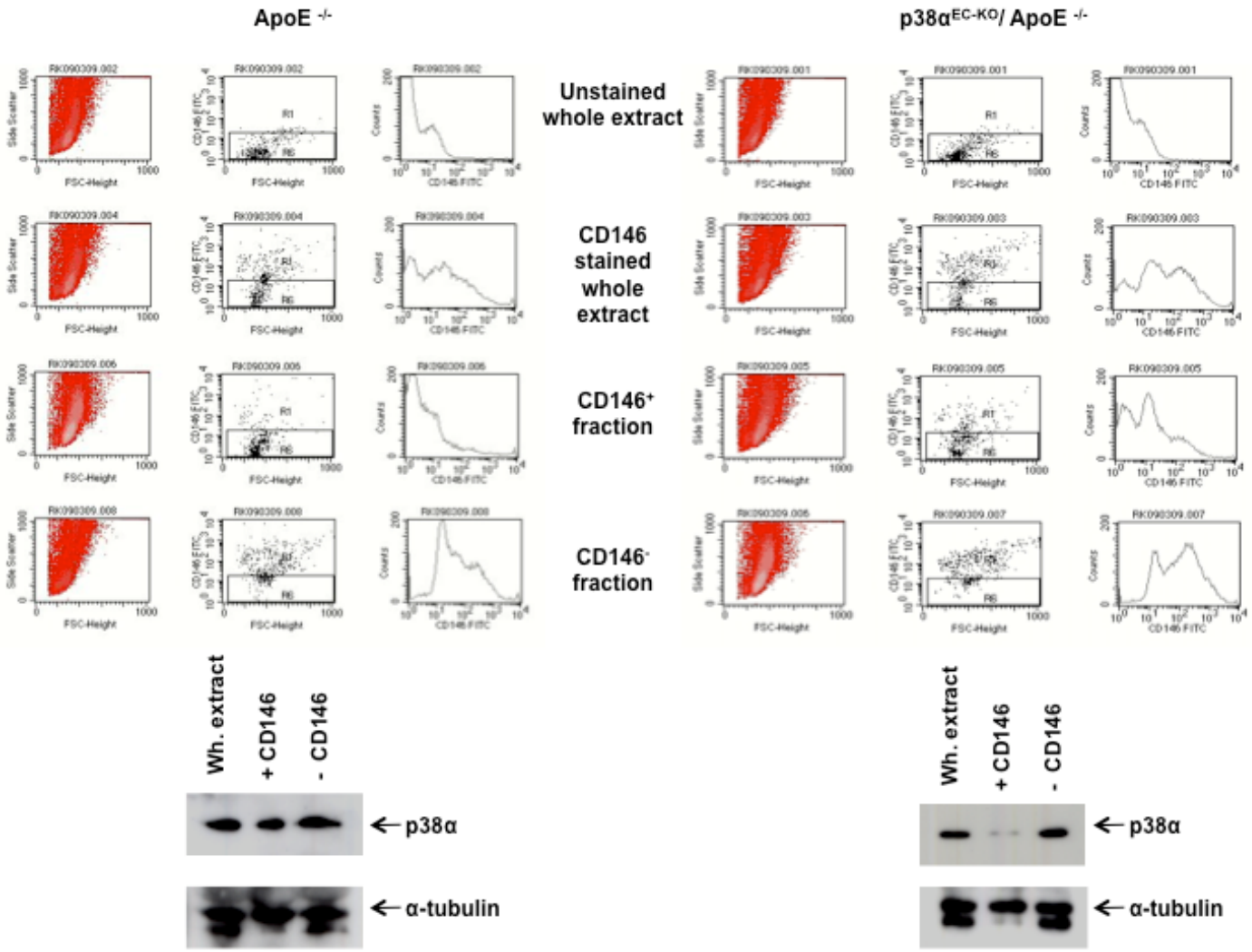

Figure 18. Deletion efficiency of p38α MAPK in primary lung endothelial cells after 10 weeks of a cholesterol rich 'western diet'. Analysis of deletion efficiency in endothelial-specific knockout mice after 5 weeks of a tamoxifen diet and 10 weeks of a cholesterol-rich 'western diet' by MACS sorting with the mouse endothelial cell marker CD146. FACS analysis of lung cell suspensions showed efficient separation of $CD146^{+}$ (positive) and $CD146^{-}$ (negative) fractions, whereas immmunoblotting of cell extracts from each sorting step showed efficient ablation of p38α in $p38α^{EC-KO}$/ApoE $^{-/-}$ mice compared to ApoE $^{-/-}$ mice. $p38^{EC-KO}$/$ApoE^{-/-}$ females, n= 9; $ApoE^{-/-}$ females, n= 6.

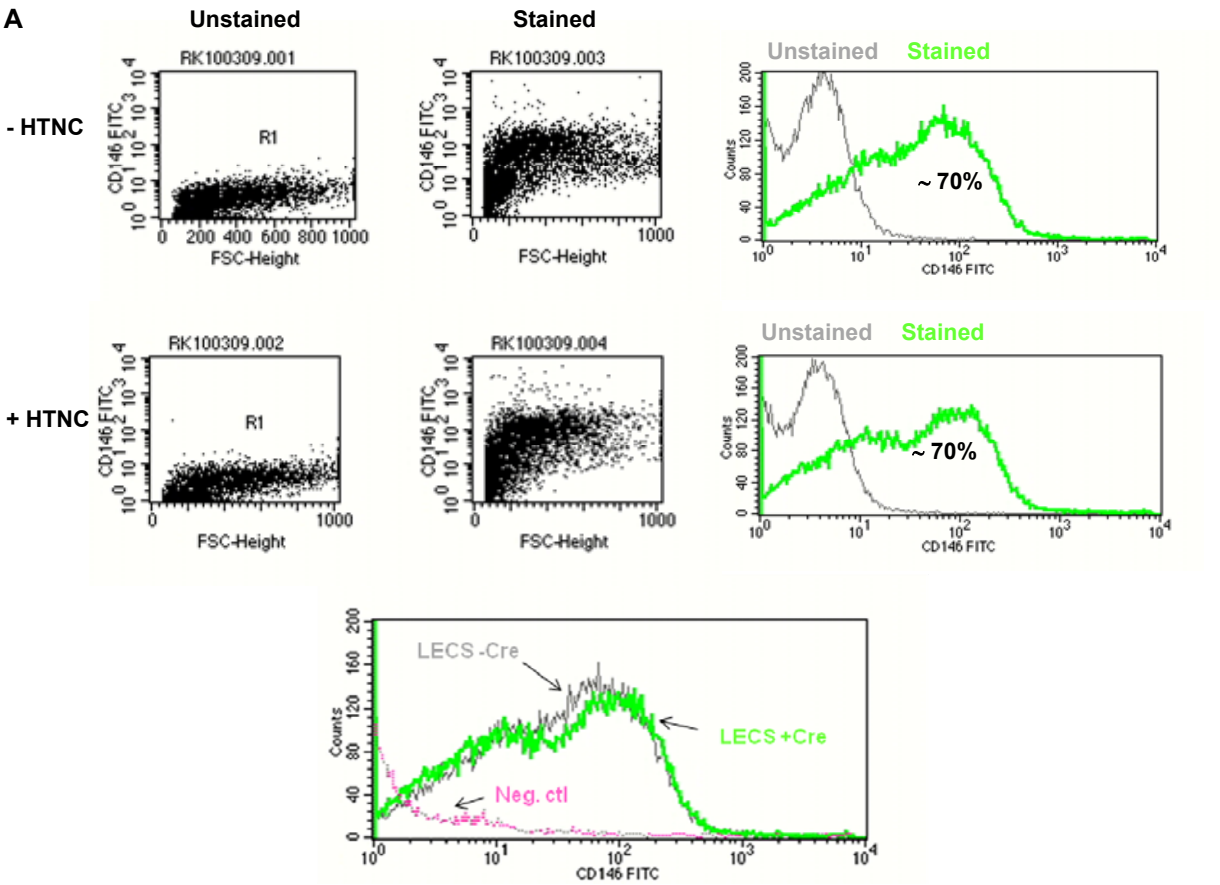

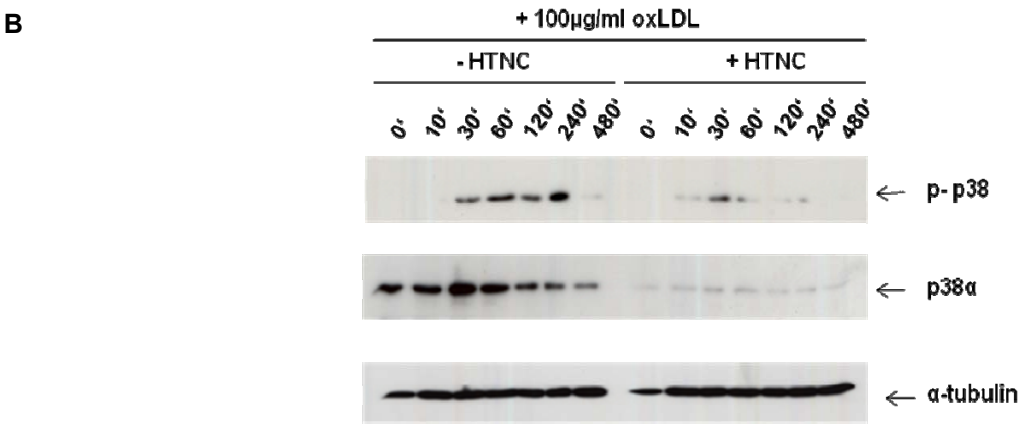

Figure 19. Efficient ablation of p38α MAPK and total p38 activation in HTNC treated p38α$^{FL/FL}$/ApoE$^{-/-}$ endothelial cells, *in vitro.* (A) FACS analysis of primary lung endothelial cells to check for purity of population, after treatment with HTNC for 16hrs at passage 8. Both HTNC treated and untreated populations showed ~70% purity for endothelial cells, when stained with the mouse endothelial cell marker CD146.(B) Immunoblotting for p38α and total p-p38 on lung endothelial extracts after stimulation with 100µg/ml oxLDL for the indicated timepoints showed strong reduction in total p38 activation and p38α expression. Cells were isolated from the lung of p38α$^{FL/FL}$/ApoE$^{-/-}$ mice and either treated or not treated with HTNC for 16hrs to induce cre recombination of p38α. Cells were passaged twice before stimulation.

2.1.2.3 *In vitro* Stimulation of Lung Primary Endothelial Cells with OxLDL Showed a Clear Reduction in Adhesion Molecule and Chemokine Expression in the Absence of p38α MAPK

In order to study the effect of p38α MAPK in endothelial cells with respect to atherosclerosis, we isolated primary lung endothelial cells from p38$\alpha^{FL/FL}$/ApoE$^{-/-}$ and treated them with HTNC as described above, to induce cre recombination of the p38α loxP flanked alleles. After assessing the purity and p38α ablation of these *in vitro* cultures (Fig.19A and B, respectively), we stimulated these cells with oxLDL (100μg/ml) for various timepoints, up to 48hrs. We then examined the expression of various chemokines and adhesion molecules that are implicated in atherosclerosis development, and have been previously reported to be regulated, at least partly, by p38. qRT-PCR for the adhesion molecule VCAM-1, but also the chemokines IP-10, MCP-1 and Gro-KC, which are all involved in the recruitment and uptake of monocytes into the arterial intima, showed a statistically significant reduction for all these molecules, in response to oxLDL (Fig 20). These results indicated an atherogenic role for p38α MAPK, and therefore we hypothesized that ablation of p38α in the endothelium would lead to a significant reduction in atherosclerosis development, compared to wild-type (ApoE$^{-/-}$) mice.

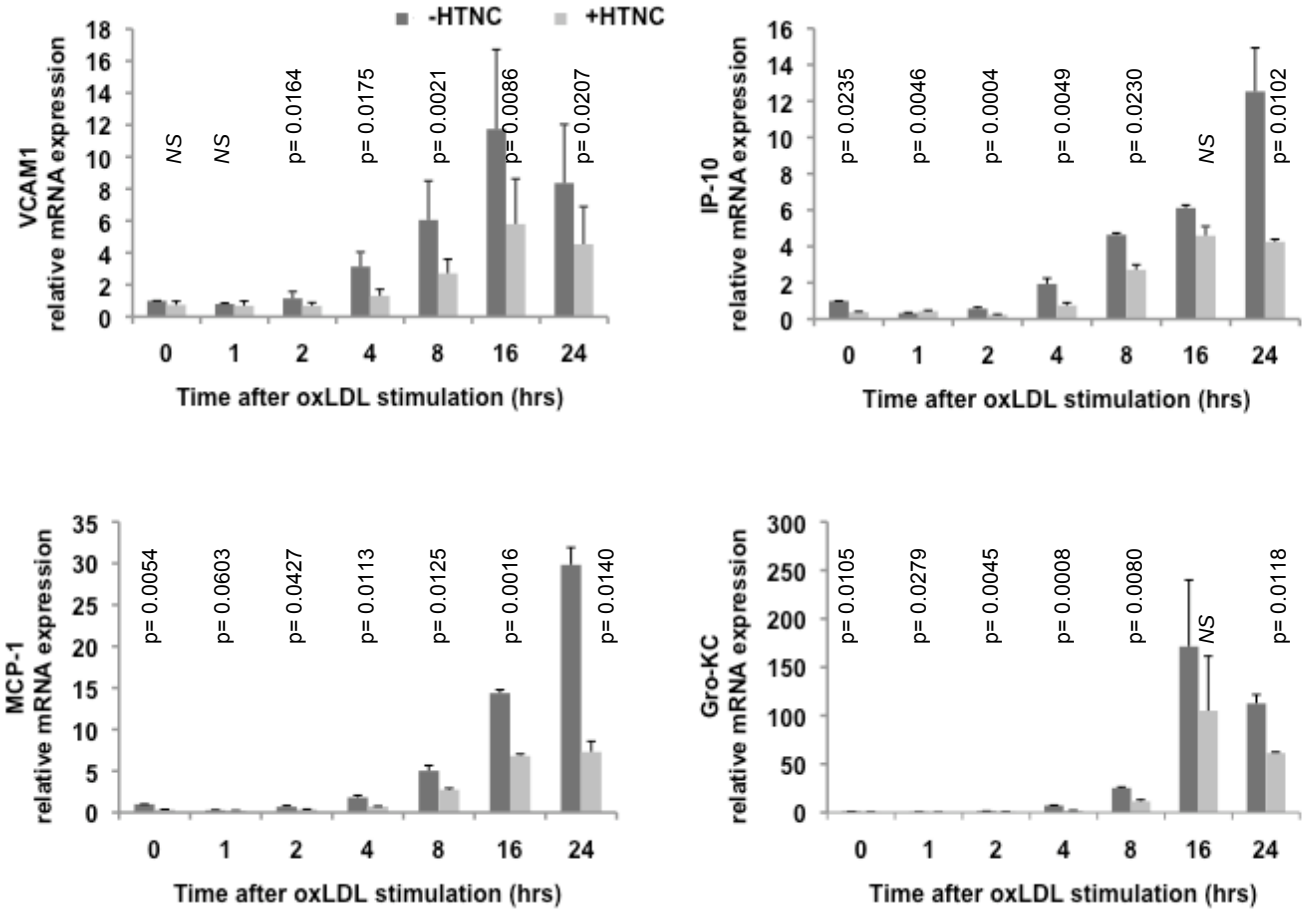

Figure 20. Downregulation of adhesion molecules and cytokines in oxLDL stimulated p38α MAPK knockout endothelial cells, *in vitro*. Relative mRNA expression levels of adhesion molecule VCAM-1 and chemokines IP-10, MCP-1 and Gro-KC in HTNC treated or untreated primary lung endothelial cells isolated from p38α$^{FL/FL}$/ ApoE$^{-/-}$ and ApoE $^{-/-}$ mice stimulated with 100μg/ml oxLDL for the indicated timepoints.

2.1.2.4 *In vitro* Stimulation of Lung Endothelial Cells Showed a Clear Reduction in JNK Signaling in the Absence of p38α MAPK

Since it has been previously shown that ablation of p38α MAPK in many cell types, including macrophages [28, 75], can lead to increased activation of JNK, we decided to also examine the effect on JNK activation when removing p38α MAPK from endothelial cells. This was a concern for us since JNK has also been implicated in atherosclerosis development [155], and its hyperactivation in the absence of MAPK could counterbalance the effect of p38α MAPK ablation. For this reason we stimulated primary lung endothelial cells with oxLDL and examined the phosphorylation of JNK. Immunoblotting for p-JNK showed decreased activation in cells where p38α MAPK had been deleted with prior HTNC treatment (Fig. 21).

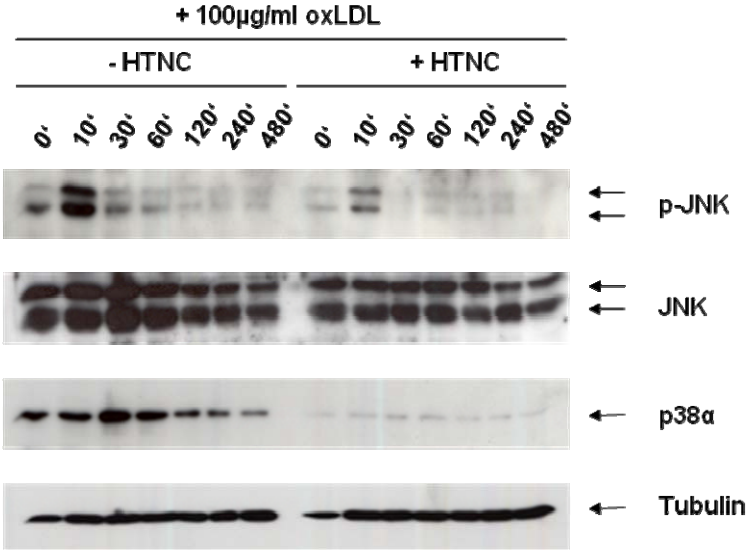

Figure 21. Decreased JNK phosphorylation upon oxLDL stimulation in primary lung endothelial cells, in the absence of p38α MAPK. Immunoblotting with p-JNK on whole cell extracts obtained from $p38^{FL/FL}/ApoE^{-/-}$ primary lung endothelial that had been pre-treated with HTNC to delete p38α MAPK and stimulated with 100µg/ml oxLDL for the indicated timepoints. Cells not treated with HTNC used as wild-type.

2.1.2.5 p38α MAPK Ablation in Vascular Endothelial Cells Does not Affect Atherosclerosis Development or Progression

In order to study the effect of endothelial-specific p38α MAPK ablation on the development of atherosclerosis, we placed groups of male and female p38α^{EC-KO}/ApoE$^{-/-}$ and their ApoE$^{-/-}$ littermates on a tamoxifen based diet for 5 weeks to induce Cre-mediated excision of the loxP-flanked p38α allele in endothelial cells. This was then followed by a cholesterol-rich 'western' diet for 10 weeks. Analysis of cholesterol levels before and after the 'western' diet revealed no differences between the two genotypes, although at week 10 cholesterol levels had increased ~ 3-fold in both male and female littermates (Fig. 22A). Bodyweight increased about 5 gr for males and 10 gr for females on average after 10 weeks of a 'western diet' (Fig. 22B).

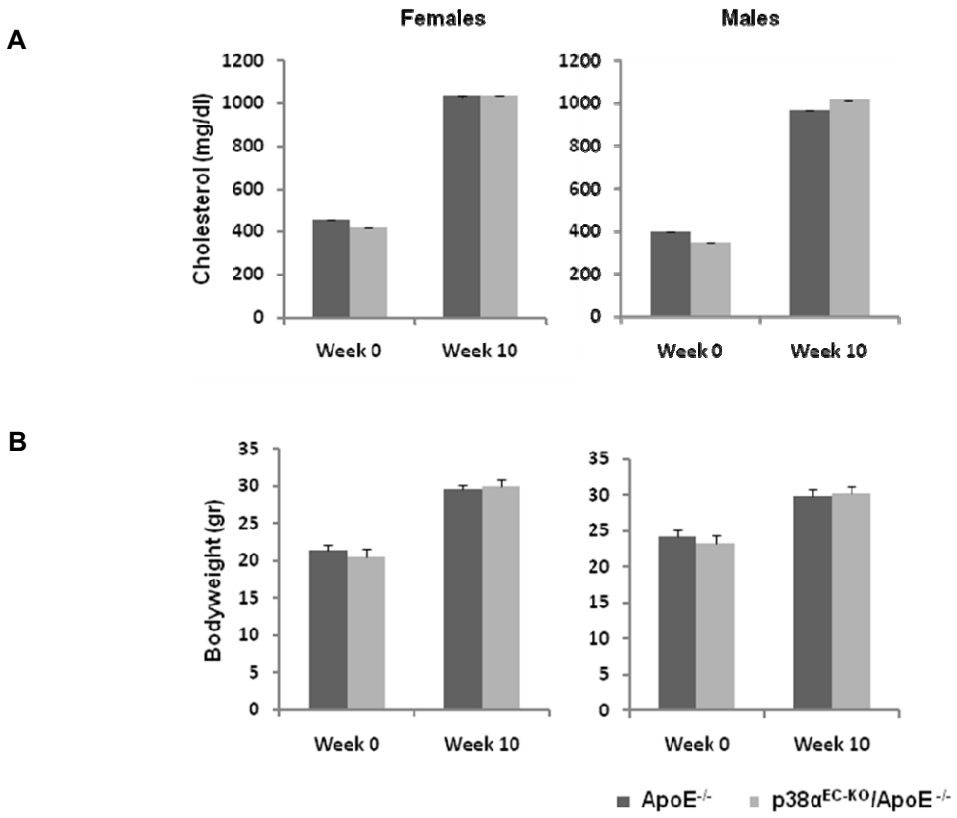

Figure 22. Bodyweight and cholesterol levels of p38α^{EC-KO}/ApoE$^{-/-}$ mice after 10 weeks of a cholesterol rich 'western' diet. (A) Cholesterol (mg/dl) and (B) weight (gr) levels of male and female p38α^{EC-KO}/ApoE$^{-/-}$ and ApoE$^{-/-}$ mice before and after 10 weeks of a cholesterol-rich 'western diet' (previously fed a tamoxifen diet for 5 weeks to induce cre expression). p38α^{EC-KO}/ApoE$^{-/-}$ males, n= 14; ApoE$^{-/-}$ males, n= 15; p38α^{EC-KO}/ApoE$^{-/-}$ females, n= 14; ApoE$^{-/-}$ females, n= 13. Error bars represent SD.

After 10 weeks on the 'western diet', mice were sacrificed and atherosclerotic lesion development was assessed in the whole aorta by *en face* Sudan IV staining (Fig. 23), but also at the aortic sinus by histological analysis of consecutive sections followed by cross-sectional plaque area quantification (Fig. 24). This analysis did not reveal any differences in lesion size between male and female p38α^{EC-KO}/ApoE$^{-/-}$ and ApoE$^{-/-}$ littermates, either in the whole aorta or in the aortic sinuses.

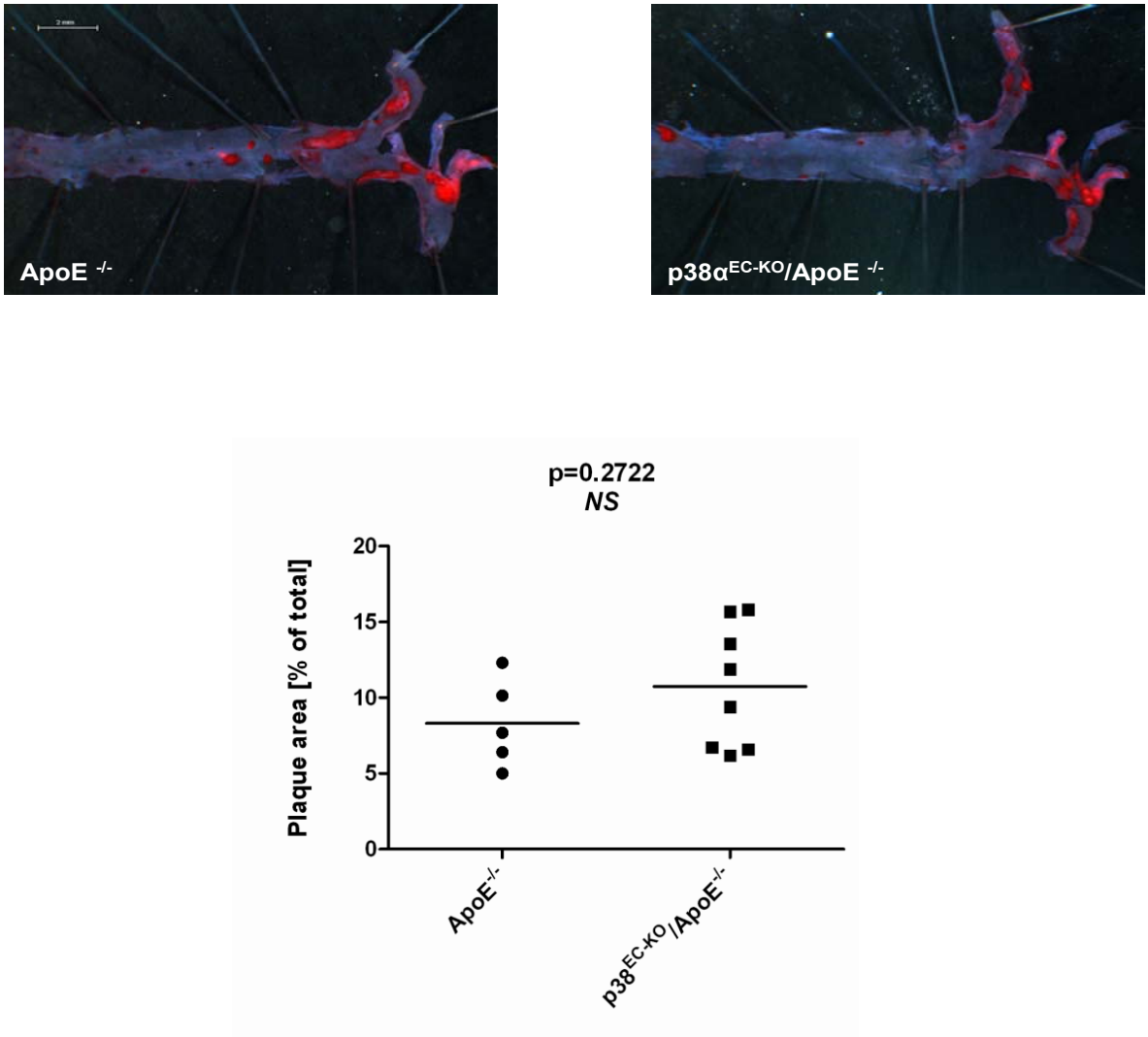

Figure 23. Deficiency of p38α MAPK in endothelial cells does not affect lesion development in the aorta of p38α^{EC-KO}/ApoE$^{-/-}$ mice. Quantification of atherosclerotic plaque size on whole aorta from female p38α^{EC-KO}/ApoE$^{-/-}$ and ApoE$^{-/-}$ mice. *En face* Sudan IV staining of plaques. p38α^{EC-KO}/ApoE$^{-/-}$ females, n= 14; ApoE$^{-/-}$ females, n= 13. Error bars represent SD.Scale bar, 2 mm

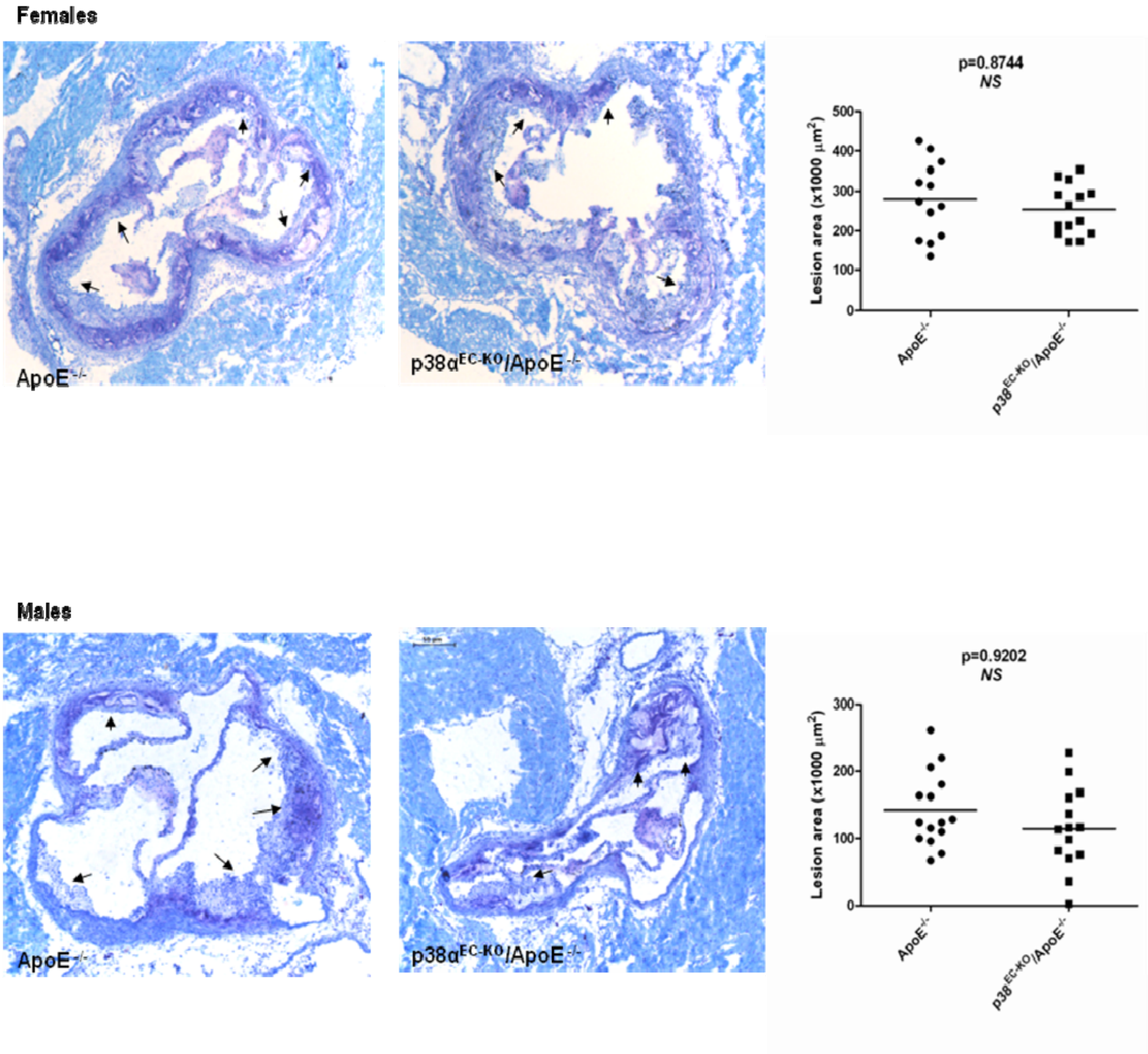

Figure 24. Development of atherosclerotic lesions in the aortic sinus of p38α^{EC-KO}/ApoE$^{-/-}$ mice. Quantification of lesion area on atherosclerotic plaques at the aortic sinus of p38α^{EC-KO}/ApoE $^{-/-}$ and ApoE $^{-/-}$ female (top) and male (bottom) mice. Plaques are marked by arrows on aortal cross sections at the height of the aortic sinus. p38α^{EC-KO}/ ApoE$^{-/-}$ males, n= 14; ApoE$^{-/-}$ males, n= 15; p38α^{EC-KO}/ ApoE$^{-/-}$ females, n= 14; ApoE$^{-/-}$ females, n= 13. Scale bar, 0.2 mm

QRT-PCR analysis on cDNA from the aortic roots of these mice did not show any significant differences in cytokine, chemokine or adhesion molecule expression (Fig. 25).

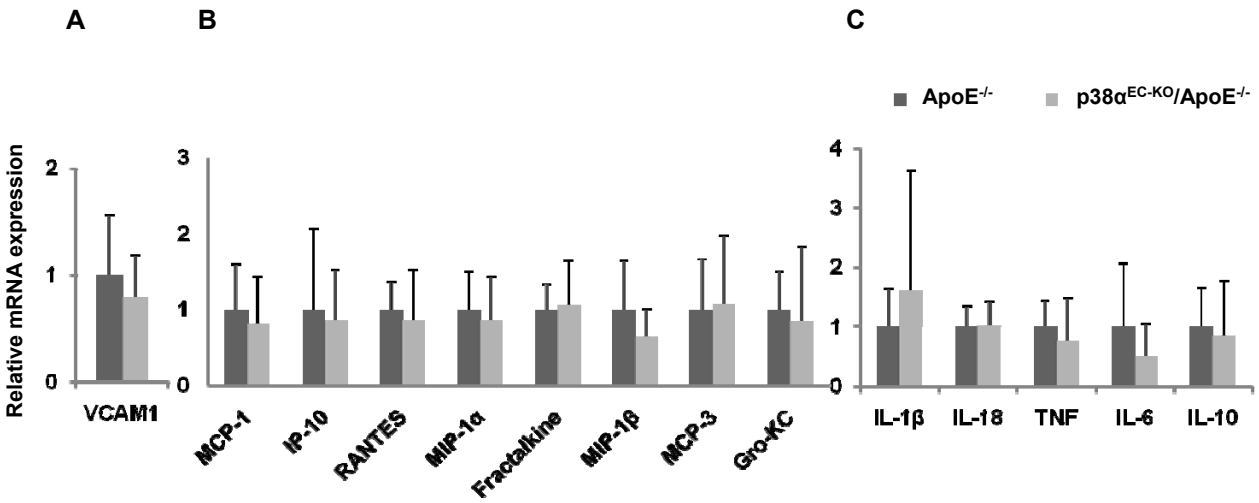

Figure 25. Similar mRNA expression of proinflammatory cytokines, chemokines and adhesion molecules in p38α^{EC-KO}/ApoE$^{-/-}$ and ApoE$^{-/-}$ mice

Relative mRNA levels of adhesion molecules (A), chemokines (B) and proinflammatory cytokines (C) of aortal arches from p38α^{EC-KO}/ApoE$^{-/-}$ and ApoE$^{-/-}$ mice after 10 weeks on western diet. p38α^{EC-KO}/ApoE$^{-/-}$ females, n= 9; ApoE $^{-/-}$ females, n = 6.Error bars represent SD.

To further characterize the progression of atherosclerotic lesions at the aortic sinus in these mice, we quantified collagen content (Fig. 26A), foam cell content (Fig. 26B) and necrotic core formation (Fig. 26C). This analysis showed that atherosclerotic plaques in p38α^{EC-KO}/ApoE$^{-/-}$ and their ApoE$^{-/-}$ littermates both developed at similar rates with neither of the genotypes showing more or less advanced lesions. So, from these results, and contrary to what we hypothesized based on our *in vitro* experiments, we can conclude that specific ablation of p38α MAPK *in vivo* does not affect the development and progression of atherosclerosis in the ApoE$^{-/-}$ mouse model.

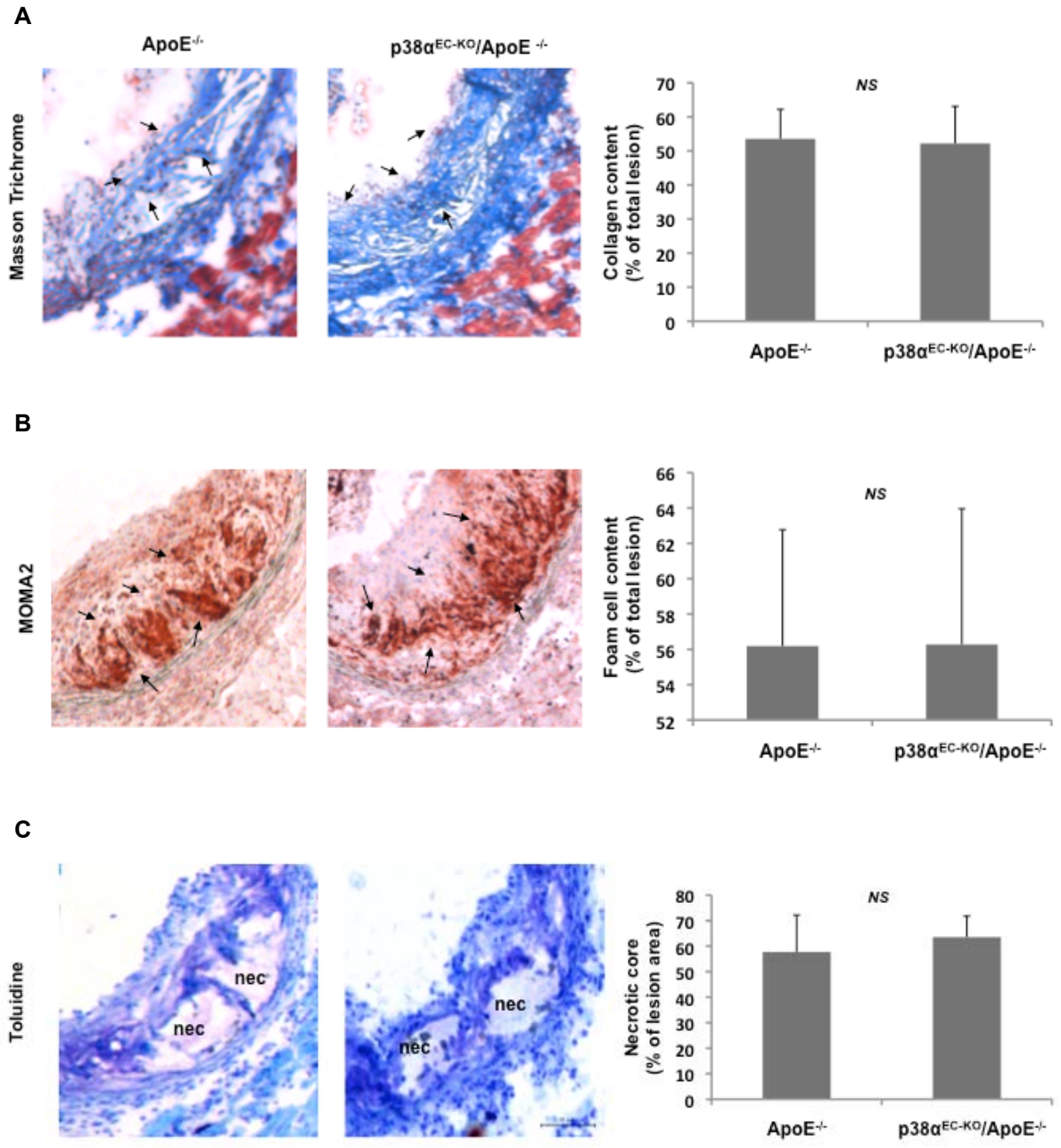

Figure 26. Similar lesion characteristics in atherosclerotic plaques of p38α^{EC-KO}/ApoE$^{-/-}$ and ApoE$^{-/-}$ mice. (A) Quantification of collagen content (Masson Trichrome staining) at the aortic sinus of p38α^{EC-KO}/ApoE$^{-/-}$ and ApoE$^{-/-}$ mice. Collagen fibers (blue) indicated by arrows. p38α^{EC-KO}/ApoE$^{-/-}$ females, n= 9; ApoE$^{-/-}$ females, n = 6. (B) Quantification of foam cell content (MOMA2 staining) at the aortic sinus of p38α^{EC-KO}/ApoE$^{-/-}$ and ApoE$^{-/-}$ mice. Foam cells (red) indicated by arrows. p38α^{EC-KO}/Apo$^{-/-}$ females, n= 9; ApoE$^{-/-}$ females, n = 6. (C) Quantification of necrotic core formation at the aortic sinus of p38α^{EC-KO}/ApoE$^{-/-}$ mice (nec=necrosis). p38α^{EC-KO}/ApoE $^{-/-}$ females, n= 9; ApoE$^{-/-}$ females, n = 6. Error bars represent SD.

2.2 Generation of p38αCA (Constitutively Active) and p38αKD (Kinase Dead) Mice

2.2.1 Generation of p38αCA (Constitutively Active) Mice

In order to produce knock-in mice expressing a constitutively active form of p38α MAPK we generated mutant forms of this kinase, by inserting point-mutations into the mouse p38α cDNA, based on a recent study involving the homologous yeast protein Hog1. In this study random mutagenesis of the *Hog1* gene generated hyperactive forms of this protein [146]. Combination of these mutations gave mutants with a 70-100 fold increase in activity [156]. The most active form of p38α MAPK was used to generate the constitutively active mice by taking advantage of the ROSA26 targeting vector that allows the insertion of a transgene into the ROSA26 locus and its ubiquitous expression.

2.2.1.1 DpnI Mutagenesis of the Mouse p38α MAPK cDNA to Generate Hyperactive Mutants

The mouse p38α MAPK (MAPK14) cDNA, obtained from the laboratory of Roger Davies (pCMV5-p38α vector), was PCR-amplified with primers containing BamHI restriction sites (see methods), and subcloned into the pGEX-2T vector (Appendix IV), which is a GST gene fusion vector that can be used for inducible, high-level intracellular expression of genes as fusions with glutathione S-transferase. Five different mutants of p38α MAPK were generated using DpnI (endonuclease specific for methylated DNA) mutagenesis and the pGEX-2T/p38α plasmid as a template, based on the previously published hyperactive mutants of the homologous Hog1 yeast protein. From these, three were single point mutations (Table 1) and two were double mutants generated by combining the mutations listed in table 1, D176A/F327L and D176A/Y323L. The mutant plasmids generated from DpnI mutagenesis were transformed into DH5α *E. coli* cells and plated on 10 cm^3 agar plates containing ampicillin (100μg/ml). DNA minipreps were prepared from six colonies, for each mutation, and sequencing allowed us to identify the clones where the correct mutations had been inserted (Fig. 27)

Mutation	Structure domain	Comments
D176A	Close to Thr[174] phosphoacceptor	Conserved residue in human, mouse and yeast
Y323L	Conserved L16 domain	Phe[318] in yeast. Mutant exhibited highest activity
F327L	Conserved L16 domain	Phe[322] in yeast. 70-fold activity in human p38

Table 1. Point mutations that hyperactivate the p38α MAPK yeast homologue, Hog1.
The point mutations listed in the table were selected based on previous random mutagenesis studies with the yeast homologue of p38α MAPK, Hog1. These mutations resulted in hyperactivation of the Hog1 protein.

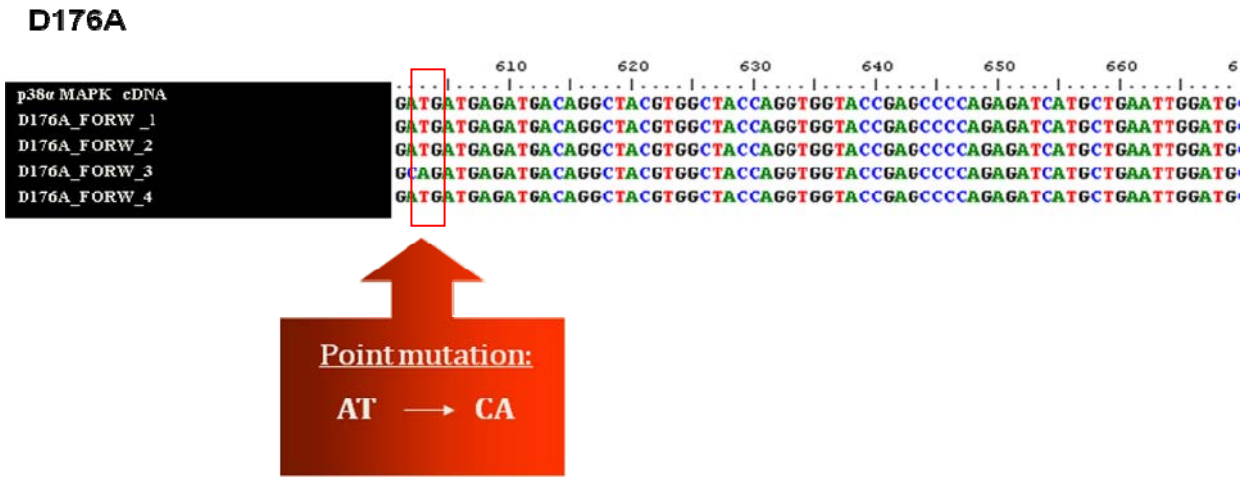

Figure 27. Sequencing of p38α MAPK mutants generated by DpnI mutagenesis. In this figure, sequencing of the D176A mutant is depicted as an example. From the four different clones sequenced, only clone three was positive for the mutation. Alignment with the p38α MAPK cDNA was performed using the program 'BioEdit', which is freely available online.

2.2.1.2 p38α MAPK Mutant GST-Purification from DH5α *E.coli* Cells

Once the clones with the correct point mutations in the p38α MAPK cDNA had been identified, all mutants were overexpressed in DH5α cells by adding 1mM IPTG to induce the *lac* promoter present in the pGEX-2T vector, and allowing the cells to grow at 37˚C for ~ 3hrs until they had reached an O.D. of ~ 0.6-0-7. After 3hrs, cells were centrifuged 10 mins/5000 rpm, the pellets were collected and GST-purification of the p38α MAPK, p38α MAPK mutants and ATF2 (substrate for p38α MAPK) was performed as described in the methods. Elution of the proteins fused to GST was performed with 5x500µl 15mM glutathione (Fig. 28). Samples containing the eluted protein were pooled. As can be seen in the figure, a large amount of the desired GST-tagged protein was lost in the pellet during the clearspin. However, there was still enough protein eluted to carry out kinase assays and examine the activity of the p38α MAPK mutants generated.

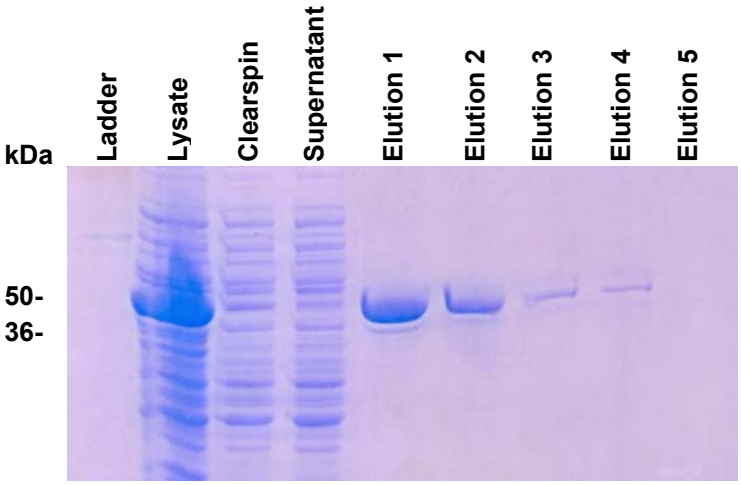

Figure 28. GST purification of p38α MAPK, p38α MAPK mutants and ATF2. In this figure a representative coomasie stained 12 % SDS polyacrylamide gel showing all the steps during the GST purification, is depicted. As can be seen, during the bacterial lysate clearspin a large amount of the desired protein is lost. However, there is still enough protein eluted for the p38 kinase assay to be performed. Elutions 1-4, containing the overexpressed protein, were pooled.

2.2.1.3 p38α Kinase Assay on GST-Purified p38α Mutants to Assess their Activity

In order to assess the activity of the p38α MAPK mutants generated we performed a kinase assay with the GST-purified wild-type and mutant p38α MAPKs. As described

in the introduction, p38α is a kinase that can activate downstream targets, including other kinases like MAPK-activated protein kinase 2 and transcription factors, like ATF2, through phosphorylation. ATP is required for this reaction to take place. In this study, the activity of p38α was assessed by examining the degree of ATF2 phosphorylation by quantifying the incorporation of [γ-^{32}P] ATP in ATF2 using phosphoimaging, as previously described by Jiang, Y. *et al*, 1997 [157]. The reaction was performed by incubating the GST-purified wild-type and mutant p38α MAPKs with GST-ATF2 for 20 mins at 37 °C, in the presence of [γ-^{32}P] ATP. The reactions were then ran on 12% SDS polyacrylamide gels, and subsequently exposed to a phosphoimager. Quantification was performed by using the program 'RANDAMES' that allowed us to quantify the volume of each band in the autoradiograph, but also the coomassie stained gel. By dividing the amount of phosphorylated ATF2 as measured from the autoradiograph, with the total amount of ATF2 as measured from the coomassie stained gel, we identified the p38α mutant D176A/Y323L as the most active one (Fig. 29) From this activity assay we also identified a p38α mutant that was less active than the wild-type p38α MAPK, mutant Y323L.

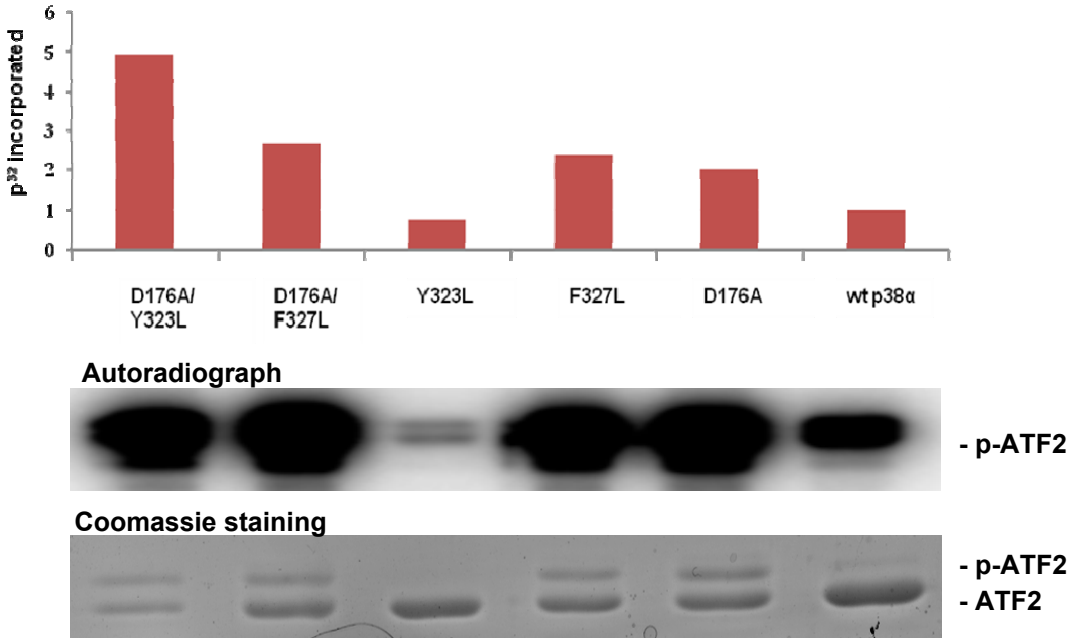

Figure 29. p38α MAPK kinase assay. The activity of the p38α MAPK mutants was assessed by quantifying the incorporation of [γ-^{32}P] ATP into ATF2 in the presence of GST-purified wild-type p38α and mutants. From this assay the mutant D176A/Y323L was revealed as the most active. Mutant Y323L appeared to be less active than wild-type p38α. This is a representative experiment of three.

2.2.1.4 Dual-Luciferase ATF2 Reporter Assay to Assess Mutant Activity in Mammalian (HEK293) Cells

After quantifying the activity of the p38α mutants overexpressed in *E.coli* cells, we went on to analyse their activity in mammalian cells. For this reason, we subcloned the wild-type and p38α mutants into the mammalian vector pIRESpuro, (see Appendix IV), which promotes the stable expression of the gene of interest over time in culture. In order to subclone wild-type p38α and the p38α mutant cDNA into the pIRESpuro vector we used a BamHI digestion. Clones with the correct orientation of the insert were selected by digesting with EcoRI (Fig. 30).

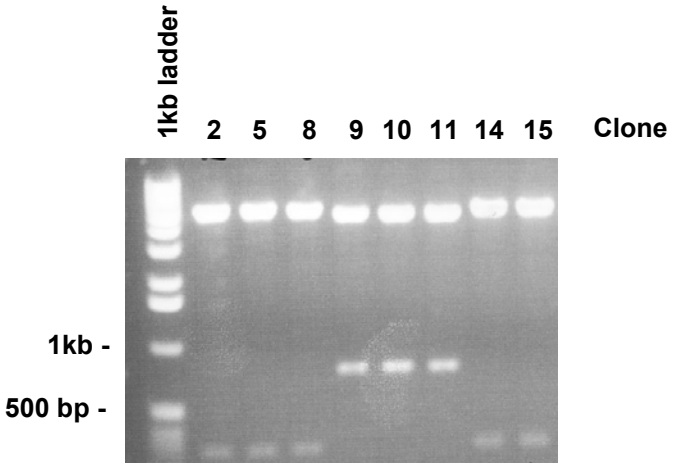

Figure 30. Subcloning of wild-type p38α and mutants into the pIRESpuro vector. EcoRI digestion was used to confirm the correct orientation of the wild-type and mutant p38α cDNA subcloned into the pIRESpuro vector. In the figure clones 2, 5, 8, 14 and 15 have the correct orientation. Correct orientation=5934 & 306 bp, Wrong orientation= 5440 & 800 bp.

The activity of the mutant forms of p38α compared to wild-type, in mammalian cells, was assessed by performing ATF2 reporter assays [158]. This reporter system is composed of the transcription factor GAL-ATF2 and the GAL4-driven firefly luciferase reporter gene (LUC), on different constructs. Higher p38α activity leads to increased luciferase expression. HEK293 (Human Embryonic Kidney Cells) cells were cotransfected with wild-type p38α or a mutant form, the two constructs of the firefly luciferase reporter system, and a control renilla luciferase reporter vector used to normalize experimental variations. From this dual-luciferase reporter assay, we confirmed the result we had seen previously, i.e. that the mutant form of p38α, D176A/Y323L has the highest activity, compared to wild-type p38α (Fig. 31). Activity

in all experiments for this mutant was between 3 & 5-fold higher than wild-type p38α MAPK.

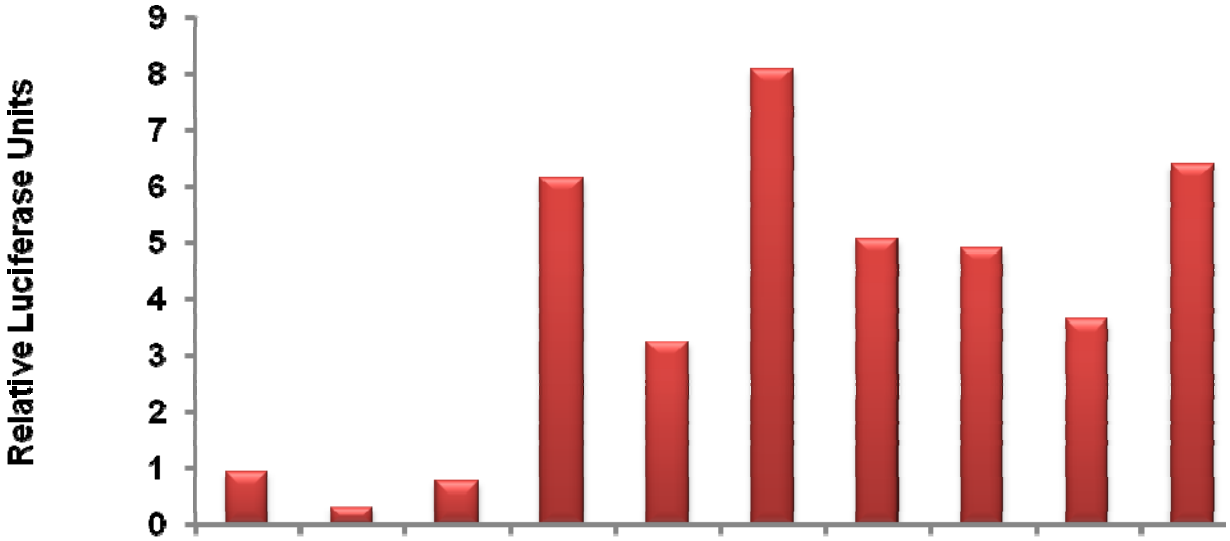

ATF2-GAL	-	+	-	+	+	+	+	+	+	+
GAL-LUC	+	-	+	+	+	+	+	+	+	+
Renilla	+	+	+	+	+	+	+	+	+	+
wt p38α	+	+	-	-	+	-	-	-	-	-
D176A	-	-	-	-	-	-	-	-	-	+
Y323L	-	-	-	-	-	-	-	-	+	-
F327L	-	-	-	-	-	-	-	+	-	-
D176A/Y323L	-	-	-	-	-	+	-	-	-	-
D176A/F327L	-	-	-	-	-	-	+	-	-	

Figure 31. Dual-luciferase ATF2 reporter assay. A dual-luciferase reporter assay was carried out in HEK293 cells to evaluate the activity of the previously generated p38α mutants, in mammalian cells. Cells were cotransfected with either wild-type p38α or a mutant form, the two constructs of the firefly luciferase reporter system (ATF2-GAL and GAL-LUC), and a control renilla luciferase reporter vector used to normalize experimental variations. The mutant with the highest activity was found to be D176A/Y323L.

2.2.1.5 Subcloning of the p38α Mutant D176A/Y323L into the ROSA26-CAGS Targeting Vector to Generate the p38αCA Targeting Construct

Once we had confirmed that the mutant form of p38α, D176A/Y323L, was the one with the highest activity compared to wt p38α, the cDNA was subcloned into the ROSA26-CAGS targeting vector: This vector allows targeting of a desired transgene to the ROSA26 locus, from where it can be expressed ubiquitously in the whole body

of a mouse under the control of a CAGS promoter [159]. Furthermore, since the transgene is placed after a transcriptional STOP cassette, which is flanked by two loxP sites, it can only be expressed in the presence of a Cre recombinase. Therefore, this construct allows for temporal control of transgene expression (Fig. 32, top). Subcloning into this targeting vector was achieved by amplifying the mutant p38α cDNA with primers that had been designed to insert AscI sites at the 5' and 3' end. This fragment was then inserted into the AscI site of the targeting vector, which is positioned on the 3' end of the loxP flanked STOP cassette (Fig. 32, top). Orientation of the inserted gene was examined through restriction digestion with EcoRI (Fig. 32, bottom)

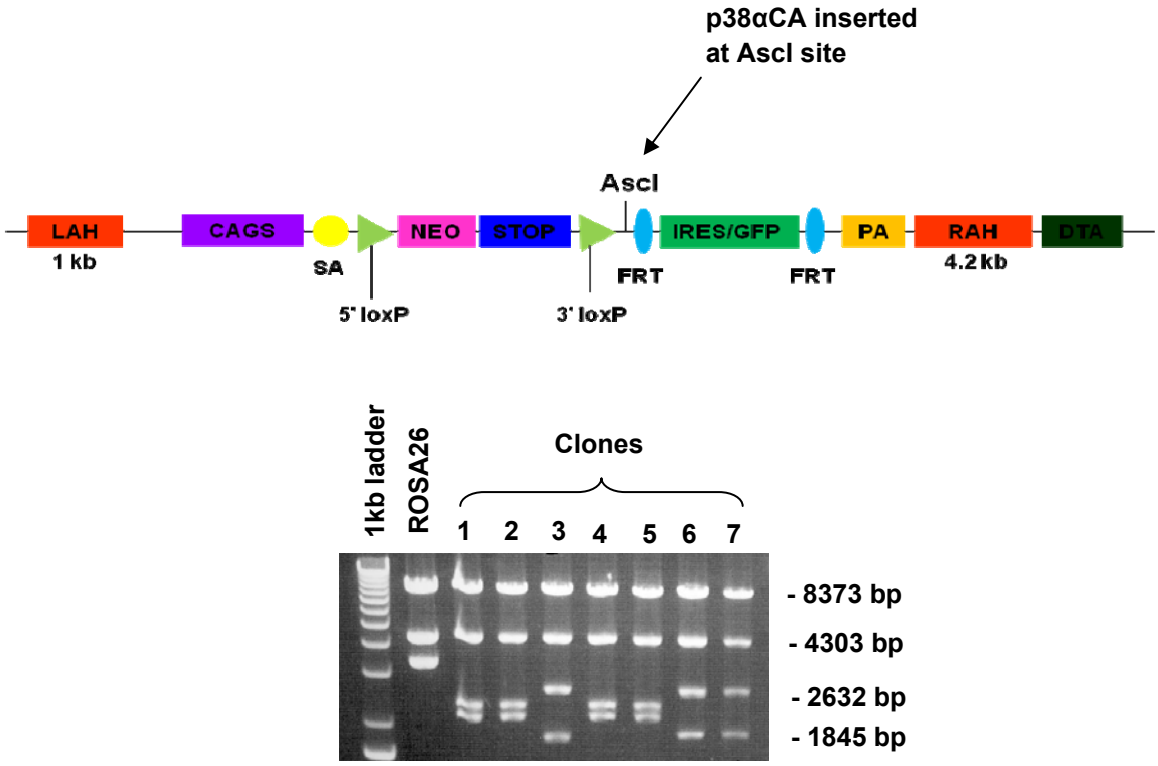

Figure 32. Subcloning of the mutant p38α D176A/Y323L (p38αCA) into the ROSA26-CAGS targeting vector. The mutant p38α was inserted at the AscI site of the targeting vector, which is placed immediately after the loxP flanked transcriptional STOP cassette. The correct orientation of the insert was examined with EcoRI digestion. The fragment sizes for correct insertion were: 8373 bp, 4303 bp, 2632 bp and 1845 bp. In the figure clones 3, 6 and 7 have the correct insert. *LAH (Left Arm of Homology), RAH (Right Arm of Homology) NEO (Neomycin resistance gene), IRES (Internal ribosomal entry site), PA (PolyA), GFP (Green fluorescent protein), FRT (Flp recombination site), SA (Splice acceptor), DTA (Diptheria toxin).*

2.2.1.6 Targeting of the Mutant p38α Transgene to the ROSA26 Locus

After subcloning the p38α mutant D176A/Y323L into the ROSA26-CAGS targeting vector and confirming the correct orientation of the insert, we then went on to target the construct to the ROSA26 locus (Fig. 34). In order to do this, the final construct was linearized with AsisI digestion (Fig. 33). It was then introduced into Bruce 4 ES cells through electroporation. After positive (neomycin resistance) and negative (diphtheria toxin) selection, two 192 clones were picked, and nine homologous recombinants were identified by southern blotting with a 5' probe (Fig. 35) external to the targeting vector.

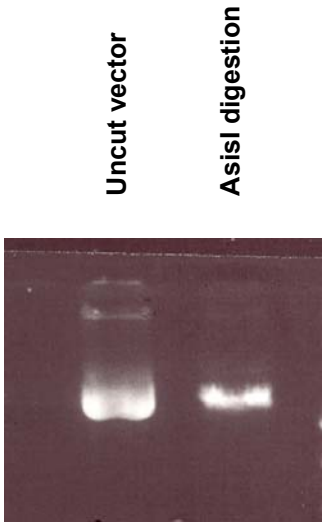

Figure 33. Linearization of the p38αCA targeting vector for electroporation into BRUCE 4 ES cells. Linearization of the final targeting vector containing the most active p38α mutant cDNA was achieved with AsisI digestion. Uncut vector was use as a control.

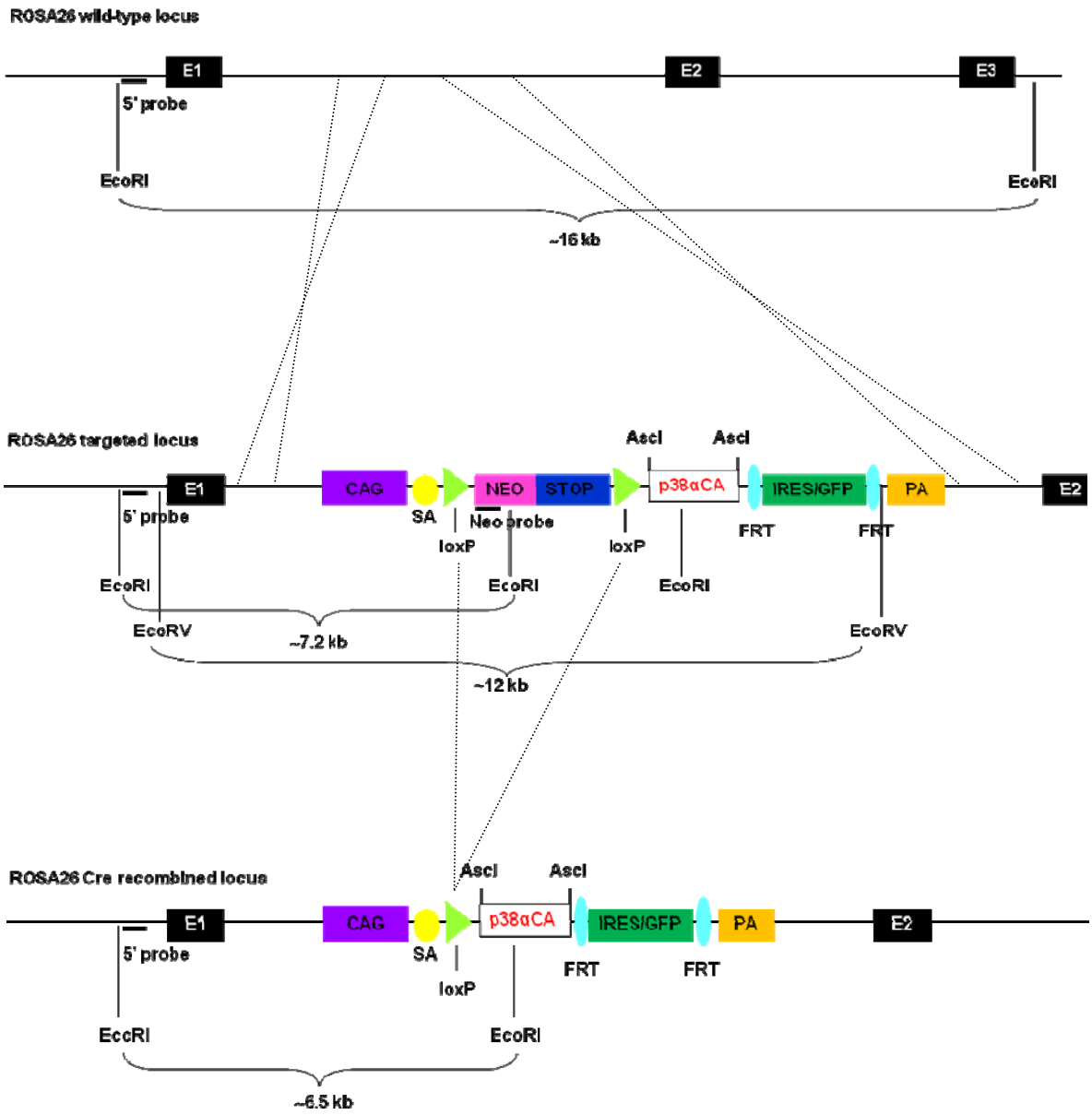

Figure 34. The p38αCA targeting strategy

Insertion of p38αCA into the ROSA26 locus by homologous recombination in mouse BRUCE 4 ES cells. After Cre-mediated excision of the STOP cassette, p38αCA is expressed under the control of the CAGS promoter. Digestion with EcoRI allowed us to identify targeted clones with an external 5' probe. EcoRV digestion and Southern Blotting with a NEO probe allowed us to exclude any random integration. In contrast with the wt ROSA26 locus that gave a band of ~16kb, the recombinant ES clones showed a band of ~7.2 kb with the 5' probe, after EcoRI digestion.

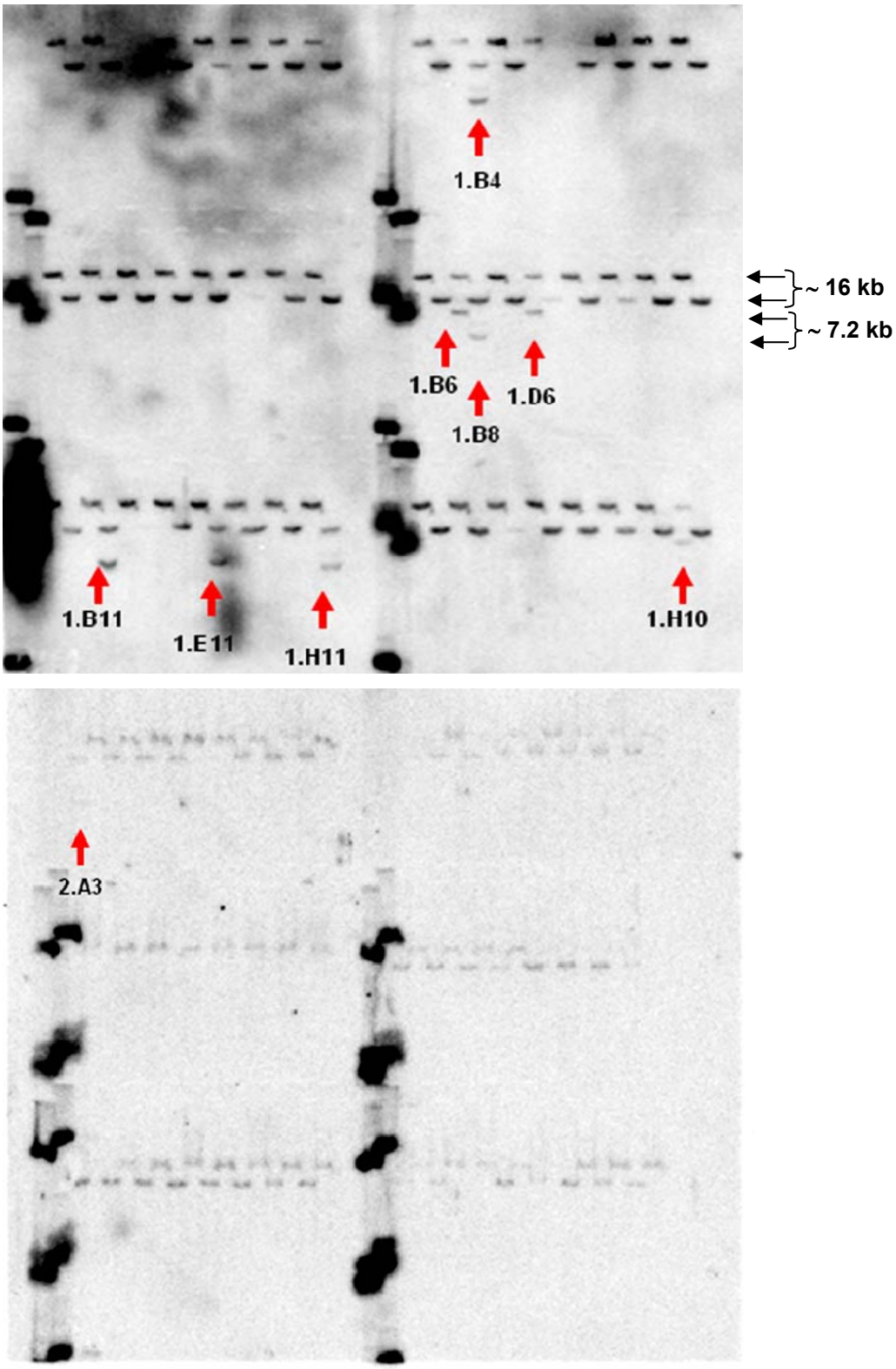

Figure 35. Southern blotting of ES clones targeted with the p38αCA vector.Southern blotting of the 192 ES clones picked, revealed 9 clones positive for homologous recombination when digesting with EcoRI and probing with a the 5' probe depicted in figure 34. They are indicated with red arrows. Wild-type bands ~16kb, targeted bands ~7.2kb.

The positive ES cell clones were further expanded and reconfirmed through Southern blotting for the 5' probe (Fig. 36A). Blotting with a NEO probe excluded random integration, but also revealed some clones previously shown to be positive with the 5' probe that were not positive for NEO, like 1.E11 (Fig. 36B).

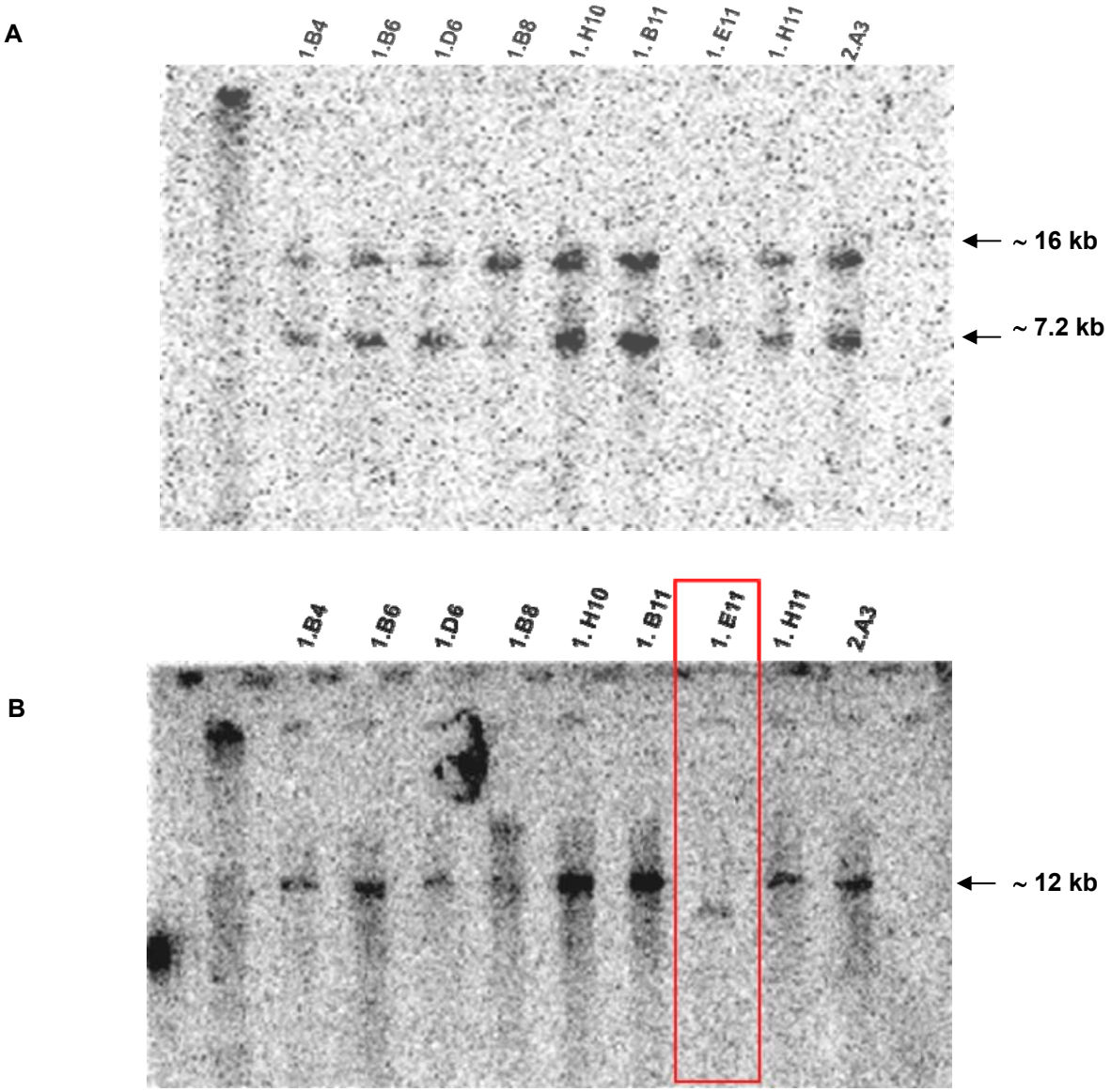

Figure 36. Confirmation of homologous recombination in ES clones targeted with the p38αCA vector. The ES cell clones that appeared positive for homologous recombination from the initial screening with Southern Blotting, were further grown in 10cm^3 and DNA extracted from these clones was used to confirm that we had indeed picked and expanded the correct clones, by (A) Southern Blotting with the external 5'probe. All 9 clones were confirmed for homologous recombination. Wild-type bands ~16kb, targeted bands ~7.2kb. (B) Random integration was excluded by digesting with EcoRV and probing with a NEO probe.

To test whether the constitutively active p38α would be expressed upon Cre-mediated recombination in these ES clones we made use of HTNC again that can be used efficiently to mediate recombination of loxP flanked alleles in ES cells [154]. If Cre recombination occurs in these cells, the STOP cassette will be excised, activating expression of the active p38α and also of GFP Treatment of ES cells with 5μM HTNC showed nearly 100% of ES cells expressing GFP, by FACS analysis (Fig. 37A). Immunoblotting for p38α and GFP on cytosolic extracts prepared from HTNC treated ES cells confirmed GFP expression in ES clones positive for homologous recombination, but also overexpression of p38α, compared to wt cells (Fig. 37B)

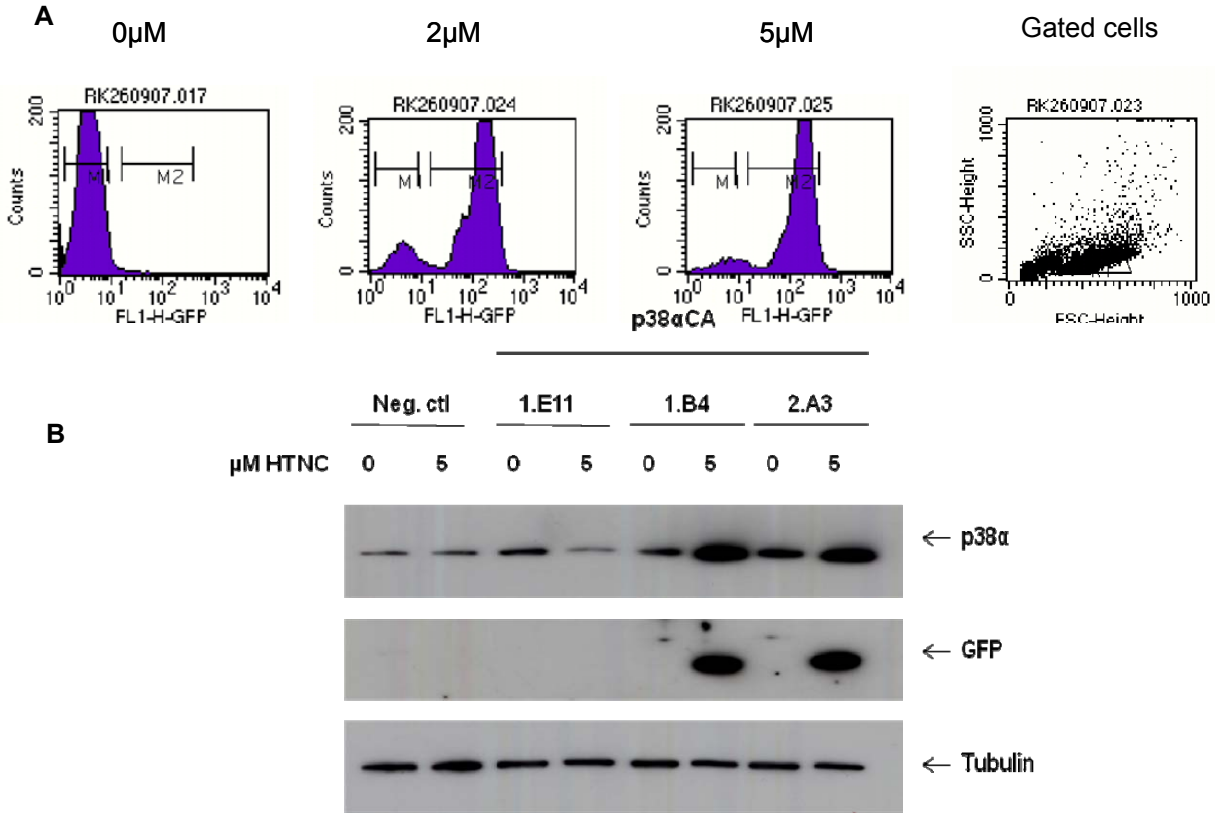

Figure 37. Treatment of ES clones positive for homologous recombination with HTNC. Positive clones were grown on 6-well plates at a density of $2x10^5$ on feeder MEFS and treated with HTNC as described in the methods. (A) FACS analysis of these cells showed GFP expression in nearly 100% of cells at a concentration of 5μM of HTNC. In the figure, clone 1.D6 is depicted as an example of GFP expression. (B) Immunoblotting with GFP and p38α antibodies showed GFP expression and increased p38α expression in p38αCA cells treated with HTNC. Negative controls were wild-type ES cells and p38αCA cells not expressing GFP when examined with FACS analysis (e.g. clone 1.E11).

2.2.1.7 From ES Cells to Mice - Chimeras and Germline Transmission

Once the ES clones positive for homologous recombination had been confirmed, two of them, 1.B4 and 2.A3, were injected into C57BL/6 blastocysts. These injections did not give rise to any chimeras, maybe due to the quality of the ES cells. From a second injection, in CB20 blastocysts, we obtained four male chimeric mice, two from clone 2.A3 (# 850 and # 851) and two from clone 1.B4 (# 861 and #862), with a chimerism of 70-80% recognized through color coating (Table 2). These male chimeras were then bred with wild-type C57BL/6 female mice in order to achieve germline transmission of the p38αCA transgene. Mice with germline transmission were identified by color coating, PCR and Southern Blotting. The result from Southern Blotting was puzzling since mice with germline transmission gave a ~2kb band higher than was expected. However, we still proceeded with breeding these mice, since this problem has been seen before with other ROSA26 targetings but the mice were still functional (Table 2 and Fig. 38). From these breedings germline transmission (GLT) was only obtained from clone 2.A3, chimera # 850.

Clone	ES-cell line	Blastocyst strain	Chimera	Bred with	Comments
2.A3	Bruce 4	CB20	**# 850 male 80%** # 851 male 70%	C57BL/6 female	**GLT** **-**
1.B4	Bruce 4	CB20	# 861 male 80% # 862 male 70%	C57BL/6 female	**-** **-**

Table 2. Chimeric mice and germline transmission obtained from the injection of BRUCE 4 ES cells carrying the p38αCA transgene in the ROSA26 locus.

Two positive ES clones, 2.A3 and 1.B4, were injected into CB20 blastocysts in order to obtain chimeric mice for the p38αCA transgene. From this injection we obtained two male chimeras from each clone with a chimerism of 70-80%. Breeding of these chimeras with female C57BL/6 mice gave germline transmission from clone 2.A3 only. Germline transmission was identified through color coating (black/brown), PCR and Southern Blotting.

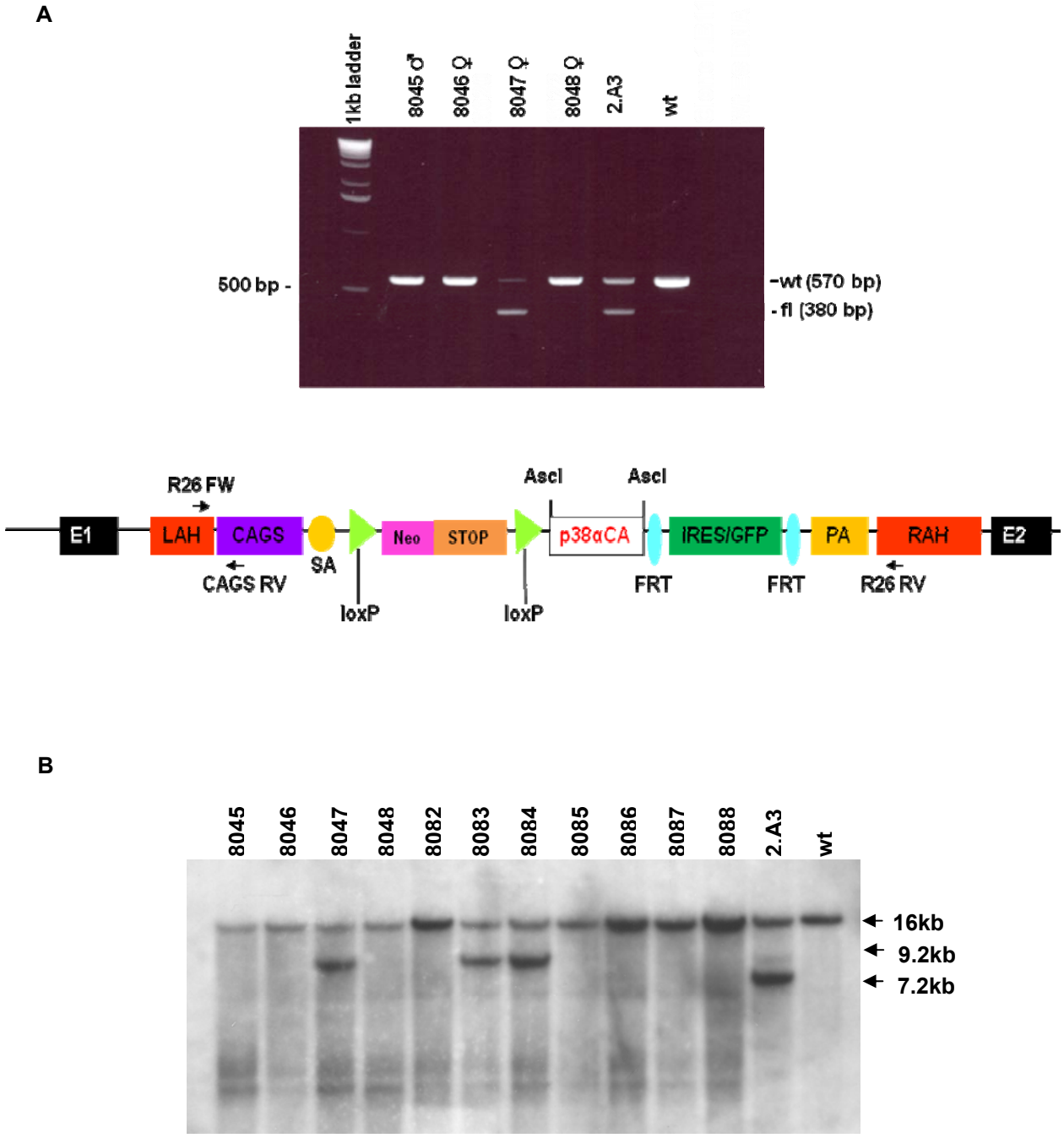

Figure 38. PCR and Southern Blotting for the identification of germline transmission of p38αCA. (A) PCR was performed to examine if germline transmission had occurred from the breeding of male chimeric mice with female C57BL/6 mice. Germline transmission was obtained from chimera # 850 (ES clone 2.A3), according to our PCR results. The primers used are depicted in the figure. Wild-type (wt) band = 570 bp, Floxed (fl) band = 380 bp. (B) We also performed Southern Blotting with the 5' probe described previously, after digesting with EcoRI. The result from this was puzzling since mice with germline transmission, according to PCR results, had a band ~2kb higher than expected (~9kb).

2.2.1.8 GFP Expression in R26wt/p38αCA^{LPC-KO} Mice

As an initial step, in order to confirm that the construct was functional, we crossed mice heterozygous for the p38αCA transgene with AlfpCre mice, which express Cre specifically in liver parenchymal cells (hepatocytes). The aim of this experiment was to isolate primary hepatocytes from these cells to examine GFP expression by performing FACS analysis. p38αCA heterozygous mice positive for AlfpCre (R26wt/p38αCA^{LPC-KO}) that were obtained from this breeding were used to isolate primary hepatocytes and look at GFP expression. p38αCA heterozygous littermates, negative for AlfpCre expression were used as negative controls. This experiment indicated that the construct inserted into these mice was functional, since we observed GFP expression in the presence of Cre recombinase in hepatocytes (Fig. 39).

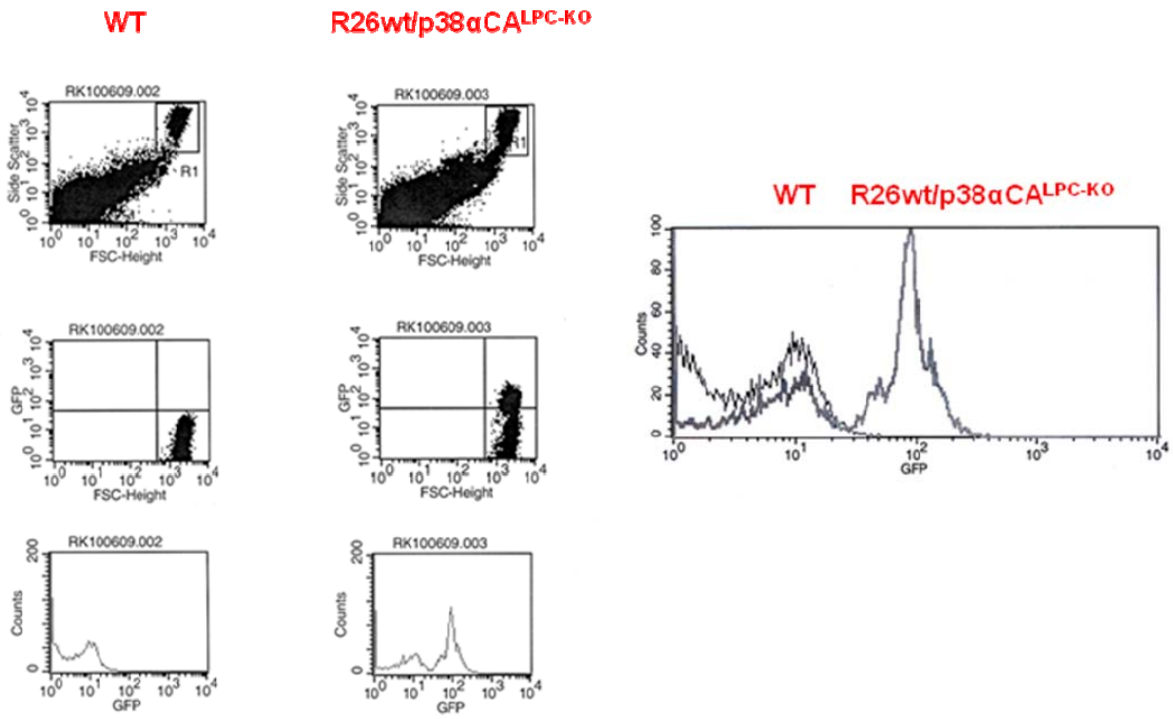

Figure 39. GFP expression in R26wt/p38αCA^{LPC-KO} mice. FACS analysis of primary hepatocytes isolated from R26wt/p38αCAC^{LPC-KO} mice showed GFP expression in these mice, which was not present in WT (wild-type) mice. Panels left: Top - gated primary hepatocytes, middle and bottom - GFP expression. Panel right: Comparison of GFP expression in Cre positive and negative cells.

We are now continuing the characterization of these mice by performing immunoblotting in order to determine if p38α is overexpressed, but also by performing activity assays as described previously in order to determine whether the overexpressed protein is hyperactivated compared to wild-type. Finally, we are breeding these mice to Deleter Cre mice that express Cre throughout the whole body, in order to determine the systemic effect this hyperactive form of p38α may have on mice.

2.2.2 Generation of p38αKD (Kinase Dead) Mice

Given the fact that p38 MAPK exists in four different isoforms and therefore when knocked out completely its activity may be compensated by other isoforms, but also that it may display another function that is not dependant on its kinase activity, we decided to generate mice that would express a kinase-dead form of this protein.

2.2.2.1 The p38αKD Targeting Construct

In order to generate mice expressing a kinase-dead form of p38α MAPK, we took advantage of a previously published mutation that is conserved between kinases and eliminates the kinase activity of the protein. More specifically, the amino acid residue lysine 53 that is located in exon 2 of the p38α MAPK locus and is essential for kinase activity was mutated to an arginine residue (K53R) to generate a kinase inactive form of p38α MAPK (Kumar, S. *et al., J. Biol. Chem.,* 1995).

After introducing this mutation into exon 2 of the p38α genomic sequence, we then went on to generate the targeting construct that would allow the generation of mice harbouring this mutation. In the generation of our construct we took advantage of the mutated asymmetric loxP sites, lox66 and lox71[160]. Normally, when positioning two loxP sites in the head-to-head or opposite orientation, the intervening sequence is inverted in the presence of Cre recombinase. However, this inversion is not continuous and is reversed upon the removal of Cre recombinase. In the case of the mutant lox66 and lox71 sites, after the first Cre-mediated recombination on wild-type and one double mutant loxP site a re formed (see fig. 40B). The latter however displays a very low affinity for Cre recombinase. Consequently, Cre-mediated recombination in the mutated Cre/loxP system has a favorable forward reaction equilibrium as depicted in the figure (Fig. 40B).

In our p38αKD targeting construct, we made use of these mutated loxP sites to switch between the native and the mutated p38α MAPK exon 2. More specifically, we subcloned both the native and the mutated exon2 in opposite and inverse orientations between lo66 and lox71 (Fig.40A). This way, the native exon 2 would be expressed in the absence of Cre recombinase, whereas introduction of Cre into the system would lead to constant expression of the mutated exon2 by inversion. The

pEASY-FLIRT vector (Appendix I) was used to generate the final targeting construct harboring the mutated exon2.

A

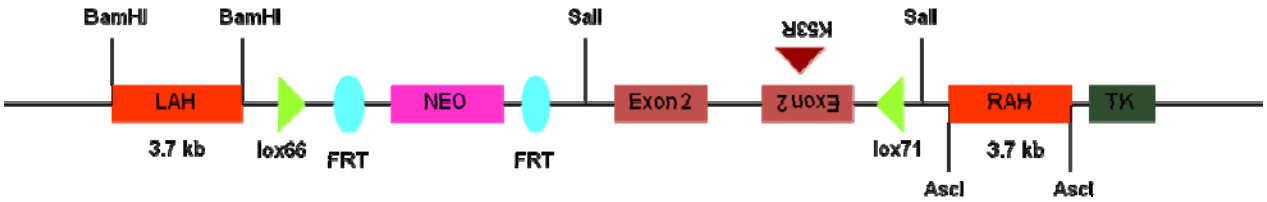

B

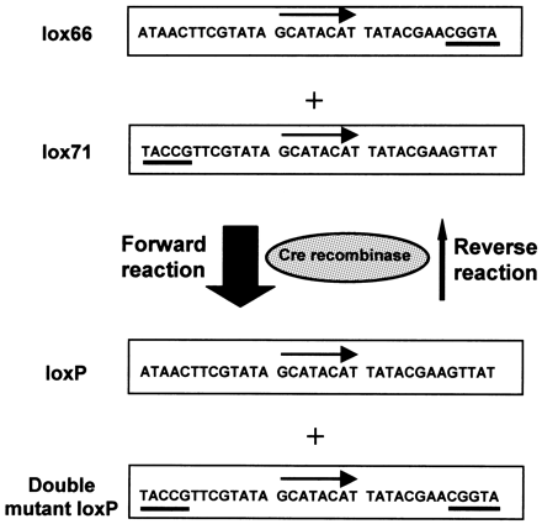

Figure 40. The p38αKD targeting strategy. (A) The targeting construct. The kinase essential lysine residue 53, in Exon 2, was mutated to an arginine. Both, the normal and the mutant Exon2 were placed between the mutant lox66-lox71 sites in an inverted order as depicted in the figure. *LAH=Left Arm of Homology, NEO=Neomycin Resistance Cassette, TK=Thymidine Kinase, K53R=Lysine to Arginine mutation* (B) Cre-mediated recombination between lox66 and lox71 sites generates one wild-type and one double mutant loxP site. Since the double mutant loxP site exhibits much reduced binding affinity for Cre recombinase, Cre- mediated inversion using the mutated Cre/loxP system prefers the forward reaction as indicated. Nucleotide sequences of loxP and its mutated derivatives are listed; mutated sequences are underlined. Arrows indicate non-palindromic core sequence. Image taken from: Nucleic Acids Research, 2002, Vol. 30, No. 17 e90© 2002, Oxford University Press.

2.2.2.2 Targeting of the p38αKD Construct to the p38α Locus

Once the final construct was generated, we targeted the kinase-dead form of p38α to the p38α MAPK locus (Fig. 42). In order to do this, the final construct was linearized with NotI digestion (Fig. 41). It was then introduced into Bruce 4 ES cells through electroporation. Three hundred eight-four clones were picked, and after positive (Neomycin) and negative (Thymidine kinase) selection, four homologous recombinants were identified by Southern blotting using a 5' and 3' probe external to the targeting vector (Fig. 43 and 44, respectively). Additional integrations were excluded in these positive clones by use of a neomycin probe. After confirmation of the clones by Southern Blotting again with the 5', 3' and NEO probe, using DNA prepared after further expanding these clones further on 10 cm^3 (Fig. 45), all four clones were injected into C57BL/6 derived blastocysts.

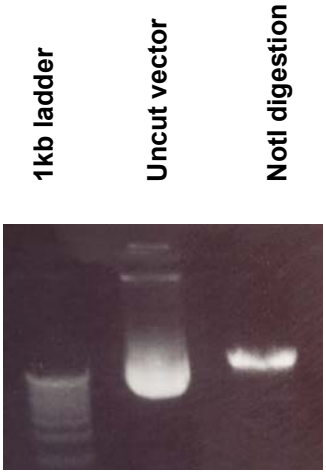

Figure 41. Linearization of the p38αKD targeting vector for electroporation into BRUCE 4 ES cells. Linearization of the final p38α kinase-dead targeting vector achieved with NotI digestion. Uncut vector was use as a control.

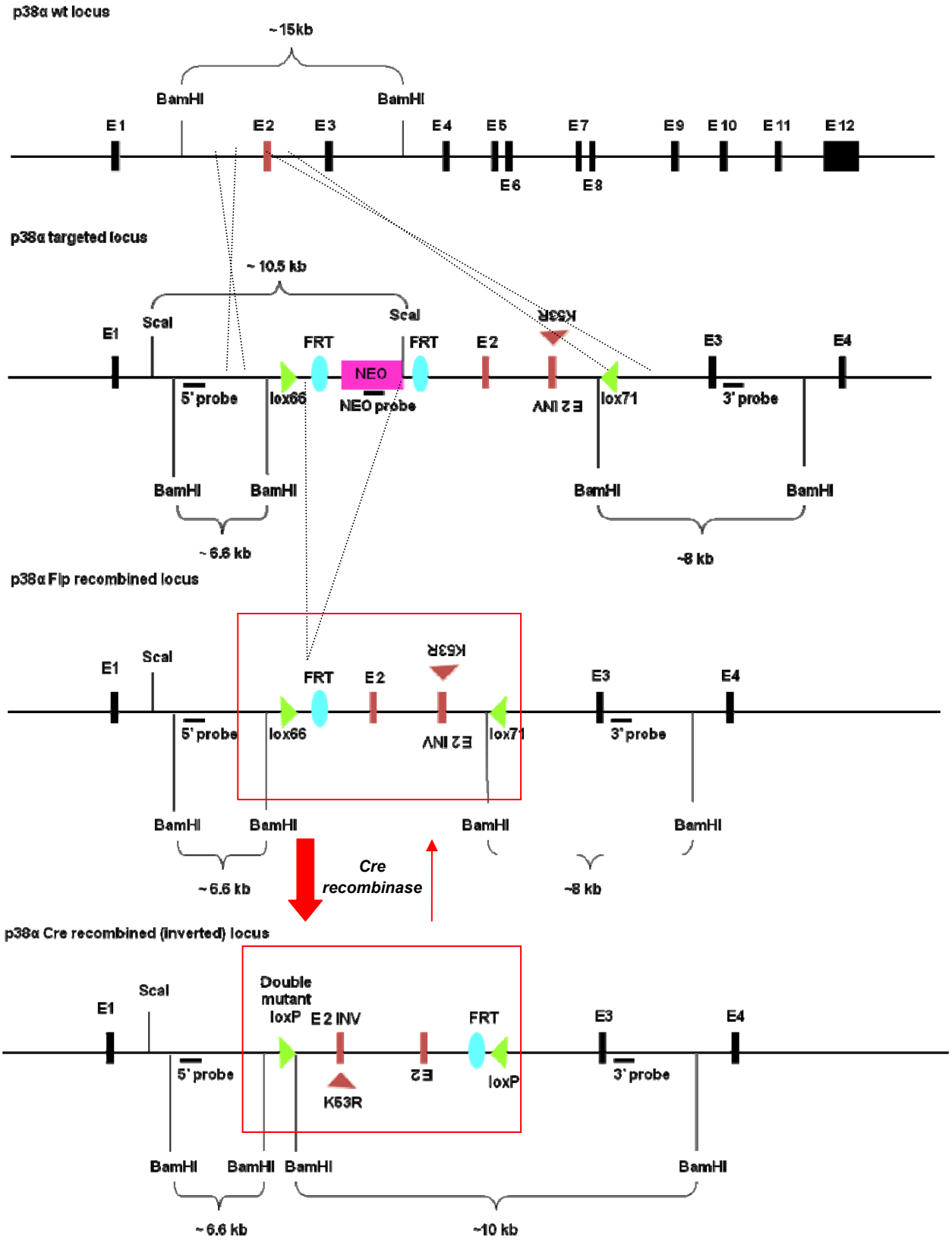

Figure 42. p38αKD targeting to the p38α locus. (A) Schematic of the wt p38α locus before homologous recombination. (B) The p38α locus after homologous recombination at Exon 2. Depicted are also the probes used to screen for homologous (5' and 3', BamHI digestion) and random recombination (NEO, ScaI digestion). (C) The Neo cassette was removed by Flp recombination, by crossing with Flp deleter mice. (D) In the presence of Cre, the region between lox66 and lox71 is inverted, leading to expression of the mutated Exon2. In this process one wt and one double mutant loxP site are generated. Since the double mutant loxP site exhibits much reduced binding affinity for Cre recombinase, Cre- mediated inversion using the mutated Cre/loxP system prefers the forward reaction as indicated.

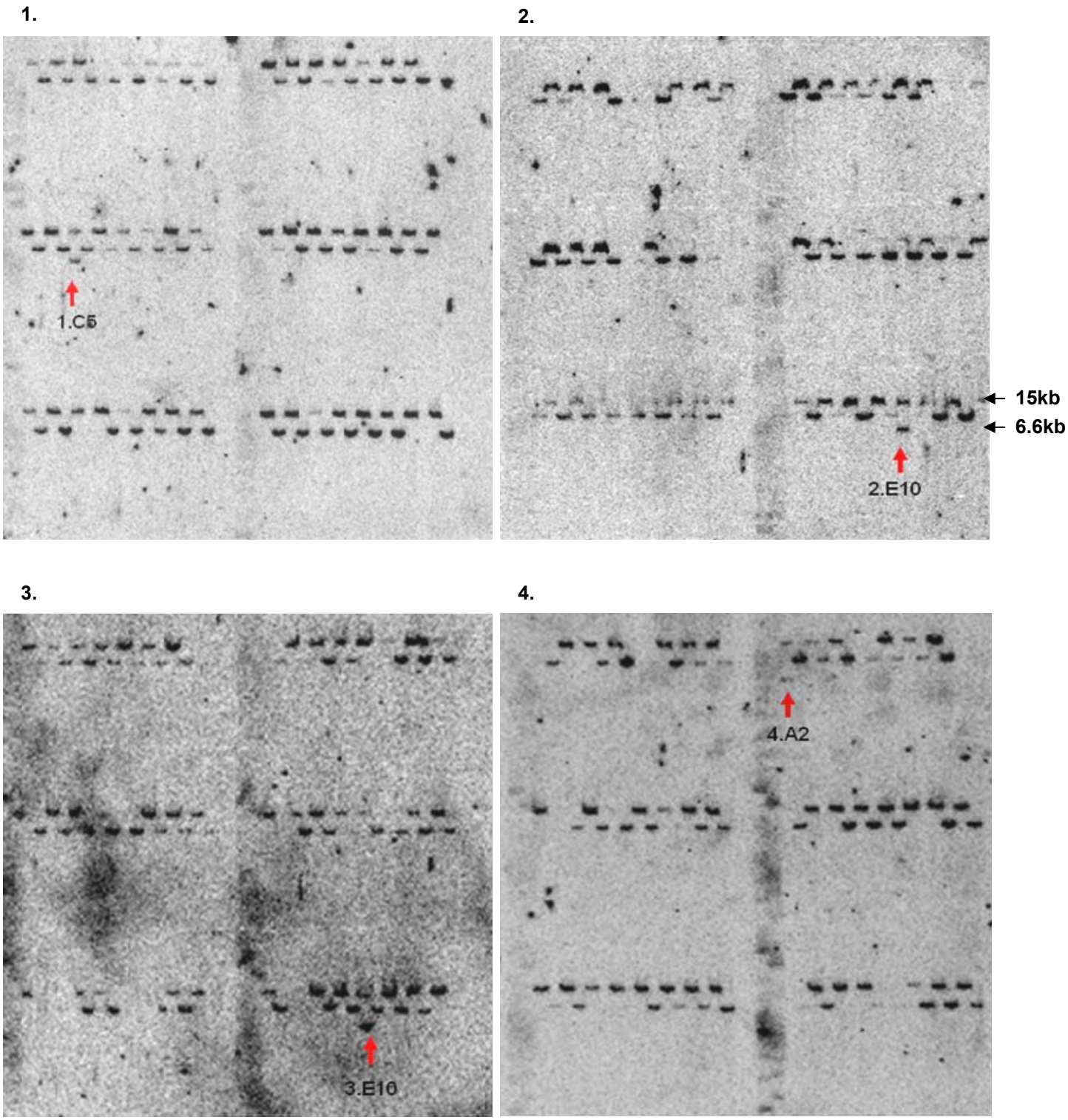

Figure 43. P38αKD targeting - Screening for homologous recombinants with a 5' probe. Southern Blotting with a 5' probe performed on DNA prepared from the 384 clones picked, after a BamHI digestion, allowed us to identify 4 ES clones positive for homologous recombination. WT = 15kb, Floxed = 6.6kb.

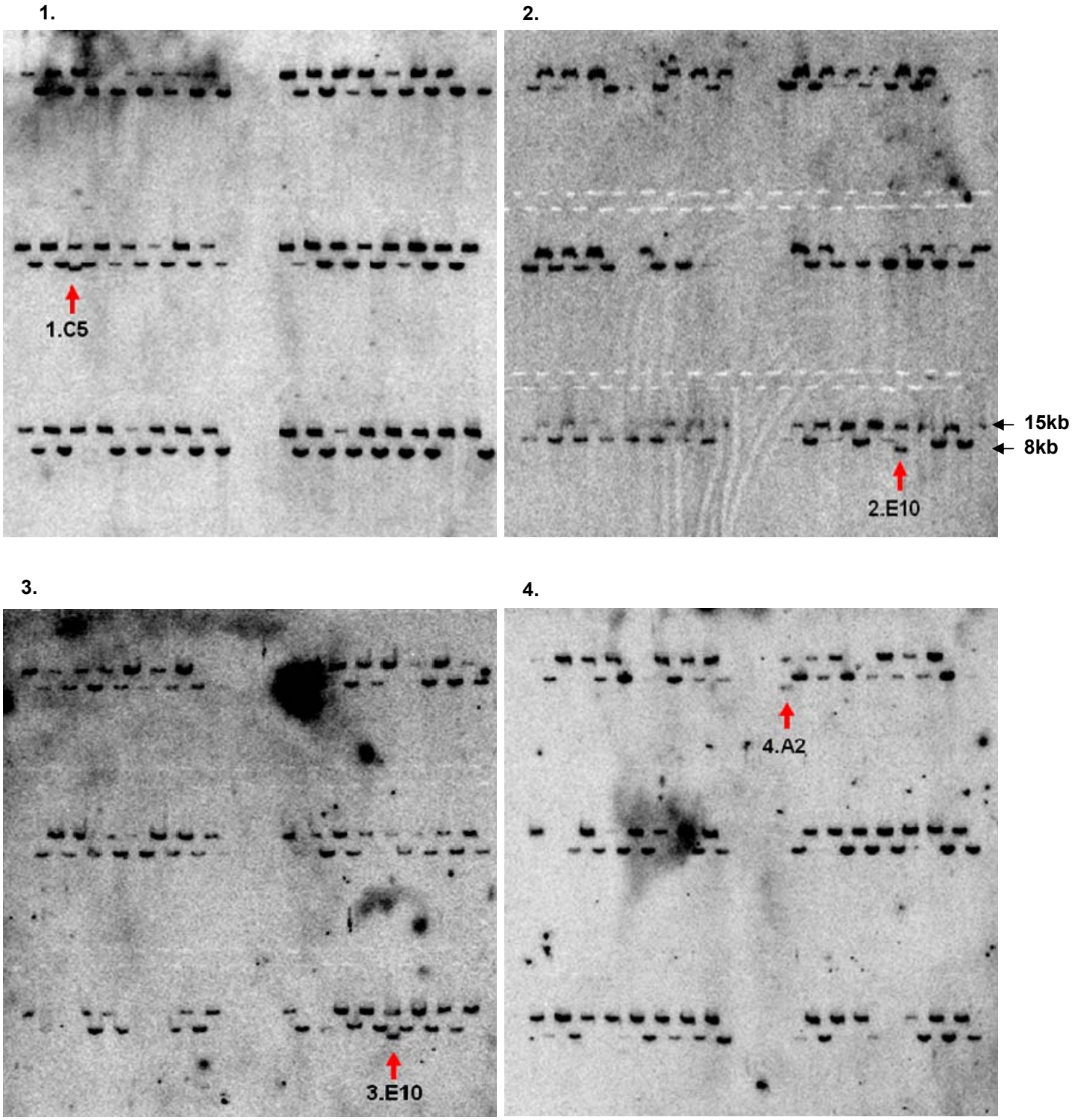

Figure 44. P38αKD targeting - Screening for homologous recombinants with a 3' probe. Southern Blotting with a 3' probe, performed on the same Southern Blots used for the 5'probe after stripping, showed that integration had also taken place on the 3' end of the 4 ES clones identified for homologous recombination previously, with the 5 ' probe. WT = 15kb, Floxed = 8kb.

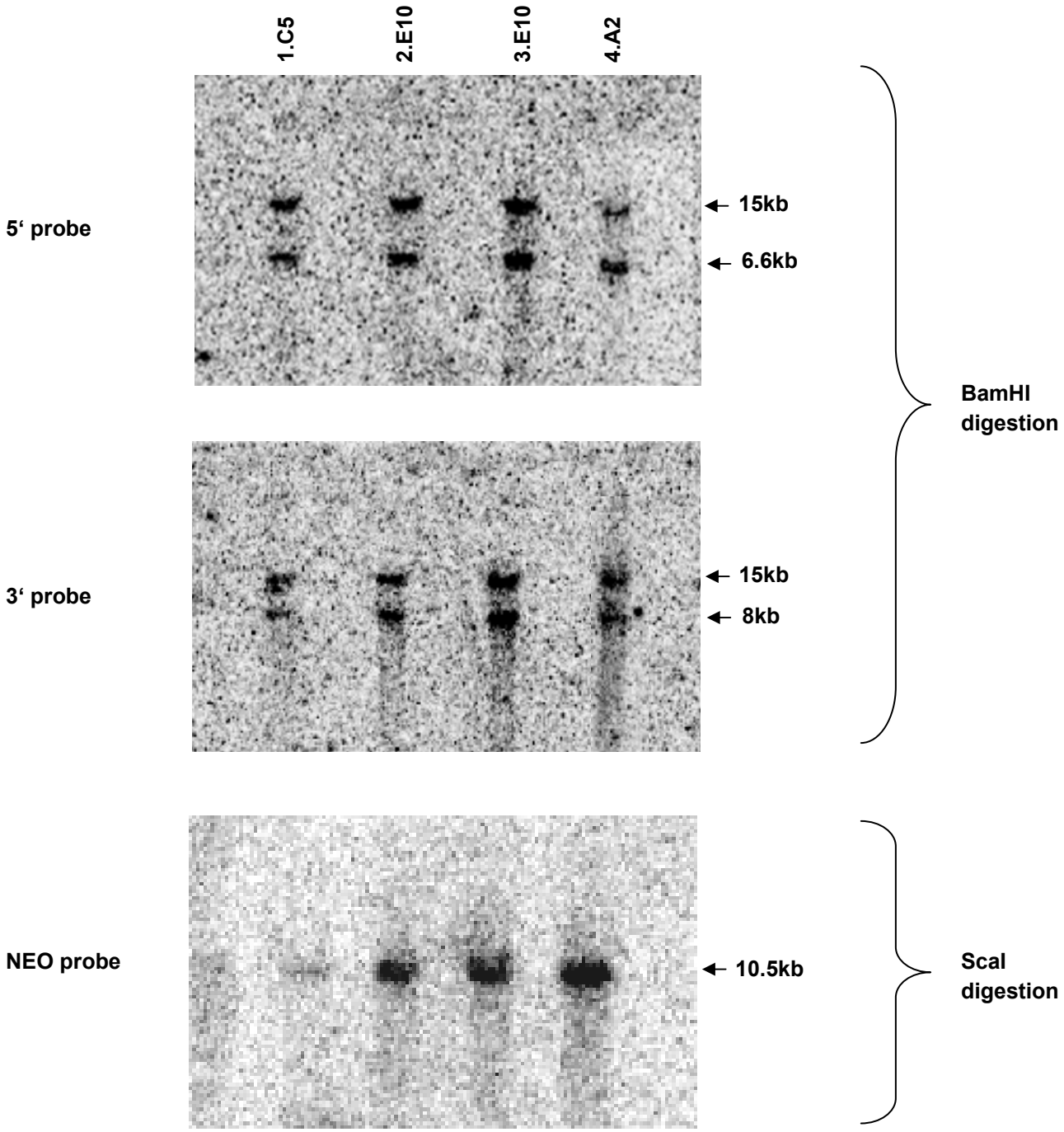

Figure 45. P38αKD targeting – Clone confirmation. ES clones positive for homologous recombination during screening with Southern Blotting were further expanded and clones were reconfirmed by Southern Blotting with the 5’ and 3’ probes used previously for screening. A NEO probe was also used (ScaI digestion) to exclude random integration. All 4 clones were confirmed.

2.2.2.3 From ES Cells to Mice - Chimeras and Germline Transmission

Once the ES clones positive for homologous recombination had been confirmed, all four of them were injected into C57BL/6 derived blastocysts. From these injections we obtained four male and two female chimeras, five from clone 1.C5, one from clone 3.E10 and one from clone 4.A2. Clone 2.E10 did not give any offspring (Table 3). Chimeras were identified through genotyping PCR (Fig. 46).

Clone	ES-cell line	Blastocyst strain	Chimera	Bred with	Comments
1.C5	Bruce 4	C57BL/6	# 4845 male **# 4846 male** # 4968 male # 4847 female # 4850 female	C57BL/6 female C57BL/6 male	- GLT - - -
2.E10	Bruce 4	C57BL/6	-	-	-
3.E10	Bruce 4	C57BL/6	# 4592 male	C57BL/6 female	-
4.A2	Bruce 4	C57BL/6	# 4852 male	C57BL/6 female	-

Table 3. Chimeric mice and germline transmission obtained from the injection of BRUCE 4 ES cells carrying the p38αCA transgene in the ROSA26 locus.

Four positive ES clones, 1.C5, 2.E10, 3.E10 and 4.A2, were injected into C57BL/6 blastocysts in order to obtain chimeric mice. From this injection we obtained five male and two female chimeras in total. Breeding of these chimeras with female and male C57BL/6 mice respectively, gave rise to germline transmission from clone 1.C5 only. Germline transmission was identified through PCR and Southern Blotting.

All the chimeras obtained were bred to C57BL/6 to produce mice with germline transmission. From all the chimeric breedings, only one gave mice where germline transmission was detected through genotyping and Southern Blotting. This was male 4846 from clone 1.C5.

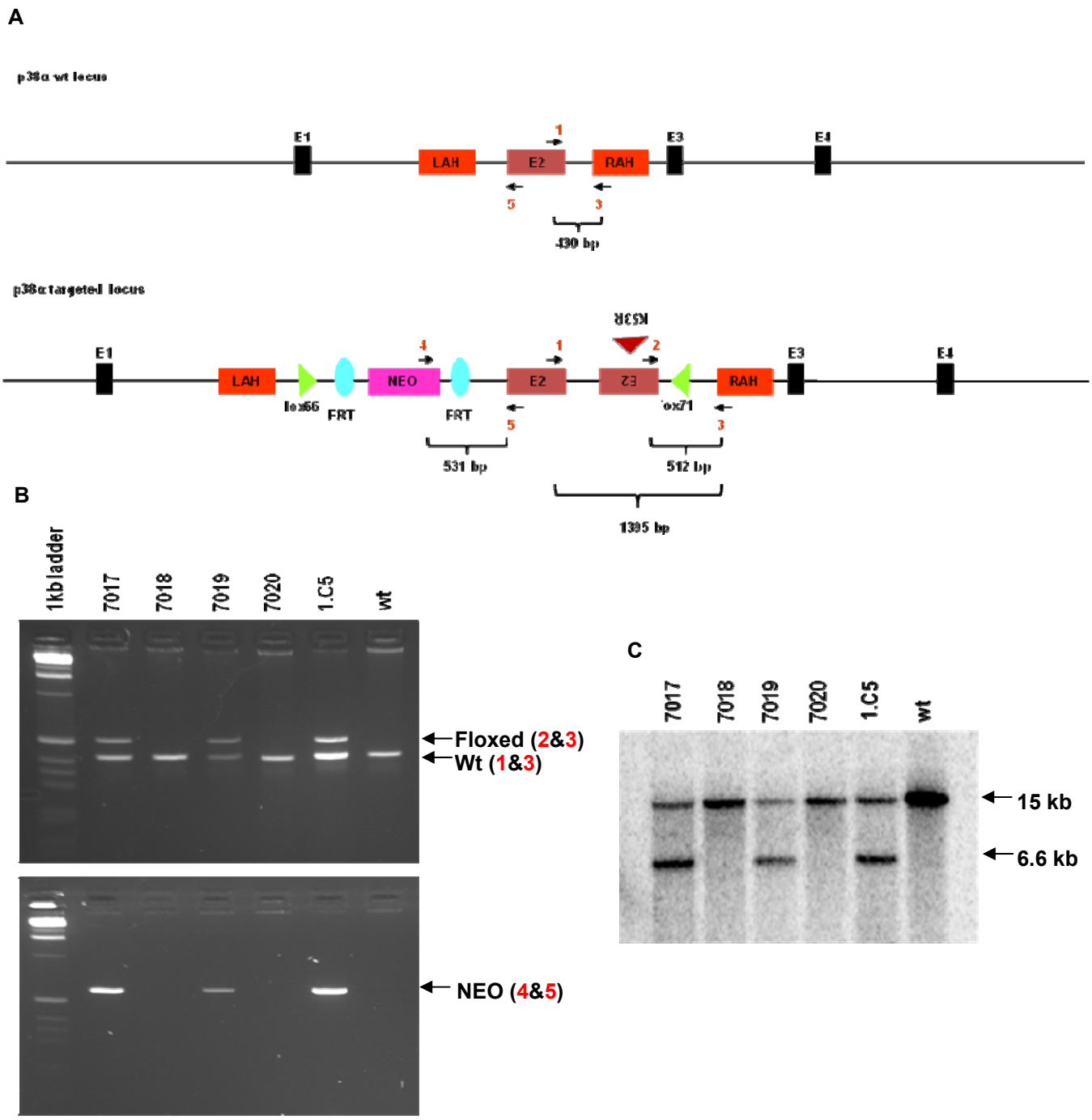

Figure 46. Identification of germline transmission through PCR and Southern blotting. (A) Genotyping strategy for p38αKD targeting. The primers used for amplification in the wt (top) and targeted (bottom) locus for chimera and germline identification are depicted in the figure. Germline transmission obtained from breeding the male chimera 4846 with a C57BL/6 female was identified through (B) PCR for the floxed and NEO bands and (C) Southern Blotting with a 5' probe described previously.

2.2.2.4 *In vivo* NEO Deletion and Breedings

Mice with germline transmission were crossed with Flp deleter mice to remove the NEO cassette so that it would not interfere with the proper expression of proteins. NEO deletion was determined by PCR using primers 4 & 5 that give a band of ~ 500bp only in the presence of the NEO cassette (see genotyping strategy fig. 46). Once we had obtained mice where the NEO cassette had been deleted, giving us heterozygous p38αKD$^{FL/wt}$ mice, these were bred with wild-type C57BL/6 mice in order to expand the line. We are also now breeding heterozygous mice in order to generate homozygous p38αKD$^{FL/FL}$ mutant mice. The homozygous mice can then be bred to Deleter Cre or other Cre lines for further characterization.

2.2.2.5 Testing of Inversion in the Presence of Cre Recombinase

Whilst the mice are breeding, once we had generated NEO deleted heterozygous mice, we isolated some BMDMs to test if the inversion in the presence of Cre recombinase was functional. This was achieved by treating the BMDMs with HTNC for 16hrs as described in the methods and isolating DNA to check for inversion by PCR and Southern Blotting. Inversion of the genomic sequence between the two mutant loxP sites was observed at all concentrations of HTNC used (1 & 2 µg/ml) in cells isolated from p38αKD$^{FL/wt}$, but not from wild-type mice, giving us a first indication that the construct we designed is functional (Fig. 47). This result still has to be confirmed by Southern Blotting. Also, the catalytic activity of p38α MAPK in these mice still remains to be examined, in the presence of Cre recombinase.

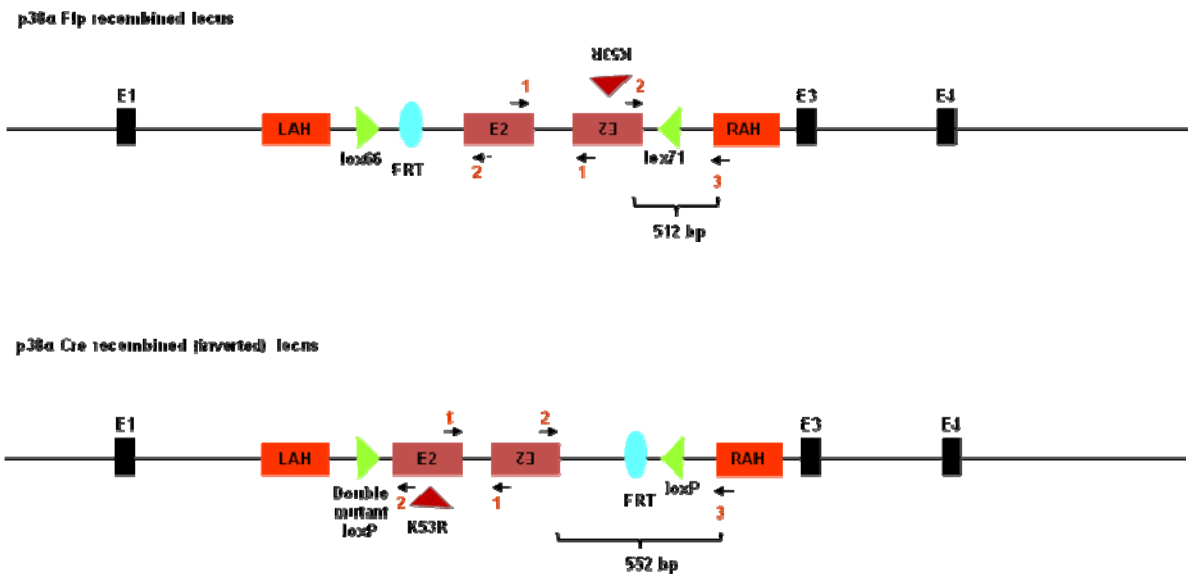

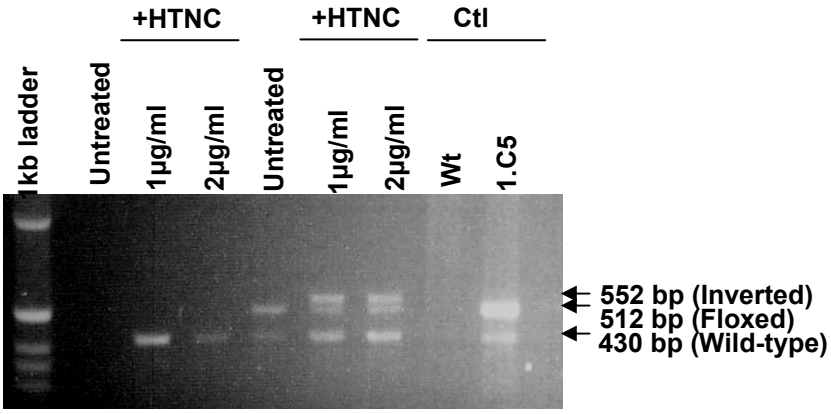

Figure 47. Genotyping for inversion in p38αKD mice after Cre recombination. PCR on DNA isolated from HTNC treated BMDMs of p38αKD$^{FL/WT}$ mice, showed that inversion of the lox66-lox71 flanked nucleotide sequence is functional. Wild-type band (as seen in fig 46)=430 bp, Floxed band (diagram top)=512 bp, Inverted band (diagram bottom)=552 bp.

3. Discussion

3.1 The Macrophage and Endothelial-Cell Specific Role of p38α MAPK in Atherosclerosis

p38α MAPK has previously been implicated in the development of atherosclerosis through various *in vitro* studies with the use of small molecule p38 inhibitors [125,126,134,161,162] but also *in vivo* in a recent study by Seimon, T.A *et al.* 2009, where they describe an anti-apoptotic role for p38α MAPK in macrophages induced by ER-stress. In this study we have investigated the macrophage and endothelial-cell specific role of p38α MAPK in atherosclerosis by taking advantage of the Cre-loxP recombination system to generate myeloid and endothelial-cell specific knockout mice, since the complete knockout of p38α MAPK has previously been described by several groups to be embryonically lethal because of severe defects in placental development [67, 70,133]. The results that we present here, surprisingly and contrary to previous studies, show that p38α MAPK does not play a significant role in atherosclerosis development.

3.1.1 p38α MAPK in Macrophages

3.1.1.1 p38α MAPK Depletion Does not Affect Foam Cell Formation *in vitro*

Lipid-laden macrophage foam cells are an early ('fatty streak') and persistent component of atherosclerotic lesions, formed by the accumulation of cholesteryl esters and triglyceride in cytoplasmic droplets [163]. Binding and endocytosis of lipids like oxLDL by macrophages is a result of the expression of various scavenger receptors, like CD36, on their surface. CD36, through functional and structural studies, has been characterized to be a member of the class B family of scavenger receptors with a substantial capacity to bind oxLDL as well as other ligands. Its importance in the initiation and perpetuation of atherosclerotic lesions has been shown in the past decade in various studies by its effect in reducing lesion formation when inactivated in ApoE deficient mouse models, the latest of which has also underlined its significance in comparison to another important scavenger receptor linked to atherosclerosis, SRA I/II [164, 165]. In this study authors claim that absence of

SRA I/II in ApoE deficient mice does not confer any further protection against atherosclerosis than what is already achieved through CD36 [165].

With the use of pharmacological inhibitors, it has been demonstrated that p38α MAPK, but not ERK or JNK, is necessary and sufficient for the transactivation of PPAR-gamma, a nuclear receptor that has been shown to play a pivotal role in oxLDL-induced CD36 expression [125, 166]. In accordance to this, it was also shown that the p38 specific inhibitor SB203580 blocked oxLDL exposed J774 cells from becoming foam cells [125]. In our studies however, when exposing p38α MAPK macrophages to oxLDL and examining lipid uptake by FACS analysis, we did not observe any significant differences, compared to wild-type mice. This was also true for the mRNA expression levels of CD36, which were increased in both wild-type and knockout cells in the presence of oxLDL in a similar manner (data not shown).

3.1.1.2 Only MIP-2α and IL-1β mRNA Expression Mildly Affected in p38α Depleted Macrophages, *in vitro*

Macrophages have also been described to play a key role in disease progression as inflammatory mediators [163]. Once monocytes have entered the arterial intima, and differentiated into macrophages under the influence of the macrophage-colony stimulating factor (MCS-F), besides scavenger receptors, they also express other pattern recognition receptors, like Toll-like receptors (TLRs). These TLRs can be activated by factors such as LPS, heat shock protein 60 (HSP60), oxLDL and other ligands that instigate the production of many proinflammatory cytokines, MMPs and other inflammatory mediators like nitric oxide (NO) and endothelin-1, by macrophages [80]. This response to TLR ligation is mediated by the activation of nuclear factor-κB (NF-κB) and MAPK signaling pathways [167, 168, 169], including p38α MAPK. Genetic deficiency of TLR4, the TLR linked to inflammatory responses to oxLDL when in complex with CD14, but also its signal transducing adaptor molecule myeloid differentiation primary-response gene 88 (Myd88), has been shown to reduce plaques in mice [170, 171].

Since, p38α MAPK is implicated in the expression of proinflammatory cytokines, chemokines, MMPs and other inflammatory mediators in atherosclerosis, downstream of TLRs, we decided to examine the expression of a panel of these mediators in macrophages after oxLDL stimulation. In this analysis, the only

difference we observed was a downregulation in MIP-2α and IL-1β, a response that has been previously shown in LPS stimulated macrophages also isolated from LysMCre mice [28]. IL-1β and MIP-2α, which are both strongly induced in monocytes in atherosclerosis, are important mediators in the progression of this disease. ApoE deficient mice lacking IL-1β showed a 30% decrease in the severity of atherosclerosis that was attributed to the downregulation of MCP-1 and VCAM-1 expression both at the mRNA and protein level [172]. MIP-2α (IL-8 in humans), a CXC chemokine, was initially thought to be insignificant as far as atherosclerosis development is concerned, since it is mainly responsible for neutrophil recruitment, which are particularly scarce in atherosclerosis. However, recent reports suggest that it may trigger firm adhesion of monocytes to vascular endothelial cells, particularly under flow conditions, by binding to the CXC chemokine receptor CXCR2 [173]. Furthermore, bone marrow transplantation studies demonstrated that the absence of the CXCR2 equivalent IL-8 receptor homologue resulted in diminished monocyte recruitment and reduced lesion size in the LDL receptor (-/-) model of atherosclerosis [174]. However, in a recent study concerning IL-8, it was also shown that reduction in this chemokine under atheroprone flow conditions, leads to an increase in VCAM-1 expression, suggesting a limiting role for the inflammatory response in endothelial cells via VCAM-1 modulation [175]. From these results, and given the findings of these previous studies, we hypothesized that p38α MAPK may not act as a mediator in foam cell formation in macrophages with respect to atherosclerosis, but it may contribute to this disease by playing a role in the recruitment of macrophages to the arterial intima, both by chemokine attraction (MCP-1 and MIP-2α) but also by promoting adhesion to the endothelial cell layer through VCAM-1 upregulation. On the other hand, taking this contradictory role of IL-8 into consideration, increased VCAM-1 expression caused by reduction of MIP-2α (IL-8), could counterbalance the effect caused by the downregulation of IL-1β.

3.1.1.3 Depletion of p38α MAPK in Macrophages Does not Affect Atherosclerosis Development *in vivo*

The results we obtained from our *in vitro* experiments, as described above, pointed towards a pro-atherogenic role for p38α MAPK in macrophages, and so depletion of this kinase should lead to a reduction in atherosclerosis development to some extent, due to a reduction in monocyte recruitment to the arterial intima. However,

when feeding groups of male and female macrophage-specific p38α^{MY-KO}/ApoE$^{-/-}$ and their ApoE$^{-/-}$ littermates a cholesterol rich 'western diet' for 10 weeks, we did not observe any significant differences in atherosclerotic plaque development either in the aortic sinus or the whole aorta of these mice. This observation correlates with that recently published by the group of Ira A. Tabas, Columbia University, New York [149]. Consistent also with our results, atherosclerotic lesion size was also unaffected when a p38 inhibitor was given to ApoE$^{-/-}$ mice infused with angiotensin II [176]. So, while other studies have shown that macrophage deletion of p38 MAPK has a marked effect on the reduction of inflammation in murine models of skin injury and septic shock [177], in our ApoE$^{-/-}$ model of atherosclerosis we found no reduction in lesion size.

Further confirmation to the fact that p38α MAPK is not an important mediator in atherosclerosis development in the context of macrophages was provided by real-time PCR (qRT-PCR) analysis on the expression of a panel of cytokines chemokines and adhesion molecules on RNA isolated from the aortic arch of p38α^{MY-KO}/ApoE$^{-/-}$ and ApoE$^{-/-}$ littermates after 10 weeks on a cholesterol rich 'western diet'. Although p38α MAPK has been shown to regulate the expression of many genes involved in the initiation and progression of atherosclerotic lesions [7,61,70,150,151], an effect thought to be mediated via a mechanism involving messenger RNA turnover and protein translation [3,61], we only observed a slight upregulation in most of the genes tested but no statistically significant differences. Not even in MIP-2α and IL-1β, which were both downregulated *in vitro* when stimulating macrophages with oxLDL. These results further confirmed that macrophage-specific deletion of p38α MAPK does not affect lesion size, and again challenged our hypothesis that it could affect atherosclerotic lesion development by promoting recruitment of macrophages to the arterial intima.

3.1.1.4 Markers of Advanced Atherosclerotic Plaque Progression not Altered in Macrophage-Specific p38α MAPK Knockout Mice

Although the above evidence was sufficient to claim that the macrophage-specific role of p38α MAPK in atheroma formation is insignificant, the recent study by Seimon, T.A *et al.* 2009 perturbed us to continue with the characterization of the plaques because of their controversial findings in plaque progression. In their study,

they claim that although there are no observable differences in plaque size between p38α^{MY-KO}/ApoE$^{-/-}$ and ApoE$^{-/-}$ mice, when deleting p38α MAPK, plaques seem to be more advanced. A significant reduction in collagen content was observed, together with a dramatic increase in mean necrotic area formation. They conclude that dramatic increase in necrotic core formation is due to a role of p38α MAPK in suppressing ER-stress induced macrophage apoptosis, subsequently promoting plaque necrosis and advanced atherosclerotic lesions. However, these findings are controversial since many studies have shown that apoptosis of macrophages can be beneficial in atherosclerosis by reducing plaque size [178, 179]. For example, administration of TRAIL to diabetic ApoE knockout mice induces apoptosis in established plaques, with most dying cells being macrophages and leads to reduced plaque size and less inflammation [178]. Also, macrophage death on its own is not adequate to increase necrotic core formation, requiring other processes including accumulation of both intracellular and extracellular lipid and death of a number of cell types, like vascular smooth muscle cell (VSMC) apoptosis. VSMC apoptosis has been shown to effectively increase necrotic core sizes (by more than 200% in some studies), in the absence of macrophage apoptosis [180, 181]. Indeed, when quantifying necrotic core formation, collagen content and foam cell content in our mice, we did not observe the effects described by Seimon, T.A *et al.* 2009.

3.1.1.5 Can JNK2 Overexpression and Activation Counterbalance the Effect of p38α MAPK Ablation?

In conclusion, our results suggest that p38α MAPK in macrophages does not play a significant role in atherosclerosis development. As this result is puzzling, since it does not correspond to the studies carried out in *vitro* thus far with p38-specific inhibitors, we can hypothesize that this is the case either because a systemic effect of p38 inhibition is required to cause a significant effect in atherosclerosis development, or p38 has a more pronounced role with respect to atherosclerosis in another cell type involved in this disease, like vascular smooth muscle cells, e.g., where it has been described to be involved in their migration and proliferation [127]. Finally, it could be that the effects observed by these inhibitors are not so specific for p38α MAPK but can also act on other kinases, like JNK2, as has been previously described 47,182, where higher concentrations of the inhibitor also inhibited JNK2

phosphorylation, but not JNK1[30]. This could be particularly important in the development of atherosclerosis, since JNK2 but not JNK1 has also been shown to have a significant role in atherosclerosis development by promoting foam cell formation [155]. Since ablation of p38α MAPK leads to hyperactivation of JNK2 [28,75], maybe this could lead to increased atherosclerosis development and counteract the reduction that is expected by diminishing p38α MAPK expression. This effect is probably missed in experiments with small molecule inhibitors if they also cause a reduction in the activation of other kinases like JNK2.

3.1.2 p38α MAPK in Endothelial Cells

3.1.2.1 p38α MAPK Depletion in Endothelial Cells Leads to Reduction of Expression in Atherosclerosis Markers like VCAM-1, *in vitro*

Endothelial cells form the 'first line' of combat in the development of atherosclerosis. When activated by various factors like oxLDL and cytokines (e.g. TNF and IL-1beta), they can express adhesion molecules and chemokines that recruit monocytes and T-cells to the arterial intima. One of the roles that has been attributed to p38α MAPK in endothelial cell activation is the regulation of adhesion molecule expression like VCAM-1 [61, 183] and expression of various proinflammatory cytokines and chemokines [3,7,63, 184]. Also, stimulation of endothelial cells with oxLDL has been shown to lead to activation of p38 via phosphorylation 185. For this reason we stimulated primary lung endothelial cells *in vitro* with oxLDL and tested with real-time PCR (qRT-PCR) the expression of a panel of cytokines, chemokines and adhesion molecules known to be involved in atherosclerosis development but also regulated by p38α MAPK, on RNA isolated from these cells. mRNA levels of VCAM-1, an endothelial adhesion molecule known to be regulated synergistically by p38α MAPK and NF-kappaB 186 and is important for atherosclerosis development [187, 188] was strongly reduced in oxLDL stimulated p38α MAPK knockout primary lung endothelial cells compared to wild-type cells. Gro-KC, deficiency of which has been associated with a loss of intimal macrophages and attenuated disease progression throughout time within established fatty streak lesions [173] was also strongly reduced. IP-10, an IFN-gamma inducible chemokine, was also significantly reduced. This chemokine has been shown to be highly and differentially expressed by human atheroma-associated cells

within lesions 189 and to attenuate atherosclerosis development in ApoE deficient mice by diminishing the influx of effector T-cells, thereby correcting the local balance with regulatory T-cells 190. Finally, MCP-1 that is a molecule critical for the initiation and development of atherosclerosis since it recruits monocytes and macrophages to the vessel wall via its receptor CCR2 was also significantly downregulated upon oxLDL stimulation. Studies with both MCP-1 and CCR2 deficient mice [191, 192] have both shown a marked decrease in lesion formation, highlighting the importance of this molecule in this disease. Again, like in our *in vitro* experiments with p38α MAPK knockout macrophages, these results pointed towards a pro-atherogenic role for this molecule in the endothelium. More specifically, it seemed to be involved in the recruitment of monocytes and macrophages into the arterial intima.

3.1.2.2 Downregulation of JNK Activation Caused by p38α MAPK Ablation

The MAPK JNK, also a stress-activated kinase like p38 MAPK has also been implicated in atherosclerosis development, with respect to endothelial cell function. Several laboratories have previously reported a possible role for JNK in endothelial cell activation [193, 194, 195]. It has been implicated in the expression of adhesion molecules by the endothelium, like E-selectin, ICAM-1 and VCAM-1, just like p38α MAPK [196, 197, 198, 199]. Since it has previously been shown that ablation of p38α MAPK in many cell types, including macrophages and liver cells[28, 75], can lead to increased activation of JNK therefore suggesting a role for p38α MAPK in the regulation of this molecule, we decided to examine JNK activation in p38α MAPK deficient endothelial cells. This was a concern for us since JNK has also been implicated in atherosclerosis development [155], and its hyperactivation in the absence of MAPK as we previously hypothesized for macrophages, could counterbalance the effect of p38α MAPK ablation. According to the results obtained from JNK knockout mice, ablation of this protein did not appear to severely affect endothelial cells 200, but nevertheless we stimulated primary lung endothelial cells with oxLDL and examined the phosphorylation of JNK. Surprisingly, immunoblotting for p-JNK showed decreased activation in cells where p38α MAPK had been deleted with HTNC treatment. This downregulation of JNK provided further evidence that p38α MAPK may have a pro-atherogenic role in endothelial cells, and in addition to promoting atherosclerosis itself, could also work to regulate other kinases involved in

atherosclerosis development. This result also excluded the possibility that hyperactivation of JNK could counterbalance the effects exerted by ablation of p38α MAPK in endothelial cells.

3.1.2.3 *In vivo* Endothelial-Cell Depletion of p38α MAPK Did not Have a Significant Effect on Atherosclerosis Development

Our *in vitro* results, with primary lung endothelial cells as described above pointed us towards a pro-atherogenic role for p38α MAPK, since its ablation resulted in the downregulation of expression of markers of atherosclerosis, such as VCAM-1. This hypothesis was also backed up by various *in vitro* and *in vivo* studies concerning atherosclerosis development that also delegate a pro-atherogenic role to this molecule in the endothelium, by mediating endothelial dysfunction, an important step in atherosclerosis initiation since it leads to adhesion molecule, proinflammatory cytokine and chemokine expression [201, 61, 63, 133, 134, 135, 136, 28]. For example, selective inhibition of p38 MAPK dose-dependently reduces TNF or LPS-induced ICAM-1 expression in cultured HUVECs 201. Patients with coronary artery disease have a significantly higher basal p38 MAPK phosphorylation and a reduced number of endothelial progenitor cells (EPCs), which are vital for angiogenesis/vascular repair. Inhibition of p38 MAPK with SB203580 (a selective inhibitor for p38α and p38β) or transfection with a dominant-negative p38 MAPK-expressing adenovirus significantly increases the basal number of endothelial progenitor cells in these patients 202. In addition, C-reactive protein inhibits endothelium-dependant NO-mediated dilation in coronary arterioles by activating p38 MAPK and reduced nicotinamide adenine dinucleotide phosphate oxidase 203. Moreover, lysophosphatidylcholine (LysoPC) which is a component of oxLDL induces apoptotic signals in endothelial cells through the p38 signaling pathway, as shown with SB203580 inhibitor studies 204. Finally, activation of p38 MAPK in the endothelium through disturbed blood flow, an important component in atherosclerosis determining where lesions occur in the aorta, can lead to VCAM-1 expression through an AKS1–dependant pathway, promoting leukocyte adhesion, inflammation and atherosclerosis 205.

Despite all these studies attributing a pro-atherogenic role to this molecule, when analyzing male and female littermates for atherosclerosis development after 10

weeks of cholesterol rich 'western diet', we did not observe any significant differences either in plaque size at the aortic sinuses or lesion size in the whole aorta. Furthermore, characterization of the stage of the plaques in the two different genotypes did not reveal any differences either in foam cell formation, collagen content or necrotic core formation, which are all characteristics of advanced plaques. A final confirmation to the fact that there was no apparent effect of the endothelial-specific deletion of p38α MAPK in atherosclerosis development compared to their $ApoE^{-/-}$ littermates was the absence of differences in cytokine chemokine and adhesion molecule expression.

3.1.2.4 Opposing Role of p38α MAPK in the Endothelium in Atherosclerosis Development Could Account for the Lack of Phenotype in $p38\alpha^{EC\text{-}KO}/ApoE^{-/-}$ Mice

In conclusion, as for the macrophage-specific knockout of p38α MAPK, endothelial-specific ablation of this protein does not affect atherosclerosis development either. This result could possibly be explained by the fact that there have also been several studies published, that attribute an opposing, i.e. atheroprotective role, to p38 MAPK in the endothelium, and that these opposing effects counterbalance its pro-atherogenic effect. For example, sheer stress can also lead to the upregulation of the Unfolded Protein Response (UPR) regulator, GRP78, by an α2β1-dependant mechanism in endothelial cells [206, 207]. Also, in response to flavonoids like black tea polyphenols, p38 MAPK activates eNOS in endothelial cells by an estrogen receptor a-dependant pathway, leading to increased NO production and thereby improved endothelial function 208. From these studies, and our results, we can see that p38α MAPK signaling in the endothelium, with respect to atherosclerosis, is much more complex than expected. So, it could be that when deleting p38α we don't only remove its pro-atherogenic, but also its atheroprotective effects, and this is why we do not see any differences in the phenotype of endothelial-specific knockout mice compared to wild-type mice after 10 weeks of a cholesterol rich 'western diet'.

3.2 The Generation of p38αCA and p38αKD Mice

The two new p38α MAPK mouse models, p38αCA and p38αKD described in this study, were initially generated to complement our studies with the ApoE$^{-/-}$ mouse model in atherosclerosis. However, both of these mouse models can be utilized for other exciting studies that will allow us to shed light and elucidate further the function and signaling pathways this molecule is involved in, in a variety of diseases and in specific cell types since both the constitutively active but also the kinase dead form of p38α MAPK are only activated in the presence of the Cre recombinase.

3.2.1 p38αCA Mice and their Applications

In this study, by taking advantage of two point mutations (D176A and Y323L), previously described in the p38 yeast homologue Hog1 to render this protein catalytically and biologically active [146, 156], we generated a mutant form of p38α MAPK that appears to be 3~5-fold more active than the native p38α MAPK in the complete absence of any upstream activators or external stimuli. The advantage of generating a mouse model where a specific MAPK is hyperactivated is the fact that we can follow the biochemical and physiological consequences of the specific MAPK more closely. This is because we do not require an extracellular stimulus or to express an active form of a component that functions upstream of that MAPK, therefore activating more than one MAPK and evoking many cellular responses. We have now generated mice carrying this hyperactive form of p38α MAPK in the ROSA26 locus, and have already established GFP expression in hepatocytes of mice crossed to the AlfpCre line that is only expressed once Cre recombination has occurred as previously described. Once we have also established the higher activation of this protein compared to wild-type p38α MAPK by performing kinase assays, these mice will be a very useful tool in many applications. Some of examples of possible applications are described below.

An interesting study where this new mouse model can be utilized is in the elucidation of the mechanisms via which p38α MAPK mediates cell survival, which has not been studied thus far, as opposed to its well known role in cell death 209 Also, since p38 MAPK is mostly considered to be associated with cell death, it is also important to answer the question as to how it discriminates its targets to mediate cell-death from

those to mediate cell survival. Finally, the p38αCA model is also an invaluable genetic tool that will allow us to obtain mechanistic insights in the tumor suppression function of p38α MAPK. Various mechanistic insights have started to emerge for the past few years concerning this function of p38α MAPK, e.g. liver-specific inactivation of the p38α MAPK pathway showed enhanced hepatocyte proliferation and tumor development that correlated with upregulation of the JNK-cJun pathway, pointing towards a new mechanism whereby p38α MAPK negatively regulates cell proliferation by antagonizing the JNK-c-Jun pathway [71]. However, the right tools in order to obtain a clearer picture of the p38α MAPK specific role in this function are still missing. One of these tools could be the p38αCA mouse model generated in this study.

3.2.2 p38αKD Mice and their Applications

The p38αKD model, as previously described, was generated by inserting a mutation (K53R) into the ATP-binding site of exon 2 of the p38α MAPK allele, which renders the synthesized protein catalytically and biologically inactive. Initial characterization of this mouse model has shown that the inversion of exon 2 to the mutated exon 2 is functional upon cre recombination. What remains to be shown now is the expression levels and the kinase inactivity of p38α MAPK in this model before it can be used for any further studies.

In studies concerned with the kinase function of p38α MAPK, a mouse model expressing a kinase-dead form of p38α MAPK is an invaluable tool, since it can exclude the possibility of compensation by other p38 MAPK isoforms as the protein is synthesized normally but is not catalytically active. This could be an issue when using the knockout model where the protein is not expressed at all. Saying this, the p38αKD model can be used as a genetic tool to confirm the results from studies that have been performed with complete genetic ablation of p38α MAPK. The p38aKD mouse model is also interesting as a genetic tool, because it resembles more closely the effect caused by p38 inhibitors, which exert their effects by inhibiting the catalytic activity of the protein and not by altering its expression levels. Due to this fact, any results obtained with this mouse model, as opposed to models where p38α MAPK

has been deleted, can show a more realistic effect as to what would happen when using p38 inhibitors for the treatment of any number of diseases.

Another intriguing possibility for the p38αKD model is its use in the study of the kinase-independent function of p38α MAPK. Use of RNAi but also small molecule p38 inhibitors to selectively inactivate p38α MAPK has revealed a novel function of this molecule in cell cycle progression that does not require its kinase activity 210. Therefore it appears that p38α MAPK has both kinase activity-dependant and kinase activity-independent functions. The kinase dependant functions of p38α MAPK have been well established, which cannot be said for its kinase-independent function. Saying this, both the p38αCA model together with the p38αKD model can be used, in conjunction with p38α knockout mice, to compare gene expression profiles in native conditions but also under various stimuli.

3.3 Concluding Remarks

In conclusion, we have investigated the macrophage and endothelial specific-role of p38α MAPK in the development of atherosclerosis and shown that it does not play a significant role in this disease, at least in the two cell types examined. In the case of macrophages this could be because of the regulating effect p38α MAPK has on JNK, which has also been shown to be strongly activated in atherosclerosis and to have a significant role in this disease by promoting foam cell formation [155]. In the case of endothelial cells, where ablation of p38α MAPK also showed a reduction in JNK phosphorylation and thus activation, the lack of effect in atherosclerosis development could be due to the opposing roles that have been proposed for p38α MAPK in the endothelium, both pro-atherogenic and atheroprotective. However, this does not exclude the possibility that it can still have an important overall (systemic) role or a more pronounced role in another cell type involved in atherosclerosis development, like vascular smooth muscle cells, e.g., where it has been describe to be involved in their migration and proliferation [127]. The effect of p38α MAPK ablation in other cell types important in atherosclerosis still remains to be investigated.

Finally, we have successfully generated two new mouse models for p38α MAPK, p38αCA and p38αKD that are both invaluable tools for the further elucidation of the pathways this kinase is involved in.

4. Materials and Methods

4.1 Design and Generation of p38αKD and p38αCA Mice

4.1.1 Design and Generation of the Targeting Vectors

4.1.1.1 Design of The Targeting Vectors

p38αKD

The p38αKD (kinase dead) targeting vector was designed to insert a *lox66/lox71* [160] flanked switch cassette (exon 2 and mutated (K53R) exon 2 in opposing orientations) into the mouse p38α (MAPK 14) locus. The pEASY-FLIRT vector (Appendix I) was utilized as a base for generating the p38αKD targeting construct. This vector was initially digested with BamHI/AscI and purified to obtain a vector of 4795 bp that contained a Herpes Simplex virus-thymidine kinase (HSV-TK) cassette for negative selection of clones with random integration of the targeting vector. PCR amplification of the vector pOG45 (plasmid #5, Pasparakis archive) using a 5' primer containing a BamHI-*lox66* sequence (sense) and a 3' primer containing an AscI-SalI-FRT sequence (antisense), generated a fragment containing a neomycin (NEO) resistance gene cassette flanked by two FRT sites. After digestion with BamHI/AscI, this fragment was subcloned into the previously digested pEASY-FLIRT vector. The Left and Right Arms of Homology (LAH and RAH respectively) were obtained from a p38α loxP-flanked targeting vector previously generated in our laboratory. The LAH (3722 bp) was obtained through BamHI digestion and immediately subcloned into the pEASY-FLIRT vector, whereas the RAH (3511 bp) was PCR-amplified with primers containing AscI sites, digested, and subsequently subcloned into the pEASY-FLIRT vector.

The next steps in the generation of the targeting vector involved the insertion of the mutated *lox71* site together with the inverted/mutated (K53R) exon 2 of the murine p38α allele. Initially, the 130 bp exon 2 flanked by 370 bp of intronic sequence on either side, was PCR-amplified with sense and antisense primers both containing a SalI site at the 5' end. The fragment obtained was cloned into the pGEMT-EASY vector (Appendix II), in the orientation of the T7 polymerase. Mutagenesis of the plasmid was performed with PCR to insert a K53R mutation in exon 2, i.e. a lysine residue in the phosphate (ATP) binding pocket responsible for catalytic activity,

mutation of which has previously been shown to render p38α MAPK, and other kinases with this conserved region, catalytically inactive 211,212. The mutated (K53R) exon 2 was then PCR-amplified from the pGEMT-EASY vector with the use of a 5' primer containing the sequence for SpeI-SalI-*lox71*-BamHI-EcoRI and a 3' primer containing the sequence for SpeI. Digestion with SpeI and subcloning of the mutated fragment into the pGEMT-EASY vector containing the original exon 2 (not mutated) yielded a vector containing the original exon 2 and an inverted/mutated (K53R) exon 2 next to each other. This vector was then digested with SalI to extract the fragment containing the exon 2, the inverted/K53R exon 2 and *lox71*. The final targeting vector was obtained by subcloning this last fragment into the pEASY-FLIRT vector described above, to yield a ~15 kb vector (Appendix III). All primers used were obtained from Metabion & Invitrogen, and all restriction enzymes from New England Biolabs.

p38αCA

The p38αCA targeting vector was designed to insert a constitutively active form of p38α MAPK into the mouse ROSA26 locus under the control of the endogenous ROSA26 promoter, but also a CAGS promoter (human cytomegalovirus very immediate early enhancer modified chicken β-actin promoter). The CAGS-ROSA26 plasmid was a kind gift from Dr. Thomas Wuenderlich, from the Institute for Genetics, University of Cologne. The p38α cDNA was obtained from the pCMV5-p38 plasmid kindly donated by the laboratory of Roger Davies, PCR-amplified with primers containing BamHI restriction sites, digested, and subcloned into the pGEX-2T plasmid (Appendix IV). Using the DpnI mutagenesis protocol, five different mutations were inserted into the murine p38α MAPK cDNA, based on previously published mutations of the yeast homologue *Hog1* that were shown to hyperactivate this protein [146,156]. These mutants were tested for activity in two ways. Through an activity assay, where we tested for incorporation of radioactive phosphate in ATF2, a well known substrate of p38 that is activated by phosphorylation, and a dual-luciferase reporter assay (described in another section).The most active mutant, D176A/Y323L, was identified. This was then PCR-amplified from the pGEX-2T vector and subcloned into the ROSA26-CAGS plasmid (Appendix IV), to yield a final targeting vector of ~17kb.

4.1.1.2 Bacterial Cell Transformation

DH5α *E.coli* bacterial cells (stored at -80˚C in 200 µl aliquots) were used for all transformations. Cells were thawed on ice, and 100 µl were mixed with 1-10 µl of ligation reaction. After sitting on ice for 30 mins, they were heat shocked at 42˚C for 60-90 secs, and placed on ice for at least 2 mins. 1 ml of LB broth was added to the transformed bacteria, and they were allowed to grow at 37˚C for 1 hr, rotating. 1/10th of the volume was plated on 10cm^3 bacterial plates containing agar, with the appropriate antibiotic resistance. The remaining volume was then spun down for 15 secs, resuspended, and again plated on 10cm^3 agar plates as above.

4.1.1.3 DNA Minipreps

DNA minipreps were prepared using the High Pure Plasmid Isolation Kit (Roche). According to the manufacturer's instructions, 0.5-4 ml of bacterial culture in LB broth was harvested by centrifuging at 6000xg for 30 secs, and the pellet was resuspended in 250µl suspension buffer/RNAse. The cells were lysed by adding 250µl Lysis Buffer, mixing gently and incubating for 5 mins at room temperature (RT). After 5 mins, 350µl Binding Buffer were added, and the bacterial lysate was mixed gently and allowed to stand on ice for 5 mins. The supernatant was collected after 10 mins of centrifugation at maximum speed, transferred to a High Pure filter tube and centrifuged at maximum speed for 30-60 secs. The flow through was discarded, and the DNA was washed by first adding 500µl Wash Buffer I and centrifuging at 13000xg for 1 min, then adding Wash Buffer II and centrifuging at 13000xg again for 1 min, plus an additional min after discarding the flow through. Finally, the DNA was eluted by adding 100µl Elution Buffer and centrifuging at 13000xg for 1 min.

4.1.1.4 DNA Maxipreps

DNA maxipreps were prepared using the QIAfilter Maxi Kit (Qiagen), according to the manufacturer's protocol. In brief, 100 ml of overnight bacterial cell culture was harvested by centrifuging at 6000xg for 15 mins at 4˚C. The bacterial pellet was homogeneously resuspended in 10ml Buffer P1. Bacteria were lysed by adding 10ml of buffer P2, mixing thoroughly by vigorously inverting 4-6 times and incubating at room temperature for 5 mins, during which the QIAfilter Cartridges were prepared.

After the 5 min incubation, 10 ml of chilled Buffer P3 were added and the lysate was mixed thoroughly by inverting 4-6 times. Clearing of the bacterial lysate was performed by pouring the lysate into the barrel of the QIAfilter Cartridge, incubating at room temperature for 10 mins, and subsequently filtering the lysate into a previously equilibrated QIAGEN-tip 500 (10 ml buffer QBT) by gently inserting the plunger. The cleared lysate was allowed to enter the resin by gravity flow. Washing of the QIAGEN-tip was performed by adding 2 x 10 ml of Buffer QC. The DNA was then eluted for the QIAGEN-tip with 15 ml of Buffer QF, and precipitated by adding 10.5 ml room temperature isopropanol, mixing, and centrifuging at 15000xg for 30 mins at 4˚C. After carefully decanting the supernatant, the pellet was allowed to air-dry for 5-10 mins. Finally, the DNA was redissolved in a suitable volume of buffer (200-300µl). DNA concentration was measured using a photometer.

4.1.1.5 Gel Extraction and PCR Purification

Gel extraction and PCR purifications were performed using the MACHEREY-NAGEL NucleoSpin Extract II Kit. For the gel extraction, the gel was cut out and weighed in a 1.5 ml eppendorf tube. Buffer NT was added at a volume of 200µl/100mg of gel, and the gel was lysed at 50˚ C for 5-10 mins. For the PCR clean up this step was not required. In this case, buffer NT was added at a volume of 200µl/100µl PCR reaction. The DNA solution was then loaded onto the columns provided and centrifuged for 1 min to bind DNA. The silica membrane was washed with 600µl buffer NT3 by centrifuging for 1 min. After discarding the flow-through, the silica membrane was dried by centrifuging for 2 mins. The DNA was eluted by adding 30µl of dH_2O, allowing the column to stand at RT for 1 min, and finally centrifuging again for 1 min. All centrifugation was performed at 11,000xg, RT.

4.1.1.6 Mammalian Cell Transfection

HEK293 (Human Embryonic Kidney cells) cells were used for all mammalian transfections. Transfections were performed with the use of Lipofectamine 2000, a proprietary formulation for the transfection of nucleic acids (DNA and RNA) into eukaryotic cells. HEK293 cells were grown on 6 well plates in DMEM medium, and transfected according to the manufacturer's protocol, in serum free medium. 4µg of DNA was diluted in 50µl serum free medium, and mixed gently. 10µl of

Lipofectamine were diluted in 50µl serum free medium and incubated for 5 mins at RT. After 5 mins of incubation, the diluted DNA was combined with the Lipofectamine to give a total volume of 100µl. This solution was then mixed gently and incubated at RT for a further 20 mins, for the DNA to form complexes (micelles) with the Lipofectamine. After 20 mins, the 100µl of complexes were added to each well containing cells and 2ml serum free medium, and mixed gently by rocking. The cells were then incubated at 37˚C in a CO_2 incubator for 18-48 hrs prior to testing for the transgene expression. The medium was changed after 4-6 hrs.

4.1.1.7 p38 MAPK *in vitro* Kinase Assay

Kinase assays were carried out using 0.2-0.4µg purified p38α MAPK, p38α MAPK mutants, or immunoprecipitates containing activated kinases were performed at 37˚C for 20 mins using 5µg of substrate (ATF2), 250µM ATP, and 10µCi of [γ-^{32}P] ATP in 20µl of kinase buffer (20mM Hepes, pH 7.6, 20mM $MgCl_2$, 25mM β-glycerophosphate, 0.1mM Na_3VO_4, and 2mM dithiothreitol (DTT)). The reactions were terminated with Laemmli sample buffer, and the products were resolved by SDS-PAGE and analyzed by autoradiography. The extent of ATF2 phosphorylation was quantified by phosphoimaging [157].

4.1.1.8 Protein Immunoprecipitation

HEK293 cells previously transfected with the wild-type and p38α MAPK mutants (pIRESPURO vector, Appendix VI) as described in the 'Mammalian Cell Transfection' section, were lysed in 1ml NP40 buffer (50 mM Tris-HCl pH 7.5, 150mM NaCl, 1% NP40, 50mM NaF, 1mM $NaVO_3$, 1mM DTT, 1mM EDTA, Complete tablet (Roche)), by rotating on a wheel at 4˚C for 1hr. After 1hr, the cytoplasmic protein extract was collected by centrifuging at 14000rpm/4˚C/10 mins to remove nuclei. Antibody was added to the cell lysates after determining protein concentration (use approximately 1 mg protein/IP), and the mix was incubated overnight at ˚C on a rotating wheel. The next day, pre-washed (2 x NP40 buffer) protein G beads were added to the protein/antibody mix (40µl 50% bead slurry / 200µl lysate) and incubated for 1hr at 4˚C on a rotating wheel. Washing 3x with 200µl NP40 buffer (without protease inhibitors) was performed by rotating for 10 mins at 4˚C and subsequently centrifuging at 1200 rpm for 5 mins. The final bead

pellet was resuspended in 50% NP40 buffer. 20μl samples were kept throughout the procedure to check immunoprecipitation efficiency with western blotting.

4.1.1.9 Isolation of Nuclear and Cytosolic Protein Extracts

In order to prepare nuclear and cytosolic extracts, cells were centrifuged and resuspended in 0.5-1ml PBS, transferred to an eppendorf tube, on ice, and centrifuged at 6000 rpm for 1 min. The pellet was resuspended in 50-100μl buffer A (10mM HEPES pH 7.6, 10mM KCl, 2mM $MgCl_2$ and 0.1mM EDTA) and incubated at 4˚C for 10 mins (swelling step). Cells were lysed by adding 3.5μl/50μl of 10% NP40, mixed, and incubated at 4˚C for 1 min. The cytoplasmic fraction was recovered by centrifuging at 14000 rpm/4˚C/1min and collecting the supernatant. The remaining pellet was washed by resuspending in 50μl of buffer A and centrifuging 14000rpm/15secs/4˚C. The supernatant was discarded and the nuclear fraction was extracted by adding 40μl buffer C (50mM HEPES pH 7.8, 50mM KCl, 300mM NaCl, 0.1mM EDTA and 10% glycerol) to the pellet, resuspending it gently and incubating on ice for 30 mins. After 30 mins, the nuclear fraction was recovered by centrifuging at 14000rpm/5-10mins/4˚C, and collecting the supernatant.

4.1.1.10 Dual-Luciferase Reporter Assay

The dual luciferase system (Promega) was used to perform a reporter gene assay for p38 mutants in mammalian (HEK293) cells. In brief, HEK293 cells were grown and maintained at 37˚C in a CO_2 incubator, in DMEM. Fresh medium was added 4 hrs before the cells were co-transfected, as described in the 'Mammalian Cell Transfection' section, with wild-type or mutant p38α previously subcloned into the pIRESPURO vector, and the GAL4-responsive luciferase plasmids (kind gift from Dr. Jun Gu, Beijing University). Luciferase activity was measured 24 hrs later after transfection following the manufacturer's instructions.

4.1.1.11 DpnI Mediated Site-Directed Mutagenesis

Mutagenesis of the p38α cDNA was performed in the pGEX-2T vector, according to the DpnI mutagenesis protocol, using the primers listed below. The primers were designed according to the QuickChange Site-Directed Mutagenesis Kit, where it is stated that the primers should be between 25 and 45 bases in length and the melting temperature (Tm) should be greater than or equal to 78˚C.

Forward (sense) primers

Mutation	Primer sequence (5'-3')	Length (bp)	Tm (˚C)
F327L	gac cct tat gac cag tcc ttA gaa agc agg gac c	34	80.41
Y323L	gat gag cct gtt gct gac cct tTA gac cag tcc ttt gaa agc	42	81.17
D176A	ggc tgg ctc ggc aca ctg CAg at gaga tga cag g	34	79.87

Reverse (antisense) primers

Mutation	Primer sequence (5'-3')	Length (bp)	Tm (˚C)
F327L	ggt ccc tgc ttt cTa agg act ggt cat aag ggt c	34	80.41
Y323L	gct ttc aaa gga ctg gtc TAa agg gtc agc aac agg ctc atc	42	81.17
D176A	cct gtc atc tca tcT Gca gtg tgc cga gcc agc c	34	79.87

Mutagenesis of the p38α cDNA was performed by amplification in the pGEX-2T vector using the primers listed above. The reaction was setup as follows:

	1x reaction (µl)
DNA template plasmid	0.5 (5-20ng)
10µM Forward primer	0.5
10µM Reverse primer	0.5
Accuprime™ *Pfx* Supermix (Invitrogen)	22.5
Total reaction volume	**24**

The PCR conditions used for the amplification are listed below:

95 ˚C	30 sec	
95 ˚C 55 ˚C 68 ˚C	30 sec 1 min 12 mins	18 x

After amplification, the methylated (parental) DNA was degraded with DpnI. This was accomplished by adding 1µl DpnI (10 units) to each PCR reaction and incubating at 37˚C for 1 hr. The mutated vectors were then transformed into DH5α *E.coli* cells as described in the bacterial transformation section. Minipreps from 6 colonies were prepared for each mutation and sequenced to confirm the change.

4.1.1.12 Sequencing

All sequencing reactions were performed at the sequencing facility, at the Institute for Genetics, University of Cologne. The reactions and PCR programme used to amplify DNA for sequencing are listed below.

1 x reaction

10µM primer	2
Big Dye Terminator (Applied Biosystems)	6
Template DNA	1
dH2O	11
Total reaction volume	**20**

PCR programme

95 ˚C	5 mins	
95 ˚C 52 ˚C 60 ˚C	15 sec 15 sec 3 mins	32 x

4.1.1.13 GST (Glutathione S-Transferase)-Purification of p38α MAPK Mutants for Activity Assays

The p38α MAPK cDNA, as described above, was subcloned into the pGEX-2T vector, a GST Gene Fusion Vector that is specifically designed for high-level intracellular expression of genes or gene fragments as fusions with *Schistostoma japonicum* glutathione S-transferase. All p38α MAPK mutants were generated using this vector. Purification of GST-fused proteins was performed using Glutathione Sepharose 4B (Amersham Biosciences), designed for rapid single step purification of recombinant derivatives of glutathione S-transferases or glutathione dependant proteins. Frozen DH5α bacterial cell pellets were resuspended in 10 ml lysis buffer (0.1% Tx-100, 1mM EDTA and Complete protease tablet (1 tablet/50 ml), in PBS). Cells were then sonicated with MS72 tip 2 x 30 secs and dounced 20 times. This step was repeated twice. An aliquot of the lysate was centrifuged 30 mins/9000rpm/4˚C. In the meantime, 500µl of bead glutathione bead slurry/ p38α

mutant was washed with 5 ml lysis buffer by centrifuging 5 mins, 1000 rpm. The supernatant of the previously centrifuged bacterial lysate was then added to the beads in a 15 ml Falcon tube, and the mix was rotated on a wheal at 4˚C for 1 hr, so the GST-fused proteins could bind to the beads. After 1hr, the beads were centrifuged 700rpm/5mins/4˚C. The supernatant was removed, and the beads were transferred into columns and washed extensively with lysis buffer without protease inhibitors. The last washes (5 ml) were performed in PBS with 1mM EDTA. GST-fused proteins were eluted in 0.5 ml fractions with 20mM in PBS and 1mM EDTA. Samples were kept at all steps of the purification protocol. After running samples on an SDS gel, samples positive for the desired protein were pooled, dialyzed overnight in PBS at 4˚C, snap frozen in liquid nitrogen and stored at -80˚C.

4.1.2 Transfection of ES Cells

Bruce-4 Embryonic stem cells (ES) derived from C57BL/6 mice were grown on Mitomycin treated murine embryonic fibroblasts (feeder cells), previously plated on 0.2% gelatin coated $10cm^3$ dishes in ES cell medium (Knockout-DMEM containing 15% FCS (Fetal Calf Serum), 2mM L-glutamine, 0.1 mM non-essential amino acids, 0.1% mM β-mercaptoethanol, 100u/ml penicillin/streptomycin, 1000u/ml LIF (Leukemia Inhibitory Factor)) at 37% in a CO_2 incubator.

Before transfection, cells were washed twice with PBS, harvested by trypsinization and resuspended in PBS at a final concentration of 1.25×10^7 cells/ml. 0.8 ml of the cell suspension were mixed with 25µg of the linearized targeting vector in a sterile 1.5 ml tube, and allowed to stand for 5 mins at room temperature. The suspension was transferred to an electroporation cuvette and the cells were electroporated using the Bio-Rad Gene Pulser Xcellset at 230V, 500µF for one pulse (8.3 ms) at RT. After pulsing, the cell suspension was diluted in complete ES medium and plated on three $10cm^3$ dishes containing feeder cells. Neomycin selection started 24 hrs after electroporation by applying 0.2mg/ml G418, on both p38αKD and p38αCA transfected ES cells. Negative selection (thymidine kinase) started 6 days after electroporation by applying 2×10^{-6} Ganciclovir to p38αKD transfected cells only.

4.1.3 Picking of Clones

ES cells were fed every day with complete ES medium. After having reached a visible size (normally 8 days) single cell clones were picked and expanded in 96-well plates on feeders in selection medium. Once the cells approached confluency, they were washed twice with PBS and trypsinized with 25µl trypsin-EDTA for 5mins at 37˚C. 100µl of ES medium was added in each well, cells were dissociated by vigorous pipetting and the content of each well was split in three feeder cell containing 96-well plates. From these plates, two were frozen at -80˚C 24 and 48hrs later, and one was further split into three gelatinized 96-well plates without feeders for DNA analysis.

4.1.4 Preparation of DNA and Southern Blot Analysis

In order to prepare genomic DNA from ES cell clones, cells were grown until fully confluent in gelatinized 96-well plates, washed with PBS and lysed with 50µl lysis buffer (10mM NaCl, 10mM Tris-HCl pH 7.5, 10mM EDTA, 0.5% Sarcosyl, 0.4-1mg/ml freshly added proteinase K) overnight at 56˚C in a humidified chamber. The next day, the box was cooled for 1hr at RT and genomic DNA was precipitated by adding 100µl of 100% EtOH to each well and allowing it to stand for 1-2hrs at RT. Once the filamentous DNA was visible, the plate was gently inverted to remove the EtOH, washed with 70% EtOH and air dried for 15 mins. Finally, the DNA was dissolved in 35µl of the digestion mix (1X restriction buffer, 1mM spermidine, 1mM DTT, 100µg/ml BSA, 50µg/ml RNase A and 50U of restriction enzyme/reaction) and incubated overnight at the appropriate temperature (37˚C) in a humidified atmosphere. The DNA fragments were separated on a 0.8% agarose gel that was denatured by soaking it for 45 mins in Denaturing solution (0.4M NaOH, 0.7% NaCl) and transferred overnight by capillary flow onto the surface of a charged nylon membrane (Hybond-XL, Amersham). The following day, the membrane was soaked for 2 mins in Neutralization solution (0.5M Tris-HCl pH 7.0), baked at 70˚C for 1 hr and pre-incubated in hybridization buffer (1M NaCl, 50Mm Tris-HCl pH, 10% dextransulphate, 1% SDS, 250µg/ml Salmon Sperm DNA) at 65˚C for 1hr. DNA probes labeled by random priming with 32Pα-dGTP were added to the hybridization buffer and allowed to hybridize to the membrane overnight at 65˚C. The next day the

membrane was washed in wash buffer (1mM EDTA, 40Mm Na-phosphate pH 7.2, 1% SDS) at 65˚C and exposed to autoradiographic film.

4.1.5 Screening for Positive ES Cell Clones

Out of 384 G418 and gancyclovir-resistant clones, 4 were identified as homologous recombinants by Southern Blot analysis of ES cell DNA digested with BamHI and probed with a 5' and 3' probe, for p38αKD. For p38αCA we identified 9 clones positive out of 192 picked clones where homologous recombination had occurred, by Southern blot analysis of ES cell DNA digested with EcoRI and probed with a R26 5' probe. DNA fragments used as probes for the p38αKD targeting were amplified from a BAC containing the murine p38α MAPK gene. The 700 bp DNA fragment used as a 5' probe for the p38αCA targeting was digested from the Orlein plasmid, with an EcoRI/PacI digestion. A NEO probe was also used in both cases to check for random integration.

For the p38αCA targeting, positive clones were also confirmed by treating ES cells *in vitro* with HTNC and looking at GFP expression by FACS analysis, as described in another section below.

The sequences of the primers and PCR programme used to amplify the probes for the p38αKD targeting are listed below. All probes were amplified using the Accuprime™ *Pfx* Supermix (Invitrogen).

Primers

Primer	Sequence (5'-3')	Length (bp)	Tm (˚C)
5' probe sense	GAT AGG GAG AGG AAG CAG CAT GTT AG	26	60
5' probe antisense	CAT GGA GGC CAT TCG TCG AGT GAG ATA C	28	60
3' probe sense	GTT CTA GGA CAG CCA GGG TTA CAC AGA G	28	63
3' probe antisense	GTG AGA GAG AAT CCT TCC AGC CCC TTA C	28	63

PCR Programme

95 ˚C	5 mins	
95 ˚C 55 ˚C 68 ˚C	15 secs 30 secs 30 secs	35 x

4.1.5.1 HTNC Treatment and FACS Analysis of p38αCA Targeted ES Cells

ES cells transfected with the p38αCA targeting vector, and found positive for homologous recombination with Southern Blotting analysis, were plated on 6-well plates on a confluent layer of Mitomycin-treated feeder cells, at a confluency of 2 x 10^5 cells/well. After allowing the cells to attach for 5 hrs, they were washed twice with PBS, and 5 or 10µM HTNC was added in Knockout-DMEM/PBS 1:1, supplemented with 100U/ml penicillin/streptomycin, for 16-20 hrs. Controls were ES cells treated with Knockout-DMEM/PBS 1:1, without HTNC. After 16-20 hrs, the cells were washed twice with PBS again and allowed to recover for 2-3 days in complete ES cell medium. On day 3, the cells were scraped off in PBS and FACS analysis was performed for GFP expression.

4.1.6 Blastocyst Injections and Germline Transmission

Chimeric mice were generated by injection of positive ES cell clones (still containing the NEO cassette) into blastocysts from C57Bl/6 or CB20 mice. Matings of male chimeras to C57Bl/6 females yielded offspring with germline transmission. p38αKD$^{FL/wt}$ mice were generated by crossing p38αKD$^{NEOFL/wt}$ mice with Flp-Deleter mice to remove the NEO cassette. p38αKD$^{FL/FL}$ mice are now being generated by crossing p38αKD$^{FL/wt}$ mice with each other. For the p38αCA mice, the NEO cassette was not necessary to remove. R26wt/p38αCA$^{FL/}$ mice are currently being crossed with Cre-Deleter mice, but also Alfp- Cre mice. Hepatocytes were isolated from R26wt/p38αCA^{FL} positive for AlfpCre (R26wt/p38αCA^{LPC-KO}) to examine GFP expression.

4.1.6.1 Hepatocyte Isolation from R26wt/p38αCA^{LPC-KO} Mice for FACS Analysis

Mice used for the isolation of hepatocytes were anaesthetized with Ketamin/Rompum (Avertin) (~ 12μl/gr bodyweight) and the abdominal cavity was opened. A bornyle was passed into the vena cava and connected with a pump, once the bornyle had been filled with blood in order to avoid bubbles. After cutting the portal vein, mice were perfused with Solution I (EBSS -Ca/+Mg (GIBCO), 0.5mM EGTA) at a speed of 7-8 for 20 secs. Once the liver had turned pale (within secs), the perfusion rate was reduced to a speed of 5 and perfusion was allowed to go on for 5 more mins. After 5 mins, the pump was stopped, the solution was exchanged for 50 ml Solution III (Solution II, Collagenase Type II (Worthington) and trypsin inhibitor (Sigma)) and the perfusion was restarted at a speed of 4-5. After perfusing with 50ml Solution III the liver was extracted and transferred into ~10ml of ice cold Solution II (EBSS +Ca/+Mg (GIBCO), 10mM HEPES). In a petri dish, the capsule of the liver was peeled away and the cells were carefully brushed out with a cell scraper. The cells were then passed through a 22μm nylon mesh and spun at 500 rpm for 5 mins. After washing 2x with high glucose DMEM or Williams E (5% FCS), the viable cells were counted and seeded at a density of ~ $2.5x10^5$ cells per 6-well collagen coated plate or immediately used for FACS analysis. The medium on the seeded cells was changed after 4 hrs.

4.2 Generation and Analysis of Macrophage and Endothelial-Specific p38α MAPK Knockout Mice in Atherosclerosis

4.2.1 Generation of Mice for Atherosclerosis Studies and Diet

The p38α MAPK mice with loxP-flanked alleles used in this study were previously described elsewhere [75]. p38α^{FL} mice were crossed with LysMCre [147] and Tie2ER^{T2}Cre [74] transgenic mice to generate myeloid and endothelial cell-specific knockouts, respectively. These mice were then crossed into ApoE$^{-/-}$ mice to render them susceptible to atherosclerosis development. For induction of Cre activity, mice carrying the Tie2-ER^{T2} transgene and their Cre negative littermates were fed a tamoxifen-containing diet as has been previously described 213. At the age of 6-8 weeks in both models, male and female littermates were placed on a cholesterol rich 'western–type' diet (Harland Tekland) for 10 weeks, to develop atherosclerosis. All animal procedures were conducted in accordance with European, national, and institutional guidelines, and protocols and were approved by local governmental authorities.

4.2.2 Analysis of Atherosclerosis

4.2.2.1 Histology of Plaques and Lesion Size

Consecutive 7 µm sections of the heart in the atrioventricular valve region were collected and stained with toluidine blue, as described previously (Kanters et al., 2003). For morphometric analysis lesion size was measured on four consecutive sections in 42 µM intervals using Adobe Photoshop.

4.2.2.2 *En face* Analysis of Atherosclerosis

Sudan IV staining and *en face* analysis of atherosclerotic lesions were performed as described previously by Holman et al., 1958 214. Plaque areas were quantified with Adobe Photoshop.

4.2.2.3 Lipid Analysis

Cholesterol measurements were performed using the CHOL reagent (Roche) and reading absorbance at 500 nm, on plasma, after overnight fasting.

4.2.2.4 Immunostainings

Frozen sections of the aortic root were fixed in ice-cold acetone for 10 minutes, dried under a ventilator, and washed with PBS. Sections were blocked in 4% fetal calf serum (FCS) with Avidin D solution (Avidin/Biotin Blocking Kit; Vector Laboratories) for 30 mins. Primary antibodies were incubated for 60 minutes (anti-mouse macrophages/ monocytes MCA519GT, rat, 1:1000 dilution, Serotec) in 4% FCS solution with Biotin (Avidin/Biotin Blocking Kit; Vector Laboratories). Sections were washed with PBS and incubated with Biotin-conjugated secondary antibody rabbit anti-rat/ biotinylated E0468, 1:100, DakoCytomation) in 4% FCS/ 2% normal mouse serum (NMS) for 60 minutes. After washing, sections were further incubated in a 1:50 Avidin/ 1:50 Biotin solution in PBS (Vectastain ABC Kit, Vector Laboratories). Sections were washed again and staining was visualized by incubation with AEC (AEC Kit, Vector Laboratories) and counterstaining with haematoxylin. Mounting of the sections was performed with Entellon (MERCK) mounting medium.

Staining for collagen on frozen sections of the aortic root was performed by using the Masson Trichrome staining kit (Sigma Aldrich) according to the instructions of the manufacturer.

4.2.2.5 Quantitative Real-Time PCR

RNA was isolated from aortas, but also macrophages and endothelial cells in *in vitro* experiments, using Trizol-reagent (Invitrogen) and RNeasy columns (QIAGEN). RNA (1 µg) was used for reverse transcription with SuperScript III reverse transcriptase (Invitrogen). The reaction was topped up to 200 µl with water, and 2 µl were used for quantitative real-time PCR reaction either with Power SYBR Green Kit (Applied Biosystems) or with TaqMan qPCR Kit from Eurogentec. Standardization was performed with primers for ubiquitin (SYBR Green) or GAPDH (TaqMan). VCAM-1, IL-1β, TNF, RANTES, MCP-1, MIP-1α, MIP-1β, MIP-2α, MCP-3, MMP-13, IP-10, IL-6, etc. were quantified with the respective TaqMan probes from Applied Biosystems. The other primer sequences are available upon request.

4.2.3 *In vitro* Experiments

4.2.3.1 Cell Culture

Bone marrow-derived macrophages

Bone marrow–derived macrophages (BMDM) were obtained according to standard procedures described elsewhere 215. Bone marrow cells were subjected to red blood cell lysis and plated on 10 cm^3 bacterial Petri dishes (Greiner) in RPMI Glutamax (Invitrogen) supplemented with 10% FCS penicillin/streptomycin and 20% L929 conditioned medium. The cells were cultured for 8 days before experiments were performed.

Thioglycolate-elicited peritoneal macrophages

For isolation of thioglycolate-elicited peritoneal macrophages, mice were injected intraperitoneally with 1 ml of sterile thioglycollate broth (4% wt/vol). After 3-4 days, cells were isolated by flushing the peritoneum with 8 ml ice-cold PBS. Red blood cells were lysed and the remaining cells were extensively washed using ice-cold PBS. Cells were seeded on bacterial Petri dishes (Greiner).

Lung endothelial cells

After perfusion with PBS, lungs were dissected from mice, passed through 75% ethanol for 10 secs and placed in fresh DMEM (Gibco). Using a blade, the lungs were cut into very small pieces to produce a pate consistency and subsequently incubated in 0.2% collagenase (Gibco) in DPBS+ $CaCl_2$ (Gibco) for 1hr at 37˚ C. After 1 hr, the solution was passed through a 19G needle to break down remaining tissue and passed through a 70μM cell strainer. The cell suspension was then centrifuged at 1500 rpm for 5 mins. The remaining pellet was resuspended in endothelial cell medium (DMEM low glucose: Ham's F-12 1:1, 20% FCS, 50μg/ml endothelial mitogen, 25μg/ ml heparin, 100U/ml penicillin/streptomycin and 2mM glutamine) and plated on a T75 flask (Corning) previously coated with coating medium (0.1% gelatin, 1. A negative (LEAF rat anti-mouse CD16/32, 1:2000 dilution, Biolegend) and positive (CD102 rat anti-mouse, 1.5:2000 dilution, BD Biosciences) sort with Dynabeads (sheep anti-rat IgG, Invitrogen) allowed us to obtain pure populations of endothelial cells. Purity of endothelial cell population was assessed by

staining with the mouse endothelial cell marker CD146 (Miltenyi Biotec) and performing FACS analysis.

4.2.3.2 Oxidized LDL Stimulation

Oxidation and fluorescence labeling of LDL

LDL was oxidized (oxLDL) as previously described 216. Briefly, human LDL (600 µl of 250 µg/ml) (Applichem) was incubated with $CuSO_4$ (22.5 µl of 1.6mM) in PBS for 9hrs at 37°C. The oxidation reaction was stopped with an excess of EDTA (100 µl of 0.5 M), and the LDL was dialyzed O/N in PBS at 4 °C. For assessment of oxLDL uptake in macrophages by FACS analysis, oxLDL was subsequently labeled with DiI 217 for 18 hrs at 37°C by adding 300µg DiI in DMSO/ mg LDL. The oxLDL-DiI solution was then dialyzed against PBS O/N at 4 °C and the next day centrifuged at 10.000 rpm/15 mins to remove any precipitate.

OxLDL stimulation of peritoneal macrophages

OxLDL stimulation of peritoneal macrophages was performed as described previously [155]. Briefly, Thioglycolate-elicited peritoneal macrophages were plated on 6 well bacterial plates in RPMI 1640 medium supplied with 10% FCS. After 2 hours, non-adherent cells were washed out and macrophages were starved for 48h. Then, fluorescence-labeled oxLDL (DiI-oxLDL) (50µg/ml) (Applichem) was added to the medium. After 2.5 hours cells were stained overnight with Oil-red O and costained with hematoxylin for 20 seconds to visualize foam cell formation. Uptake of oxLDL was quantified by FACs analysis. Scavenger receptor and cytokine, chemokine and MMP expression was assessed by collecting RNA and performing RT-PCR as described previously.

OxLDL stimulation of lung endothelial cells

Lung endothelial cells were isolated from $p38\alpha^{FL/FL}$/$ApoE^{-/-}$ mice as described above. At passage 8, they were either treated or not treated with HTNC overnight (16 hrs) in DMEM (low glucose): PBS 1:1 with 100U/ml penicillin/streptomycin. The next day HTNC was removed and replaced with normal endothelial cell medium. The cells were allowed to reach confluency and split 1-2 more timed before being used for any

experiments to ensure that they were not previously activated due to the Cre. For oxLDL stimulation, the cells were starved overnight in starving medium (endothelial cell medium supplemented with 2% FCS, without endothelial mitogen). The next day, 100µg/ml oxLDL was added to the medium for indicated timepoints. Cells were centrifuged 3000rpm/5 minutes and pellets collected for protein lysates.

4.2.3.3 MACS Sorting of Lung Endothelial Cells

Lung endothelial cells were isolated from female p38α^{EC-KO}/ApoE$^{-/-}$ and ApoE$^{-/-}$ littermates that had been previously fed a tamoxifen diet for 5 weeks to induce cre expression, and subsequently fed a cholesterol rich 'western diet' for 10 weeks, as described above. After passing the collagenase dissociated lung through a 19G needle, the cell suspension was passed through a 100µm, then a 70µm and a 40µm cell strainer and cells were collected in a 50ml tube (Falcon). Cells were washed twice with PBS by centrifuging 300xg/10 mins. Removal of debris and cell enrichment was achieved by mixing cell suspension with 30% Histodenz solution (Sigma-Aldrich, and centrifuging 1500xg/2mins. Low-density cells at the interface were harvested and washed twice in degassed MACS buffer (PBS pH 7.2, 0.5% BSA and 2mM EDTA). Cells were resuspended in MACS buffer (90µl/10^7 cells) and labeled with Anti-LSEC MicroBeads (beads coupled to the mouse endothelial cell marker CD146, Miltenyi Biotec) by adding 10µl beads/ 10^7 cells and incubating 15 mins/ 4˚C. After washing, the cells were resuspended in 500µl buffer/10^8 cells. Magnetic separation of the cells was performed by use of an MACS column (MS, Miltenyi Biotec) and a magnetic field. Once the cell suspension was loaded onto the column, magnetically labeled cells (endothelial cells) were retained on the column, whereas unlabelled cells (CD146 negative fraction) ran through. After removal of the column from the magnetic field, the magnetically retained cells were eluted (CD146 positive fraction). CD146 sorting of lung endothelial cells was confirmed through FACS analysis. Protein lysates were prepared from sorted cells in order to perform immunobloting.

4.2.3.4 Whole Cell Protein Extraction

Whole cell protein extracts were prepared from endothelial cells and macrophages by lysing with high salt RIPA buffer. In general, after harvesting cells by washing 2 x PBS, cells were scraped off plates in PBS and collected by centrifuging at 6000 rpm for 5 mins at 4˚C. The PBS was aspirated and the cell pellet was resuspended in 50-100µl high salt RIPA buffer (20 mM Hepes, 350 mM NaCl, 20% Glycerol, 1mM $MgCl_2$, 0.5mM EDTA, 0.1 mM EGTA, 0.1% NP40, 1mM DTT, 1mM $NaVO_3$, 1mM NaF, and 1 mini Complete tablet/10 ml). The cell suspension was mixed thoroughly by pipetting and vortexing, and lysed by incubating 30 mins on ice and sonicating 7.5 mins in a cooled sonicating bath. Protein extracts were collected by centrifuging at maximum speed (14000 rpm) for 20 mins at 4˚C and collecting the supernatant. Protein concentration was measured by Bradford assay, at 595 nm, and extracts were prepared for SDS gel analysis by boiling for 5 mins with SDS sample buffer.

4.2.3.5 Immunoblot analysis

Protein lysates were prepared from macrophage and endothelial cells, separated by SDS-polyacrylamide gel electrophoresis, transferred to nitrocellulose and analysed by immunoblotting. Membranes were probed with antibodies specific for: α-tubulin (Sigma-Aldrich, T6074), p38α (Cell signaling, #9218), p-p38 (Cell Signaling, #9211), p-JNK (Cell Signaling, #9251) and JNK (Cell Signaling, #9252). Horseradish peroxidase-conjugated anti-rabbit, anti-mouse and anti-rat secondary antibodies were used (Amersham).

4.2.3.6 Statistical Analysis

All statistical analyses were performed using Prism program (GraphPad Software Inc., San Diego, CA), and Excel. Statistical significance between experimental groups was assessed using an unpaired two sample Student's t test.

4.3 Genomic DNA Isolation from Mutant Mice and Genotyping

4.3.1 Genomic DNA isolation from Mutant Mice

Genomic DNA was isolated from 5mm tail taken from 3-week old pups, after overnight digestion in 500 µl of Tail buffer (100mM Tris-HCl, pH 8.5, 200mM NaCl, 5mM EDTA, 0.2% SDS) with 200µg/ml proteinase K at 56˚C. The following day, the digested tails were centrifuged at 14.000 rpm for 5 mins. The supernatant was transferred to a fresh tube, and genomic DNA was extracted by mixing with an equal volume of isopropanol and allowing it to precipitate. After centrifuging 14000 rpm for 5 mins to pellet DNA, it was washed in 70%, air dried and resuspended in 50-100µl Tris-EDTA (TE). 2µl of resuspended DNA was used for each PCR reaction.

4.3.2 Genotyping PCR Protocols

Genotyping on murine genomic tail DNA was performed using the primers listed below:

PCR	Primers (Pasparakis database #) (5'-3')	Annealing Tm (˚C)	Expected bands (bp)
p38αKD	# 1823: GCT GAA GCA CAT GAA ACA CG # 1824: GCA AAG AGT GGG GGT TAC # 1825: CTG AAA CGG TCT CGA CAG C	60	Wt 430 Floxed 512 Floxed/Inverted 552
p38αKD Neo	# 697: GAT TCG CAG CGC ATC GCC # 1822: GAT GCC CCG TCT TTG TAT C	62	Neo +ve 531
General Cre	# 101: GTC CAA TTT ACT GAC CGT ACA C # 102: CTG TCA CTT GGT CGT GGC AGC	61	Cre +ve 350
ApoE	# 363: GCC TAG CCG AGG GAG AGC CG # 364: TGT GAC TTG GGA GCT CTG CAG C # 365: GCC GCC CCG ACT GCA TCT	68	Wt 155 Ko 245
Flp-Deleter	# 483: TTA GTT CAG CAG CAC ATG ATG # 608: GGA GGA TTT GAT ATT CAC CTG	54	Flp +ve 450

Deleter Cre	# 750: CGC ATA ACC AGT GAA ACA GCA T # 745: GAA AGT CGA GTA GGC GTG TAC G	58	Cre +ve 600
Alfp-Cre	# 831: TCC AGA TGG CAA ACA TAC GC # 699: GTG TAC GGT CAG TAA ATT GGA C	60	Cre +ve 300
LysM-Cre	# 741: CTT GGG CTG CCA GAA TTT CTC # 742: TTA CAG TCG GCC AGG CTG AC # 743: CCC AGA AAT GCC AGA TTA CG	63	Wt 350 Cre +ve 700
p38	# 688: CTA CAG AAT GCA CCT CGG ATG # 689: AGA AGG CTG GAT TTG CAC AAG # 690: CCA GCA CTT GGA AGG CTA TTC	62	Wt 121 Floxed 188 Deleted 411
CAGS ROSA26	# 878: TGT CGC AAA TTA ACT GTG AAT C # R26 RV: GAT ATG AAG TAC TGG GCT CTT # R26 FW: AAA GTC GCT CTG AGT TGT TAT C	56	Wt 570 Floxed 380

All the genotyping reactions were setup as listed below:

	1x reaction (µl)
10 x Taq buffer	3
2mM dNTPs	3
10 x Primer mix (33 µM)	3
25 mM MgCl2	1.8
Tail DNA	2
5 U/µl Taq	0.2
dH20	17
Total reaction volume	**30**

The general PCR programme used can be seen below. Annealing temperatures for each genotyping reaction were as listed in the primers table above.

94 ˚C	3 mins	
94 ˚C Annealing 72 ˚C	30 sec 30 sec 30 sec	35 x
72 ˚C	3 mins	

Some special settings were required for the CAGS ROSA26, the LysMCre, ApoE and Deleter Cre PCRs. These are listed below.

CAGS ROSA26

94 ˚C	3 mins	
94 ˚C Annealing 72 ˚C	30 sec 45 sec 1.5 mins	45 x
72 ˚C	10 mins	

LysMCre

94 ˚C	3 mins	
94 ˚C Annealing 72 ˚C	30 sec 30 sec 1.4 mins	35 x
72 ˚C	5 mins	

ApoE

94 ˚C	3 mins	
94 ˚C Annealing 72 ˚C	20 sec 40 sec 30 sec	30 x
72 ˚C	3 mins	

Deleter Cre

94 ˚C	3 mins	
94 ˚C Annealing 72 ˚C	30 sec 30 sec 1 min	35 x
72 ˚C	3 mins	

5. Bibliography

1 Rouse, J. *et al.*, A novel kinase cascade triggered by stress and heat shock that stimulates MAPKAP kinase-2 and phosphorylation of the small heat shock proteins. *Cell* 78 (6), 1027-1037 (1994).

2 Chang, L. & Karin, M., Mammalian MAP kinase signalling cascades. *Nature* 410 (6824), 37-40 (2001).

3 Kumar, S., Boehm, J., & Lee, J.C., p38 MAP kinases: key signalling molecules as therapeutic targets for inflammatory diseases. *Nat Rev Drug Discov* 2 (9), 717-726 (2003).

4 Zarubin, T. & Han, J., Activation and signaling of the p38 MAP kinase pathway. *Cell Res* 15 (1), 11-18 (2005).

5 Beardmore, V.A. *et al.*, Generation and characterization of p38beta (MAPK11) gene-targeted mice. *Mol Cell Biol* 25 (23), 10454-10464 (2005).

6 Pearson, G. *et al.*, Mitogen-activated protein (MAP) kinase pathways: regulation and physiological functions. *Endocr Rev* 22 (2), 153-183 (2001).

7 Herlaar, E. & Brown, Z., p38 MAPK signalling cascades in inflammatory disease. *Mol Med Today* 5 (10), 439-447 (1999).

8 English, J. *et al.*, New insights into the control of MAP kinase pathways. *Exp Cell Res* 253 (1), 255-270 (1999).

9 Lee, J.C. *et al.*, A protein kinase involved in the regulation of inflammatory cytokine biosynthesis. *Nature* 372 (6508), 739-746 (1994).

10 Han, J., Lee, J.D., Bibbs, L., & Ulevitch, R.J., A MAP kinase targeted by endotoxin and hyperosmolarity in mammalian cells. *Science* 265 (5173), 808-811 (1994).

11 Freshney, N.W. *et al.*, Interleukin-1 activates a novel protein kinase cascade that results in the phosphorylation of Hsp27. *Cell* 78 (6), 1039-1049 (1994).

12 Jiang, Y. *et al.*, Characterization of the structure and function of a new mitogen-activated protein kinase (p38beta). *The Journal of biological chemistry* 271 (30), 17920-17926 (1996).

13 Li, Z., Jiang, Y., Ulevitch, R.J., & Han, J., The primary structure of p38 gamma: a new member of p38 group of MAP kinases. *Biochem Biophys Res Commun* 228 (2), 334-340 (1996).

14 Kumar, S. *et al.*, Novel homologues of CSBP/p38 MAP kinase: activation, substrate specificity and sensitivity to inhibition by pyridinyl imidazoles. *Biochem Biophys Res Commun* 235 (3), 533-538 (1997).

15 Hale, K.K., Trollinger, D., Rihanek, M., & Manthey, C.L., Differential expression and activation of p38 mitogen-activated protein kinase alpha, beta, gamma, and delta in inflammatory cell lineages. *J Immunol* 162 (7), 4246-4252 (1999).

16 Enslen, H., Raingeaud, J., & Davis, R.J., Selective activation of p38 mitogen-activated protein (MAP) kinase isoforms by the MAP kinase kinases MKK3 and MKK6. *J Biol Chem* 273 (3), 1741-1748 (1998).

17 Jiang, Y. *et al.*, Characterization of the structure and function of the fourth member of p38 group mitogen-activated protein kinases, p38delta. *J Biol Chem* 272 (48), 30122-30128 (1997).

18 Adams, J.L., Badger, A.M., Kumar, S., & Lee, J.C., p38 MAP kinase: molecular target for the inhibition of pro-inflammatory cytokines. *Prog Med Chem* 38, 1-60 (2001).

19 Kyriakis, J.M. & Avruch, J., Mammalian mitogen-activated protein kinase signal transduction pathways activated by stress and inflammation. *Physiol Rev* 81 (2), 807-869 (2001).

20 Ge, B. *et al.*, MAPKK-independent activation of p38alpha mediated by TAB1-dependent autophosphorylation of p38alpha. *Science* 295 (5558), 1291-1294 (2002).

21 Salvador, J.M., Mittelstadt, P.R., Belova, G.I., Fornace, A.J., Jr., & Ashwell, J.D., The autoimmune suppressor Gadd45alpha inhibits the T cell alternative p38 activation pathway. *Nat Immunol* 6 (4), 396-402 (2005).

22 Salvador, J.M. *et al.*, Alternative p38 activation pathway mediated by T cell receptor-proximal tyrosine kinases. *Nat Immunol* 6 (4), 390-395 (2005).

23 Cuenda, A. & Rousseau, S., p38 MAP-kinases pathway regulation, function and role in human diseases. *Biochim Biophys Acta* 1773 (8), 1358-1375 (2007).

24 Takekawa, M., Maeda, T., & Saito, H., Protein phosphatase 2Calpha inhibits the human stress-responsive p38 and JNK MAPK pathways. *EMBO J* 17 (16), 4744-4752 (1998).

[25] Masuda, K., Shima, H., Watanabe, M., & Kikuchi, K., MKP-7, a novel mitogen-activated protein kinase phosphatase, functions as a shuttle protein. *J Biol Chem* 276 (42), 39002-39011 (2001).

[26] Tanoue, T., Yamamoto, T., Maeda, R., & Nishida, E., A Novel MAPK phosphatase MKP-7 acts preferentially on JNK/SAPK and p38 alpha and beta MAPKs. *J Biol Chem* 276 (28), 26629-26639 (2001).

[27] Theodosiou, A., Smith, A., Gillieron, C., Arkinstall, S., & Ashworth, A., MKP5, a new member of the MAP kinase phosphatase family, which selectively dephosphorylates stress-activated kinases. *Oncogene* 18 (50), 6981-6988 (1999).

[28] Kim, C. *et al.*, The kinase p38 alpha serves cell type-specific inflammatory functions in skin injury and coordinates pro- and anti-inflammatory gene expression. *Nature immunology* 9 (9), 1019-1027 (2008).

[29] Cuenda, A. *et al.*, SB 203580 is a specific inhibitor of a MAP kinase homologue which is stimulated by cellular stresses and interleukin-1. *FEBS Lett* 364 (2), 229-233 (1995).

[30] Davies, S.P., Reddy, H., Caivano, M., & Cohen, P., Specificity and mechanism of action of some commonly used protein kinase inhibitors. *Biochem J* 351 (Pt 1), 95-105 (2000).

[31] Raingeaud, J. *et al.*, Pro-inflammatory cytokines and environmental stress cause p38 mitogen-activated protein kinase activation by dual phosphorylation on tyrosine and threonine. *J Biol Chem* 270 (13), 7420-7426 (1995).

[32] McLaughlin, M.M. *et al.*, Identification of mitogen-activated protein (MAP) kinase-activated protein kinase-3, a novel substrate of CSBP p38 MAP kinase. *J Biol Chem* 271 (14), 8488-8492 (1996).

[33] Stokoe, D., Engel, K., Campbell, D.G., Cohen, P., & Gaestel, M., Identification of MAPKAP kinase 2 as a major enzyme responsible for the phosphorylation of the small mammalian heat shock proteins. *FEBS Lett* 313 (3), 307-313 (1992).

[34] Huang, C.K., Zhan, L., Ai, Y., & Jongstra, J., LSP1 is the major substrate for mitogen-activated protein kinase-activated protein kinase 2 in human neutrophils. *J Biol Chem* 272 (1), 17-19 (1997).

[35] Tan, Y. *et al.*, FGF and stress regulate CREB and ATF-1 via a pathway involving p38 MAP kinase and MAPKAP kinase-2. *EMBO J* 15 (17), 4629-4642 (1996).

[36] Heidenreich, O. *et al.*, MAPKAP kinase 2 phosphorylates serum response factor in vitro and in vivo. *J Biol Chem* 274 (20), 14434-14443 (1999).

[37] Thomas, G., Haavik, J., & Cohen, P., Participation of a stress-activated protein kinase cascade in the activation of tyrosine hydroxylase in chromaffin cells. *Eur J Biochem* 247 (3), 1180-1189 (1997).

[38] Mahtani, K.R. *et al.*, Mitogen-activated protein kinase p38 controls the expression and posttranslational modification of tristetraprolin, a regulator of tumor necrosis factor alpha mRNA stability. *Mol Cell Biol* 21 (19), 6461-6469 (2001).

[39] Waskiewicz, A.J., Flynn, A., Proud, C.G., & Cooper, J.A., Mitogen-activated protein kinases activate the serine/threonine kinases Mnk1 and Mnk2. *EMBO J* 16 (8), 1909-1920 (1997).

[40] Fukunaga, R. & Hunter, T., MNK1, a new MAP kinase-activated protein kinase, isolated by a novel expression screening method for identifying protein kinase substrates. *EMBO J* 16 (8), 1921-1933 (1997).

[41] New, L. *et al.*, PRAK, a novel protein kinase regulated by the p38 MAP kinase. *EMBO J* 17 (12), 3372-3384 (1998).

[42] Deak, M., Clifton, A.D., Lucocq, L.M., & Alessi, D.R., Mitogen- and stress-activated protein kinase-1 (MSK1) is directly activated by MAPK and SAPK2/p38, and may mediate activation of CREB. *EMBO J* 17 (15), 4426-4441 (1998).

[43] Pierrat, B., Correia, J.S., Mary, J.L., Tomas-Zuber, M., & Lesslauer, W., RSK-B, a novel ribosomal S6 kinase family member, is a CREB kinase under dominant control of p38alpha mitogen-activated protein kinase (p38alphaMAPK). *J Biol Chem* 273 (45), 29661-29671 (1998).

[44] New, L. *et al.*, Cloning and characterization of RLPK, a novel RSK-related protein kinase. *J Biol Chem* 274 (2), 1026-1032 (1999).

[45] Zheng, L., Roeder, R.G., & Luo, Y., S phase activation of the histone H2B promoter by OCA-S, a coactivator complex that contains GAPDH as a key component. *Cell* 114 (2), 255-266 (2003).

[46] Hazzalin, C.A. *et al.*, p38/RK is essential for stress-induced nuclear responses: JNK/SAPKs and c-Jun/ATF-2 phosphorylation are insufficient. *Curr Biol* 6 (8), 1028-1031 (1996).

47 Whitmarsh, A.J., Yang, S.H., Su, M.S., Sharrocks, A.D., & Davis, R.J., Role of p38 and JNK mitogen-activated protein kinases in the activation of ternary complex factors. *Molecular and cellular biology* 17 (5), 2360-2371 (1997).
48 Janknecht, R. & Hunter, T., Convergence of MAP kinase pathways on the ternary complex factor Sap-1a. *EMBO J* 16 (7), 1620-1627 (1997).
49 Wang, X.Z. & Ron, D., Stress-induced phosphorylation and activation of the transcription factor CHOP (GADD153) by p38 MAP Kinase. *Science* 272 (5266), 1347-1349 (1996).
50 Han, J., Jiang, Y., Li, Z., Kravchenko, V.V., & Ulevitch, R.J., Activation of the transcription factor MEF2C by the MAP kinase p38 in inflammation. *Nature* 386 (6622), 296-299 (1997).
51 Zhao, M. *et al.*, Regulation of the MEF2 family of transcription factors by p38. *Mol Cell Biol* 19 (1), 21-30 (1999).
52 Huang, C., Ma, W.Y., Maxiner, A., Sun, Y., & Dong, Z., p38 kinase mediates UV-induced phosphorylation of p53 protein at serine 389. *J Biol Chem* 274 (18), 12229-12235 (1999).
53 Yee, A.S. *et al.*, The HBP1 transcriptional repressor and the p38 MAP kinase: unlikely partners in G1 regulation and tumor suppression. *Gene* 336 (1), 1-13 (2004).
54 Galibert, M.D., Carreira, S., & Goding, C.R., The Usf-1 transcription factor is a novel target for the stress-responsive p38 kinase and mediates UV-induced Tyrosinase expression. *EMBO J* 20 (17), 5022-5031 (2001).
55 Pereira, R.C., Delany, A.M., & Canalis, E., CCAAT/enhancer binding protein homologous protein (DDIT3) induces osteoblastic cell differentiation. *Endocrinology* 145 (4), 1952-1960 (2004).
56 Gomez del Arco, P., Martinez-Martinez, S., Maldonado, J.L., Ortega-Perez, I., & Redondo, J.M., A role for the p38 MAP kinase pathway in the nuclear shuttling of NFATp. *J Biol Chem* 275 (18), 13872-13878 (2000).
57 Kramer, R.M. *et al.*, p38 mitogen-activated protein kinase phosphorylates cytosolic phospholipase A2 (cPLA2) in thrombin-stimulated platelets. Evidence that proline-directed phosphorylation is not required for mobilization of arachidonic acid by cPLA2. *J Biol Chem* 271 (44), 27723-27729 (1996).
58 Kuma, Y., Campbell, D.G., & Cuenda, A., Identification of glycogen synthase as a new substrate for stress-activated protein kinase 2b/p38beta. *Biochem J* 379 (Pt 1), 133-139 (2004).
59 Roux, P.P. & Blenis, J., ERK and p38 MAPK-activated protein kinases: a family of protein kinases with diverse biological functions. *Microbiol Mol Biol Rev* 68 (2), 320-344 (2004).
60 Hashimoto, S. *et al.*, p38 Mitogen-activated protein kinase regulates IL-8 expression in human pulmonary vascular endothelial cells. *Eur Respir J* 13 (6), 1357-1364 (1999).
61 Pietersma, A. *et al.*, p38 mitogen activated protein kinase regulates endothelial VCAM-1 expression at the post-transcriptional level. *Biochem Biophys Res Commun* 230 (1), 44-48 (1997).
62 Pouliot, M., Baillargeon, J., Lee, J.C., Cleland, L.G., & James, M.J., Inhibition of prostaglandin endoperoxide synthase-2 expression in stimulated human monocytes by inhibitors of p38 mitogen-activated protein kinase. *J Immunol* 158 (10), 4930-4937 (1997).
63 Viemann, D. *et al.*, Transcriptional profiling of IKK2/NF-kappa B- and p38 MAP kinase-dependent gene expression in TNF-alpha-stimulated primary human endothelial cells. *Blood* 103 (9), 3365-3373 (2004).
64 Goedert, M., Cuenda, A., Craxton, M., Jakes, R., & Cohen, P., Activation of the novel stress-activated protein kinase SAPK4 by cytokines and cellular stresses is mediated by SKK3 (MKK6); comparison of its substrate specificity with that of other SAP kinases. *EMBO J* 16 (12), 3563-3571 (1997).
65 Godl, K. *et al.*, An efficient proteomics method to identify the cellular targets of protein kinase inhibitors. *Proc Natl Acad Sci U S A* 100 (26), 15434-15439 (2003).
66 Karaman, M.W. *et al.*, A quantitative analysis of kinase inhibitor selectivity. *Nat Biotechnol* 26 (1), 127-132 (2008).
67 Mudgett, J.S. *et al.*, Essential role for p38alpha mitogen-activated protein kinase in placental angiogenesis. *Proc Natl Acad Sci U S A* 97 (19), 10454-10459 (2000).
68 Adams, R.H. *et al.*, Essential role of p38alpha MAP kinase in placental but not embryonic cardiovascular development. *Mol Cell* 6 (1), 109-116 (2000).
69 Tamura, K. *et al.*, Requirement for p38alpha in erythropoietin expression: a role for stress kinases in erythropoiesis. *Cell* 102 (2), 221-231 (2000).

[70] Allen, M. *et al.*, Deficiency of the stress kinase p38alpha results in embryonic lethality: characterization of the kinase dependence of stress responses of enzyme-deficient embryonic stem cells. *The Journal of experimental medicine* 191 (5), 859-870 (2000).
[71] Hui, L. *et al.*, p38alpha suppresses normal and cancer cell proliferation by antagonizing the JNK-c-Jun pathway. *Nat Genet* 39 (6), 741-749 (2007).
[72] Ventura, J.J. *et al.*, p38alpha MAP kinase is essential in lung stem and progenitor cell proliferation and differentiation. *Nat Genet* 39 (6), 750-758 (2007).
[73] Sauer, B., Inducible gene targeting in mice using the Cre/lox system. *Methods* 14 (4), 381-392 (1998).
[74] Forde, A., Constien, R., Grone, H.J., Hammerling, G., & Arnold, B., Temporal Cre-mediated recombination exclusively in endothelial cells using Tie2 regulatory elements. *Genesis* 33 (4), 191-197 (2002).
[75] Heinrichsdorff, J., Luedde, T., Perdiguero, E., Nebreda, A.R., & Pasparakis, M., p38 alpha MAPK inhibits JNK activation and collaborates with IkappaB kinase 2 to prevent endotoxin-induced liver failure. *EMBO reports* 9 (10), 1048-1054 (2008).
[76] Ross, R., The pathogenesis of atherosclerosis--an update. *N Engl J Med* 314 (8), 488-500 (1986).
[77] Ross, R., The pathogenesis of atherosclerosis: a perspective for the 1990s. *Nature* 362 (6423), 801-809 (1993).
[78] Ross, R., Atherosclerosis--an inflammatory disease. *N Engl J Med* 340 (2), 115-126 (1999).
[79] Lusis, A.J., Atherosclerosis. *Nature* 407 (6801), 233-241 (2000).
[80] Hansson, G.K. & Libby, P., The immune response in atherosclerosis: a double-edged sword. *Nat Rev Immunol* 6 (7), 508-519 (2006).
[81] Stout, R.W., Ageing and atherosclerosis. *Age Ageing* 16 (2), 65-72 (1987).
[82] Minamino, T. & Komuro, I., Vascular cell senescence: contribution to atherosclerosis. *Circ Res* 100 (1), 15-26 (2007).
[83] Gordon, T., Kannel, W.B., Hjortland, M.C., & McNamara, P.M., Menopause and coronary heart disease. The Framingham Study. *Ann Intern Med* 89 (2), 157-161 (1978).
[84] Stampfer, M.J. *et al.*, Postmenopausal estrogen therapy and cardiovascular disease. Ten-year follow-up from the nurses' health study. *N Engl J Med* 325 (11), 756-762 (1991).
[85] Hulley, S. *et al.*, Randomized trial of estrogen plus progestin for secondary prevention of coronary heart disease in postmenopausal women. Heart and Estrogen/progestin Replacement Study (HERS) Research Group. *JAMA* 280 (7), 605-613 (1998).
[86] Malkin, C.J., Pugh, P.J., Jones, R.D., Jones, T.H., & Channer, K.S., Testosterone as a protective factor against atherosclerosis--immunomodulation and influence upon plaque development and stability. *J Endocrinol* 178 (3), 373-380 (2003).
[87] Tedgui, A. & Mallat, Z., Hypertension: a novel regulator of adaptive immunity in atherosclerosis? *Hypertension* 44 (3), 257-258 (2004).
[88] O'Leary, D.H. *et al.*, Carotid-artery intima and media thickness as a risk factor for myocardial infarction and stroke in older adults. Cardiovascular Health Study Collaborative Research Group. *N Engl J Med* 340 (1), 14-22 (1999).
[89] Chobanian, A.V. & Alexander, R.W., Exacerbation of atherosclerosis by hypertension. Potential mechanisms and clinical implications. *Arch Intern Med* 156 (17), 1952-1956 (1996).
[90] Xu, C.P., Glagov, S., Zatina, M.A., & Zarins, C.K., Hypertension sustains plaque progression despite reduction of hypercholesterolemia. *Hypertension* 18 (2), 123-129 (1991).
[91] Knowles, J.W. & Maeda, N., Genetic modifiers of atherosclerosis in mice. *Arterioscler Thromb Vasc Biol* 20 (11), 2336-2345 (2000).
[92] Meyer, G., Merval, R., & Tedgui, A., Effects of pressure-induced stretch and convection on low-density lipoprotein and albumin uptake in the rabbit aortic wall. *Circ Res* 79 (3), 532-540 (1996).
[93] Landmesser, U., Hornig, B., & Drexler, H., Endothelial function: a critical determinant in atherosclerosis? *Circulation* 109 (21 Suppl 1), II27-33 (2004).
[94] Wang, H. *et al.*, The upregulation of ICAM-1 and P-selectin requires high blood pressure but not circulating renin-angiotensin system in vivo. *J Hypertens* 22 (7), 1323-1332 (2004).
[95] Libby, P., Inflammation in atherosclerosis. *Nature* 420 (6917), 868-874 (2002).
[96] Nabel, E.G., Cardiovascular disease. *N Engl J Med* 349 (1), 60-72 (2003).
[97] Rubin, E.M. & Tall, A., Perspectives for vascular genomics. *Nature* 407 (6801), 265-269 (2000).

98 Milewicz, D.M. & Seidman, C.E., Genetics of cardiovascular disease. *Circulation* 102 (20 Suppl 4), IV103-111 (2000).
99 Seo, D.M. & Goldschmidt-Clermont, P.J., Unraveling the genetics of atherosclerosis: implications for diagnosis and treatment. *Expert Rev Mol Diagn* 7 (1), 45-51 (2007).
100 Howard, G. *et al.*, Cigarette smoking and progression of atherosclerosis: The Atherosclerosis Risk in Communities (ARIC) Study. *JAMA* 279 (2), 119-124 (1998).
101 Wang, Z. *et al.*, Protein carbamylation links inflammation, smoking, uremia and atherogenesis. *Nat Med* 13 (10), 1176-1184 (2007).
102 Chait, A. & Bornfeldt, K.E., Diabetes and atherosclerosis: is there a role for hyperglycemia? *J Lipid Res* 50 Suppl, S335-339 (2009).
103 Kannel, W.B. & McGee, D.L., Diabetes and glucose tolerance as risk factors for cardiovascular disease: the Framingham study. *Diabetes Care* 2 (2), 120-126 (1979).
104 Galla, J.M. & Nicholls, S.J., Pharmacologic therapy for coronary atherosclerosis in patients with Type 2 diabetes mellitus. *Expert Rev Cardiovasc Ther* 7 (1), 85-93 (2009).
105 Dantuma, N.P. *et al.*, An insect homolog of the vertebrate very low density lipoprotein receptor mediates endocytosis of lipophorins. *J Lipid Res* 40 (5), 973-978 (1999).
106 de Winther, M.P. *et al.*, Scavenger receptor deficiency leads to more complex atherosclerotic lesions in APOE3Leiden transgenic mice. *Atherosclerosis* 144 (2), 315-321 (1999).
107 de Winther, M.P. *et al.*, Macrophage specific overexpression of the human macrophage scavenger receptor in transgenic mice, using a 180-kb yeast artificial chromosome, leads to enhanced foam cell formation of isolated peritoneal macrophages. *Atherosclerosis* 147 (2), 339-347 (1999).
108 van Dijk, K.W. *et al.*, Hyperlipidemia of ApoE2(Arg(158)-Cys) and ApoE3-Leiden transgenic mice is modulated predominantly by LDL receptor expression. *Arterioscler Thromb Vasc Biol* 19 (12), 2945-2951 (1999).
109 Cyrus, T. *et al.*, Disruption of the 12/15-lipoxygenase gene diminishes atherosclerosis in apo E-deficient mice. *J Clin Invest* 103 (11), 1597-1604 (1999).
110 Hegele, R.A., Paraoxonase genes and disease. *Ann Med* 31 (3), 217-224 (1999).
111 Shih, D.M. *et al.*, Combined serum paraoxonase knockout/apolipoprotein E knockout mice exhibit increased lipoprotein oxidation and atherosclerosis. *J Biol Chem* 275 (23), 17527-17535 (2000).
112 Glagov, S., Zarins, C., Giddens, D.P., & Ku, D.N., Hemodynamics and atherosclerosis. Insights and perspectives gained from studies of human arteries. *Arch Pathol Lab Med* 112 (10), 1018-1031 (1988).
113 Gimbrone, M.A., Jr., Vascular endothelium, hemodynamic forces, and atherogenesis. *Am J Pathol* 155 (1), 1-5 (1999).
114 Boren, J. *et al.*, Identification of the principal proteoglycan-binding site in LDL. A single-point mutation in apo-B100 severely affects proteoglycan interaction without affecting LDL receptor binding. *J Clin Invest* 101 (12), 2658-2664 (1998).
115 Young, I.S. & McEneny, J., Lipoprotein oxidation and atherosclerosis. *Biochem Soc Trans* 29 (Pt 2), 358-362 (2001).
116 Steinberg, D., Low density lipoprotein oxidation and its pathobiological significance. *J Biol Chem* 272 (34), 20963-20966 (1997).
117 Gerhard, G.T. & Duell, P.B., Homocysteine and atherosclerosis. *Curr Opin Lipidol* 10 (5), 417-428 (1999).
118 Bobryshev, Y.V. & Lord, R.S., S-100 positive cells in human arterial intima and in atherosclerotic lesions. *Cardiovasc Res* 29 (5), 689-696 (1995).
119 Kovanen, P.T., Kaartinen, M., & Paavonen, T., Infiltrates of activated mast cells at the site of coronary atheromatous erosion or rupture in myocardial infarction. *Circulation* 92 (5), 1084-1088 (1995).
120 Jonasson, L., Holm, J., Skalli, O., Bondjers, G., & Hansson, G.K., Regional accumulations of T cells, macrophages, and smooth muscle cells in the human atherosclerotic plaque. *Arteriosclerosis* 6 (2), 131-138 (1986).
121 Watson, K.E. *et al.*, TGF-beta 1 and 25-hydroxycholesterol stimulate osteoblast-like vascular cells to calcify. *J Clin Invest* 93 (5), 2106-2113 (1994).
122 Libby, P., The molecular mechanisms of the thrombotic complications of atherosclerosis. *J Intern Med* 263 (5), 517-527 (2008).
123 Hansson, G.K., Atherosclerosis--an immune disease: The Anitschkov Lecture 2007. *Atherosclerosis* 202 (1), 2-10 (2009).

[124] Hansson, G.K., Immune mechanisms in atherosclerosis. *Arterioscler Thromb Vasc Biol* 21 (12), 1876-1890 (2001).
[125] Zhao, M. *et al.*, Activation of the p38 MAP kinase pathway is required for foam cell formation from macrophages exposed to oxidized LDL. *APMIS* 110 (6), 458-468 (2002).
[126] Lei, Z.B. *et al.*, OxLDL upregulates CXCR2 expression in monocytes via scavenger receptors and activation of p38 mitogen-activated protein kinase. *Cardiovascular research* 53 (2), 524-532 (2002).
[127] Wang, Z., Castresana, M.R., & Newman, W.H., Reactive oxygen species-sensitive p38 MAPK controls thrombin-induced migration of vascular smooth muscle cells. *Journal of molecular and cellular cardiology* 36 (1), 49-56 (2004).
[128] Rousseau, S. *et al.*, Vascular endothelial growth factor (VEGF)-driven actin-based motility is mediated by VEGFR2 and requires concerted activation of stress-activated protein kinase 2 (SAPK2/p38) and geldanamycin-sensitive phosphorylation of focal adhesion kinase. *The Journal of biological chemistry* 275 (14), 10661-10672 (2000).
[129] Denes, L. *et al.*, Pharmacologically activated migration of aortic endothelial cells is mediated through p38 SAPK. *British journal of pharmacology* 136 (4), 597-603 (2002).
[130] McMullen, M.E., Bryant, P.W., Glembotski, C.C., Vincent, P.A., & Pumiglia, K.M., Activation of p38 has opposing effects on the proliferation and migration of endothelial cells. *The Journal of biological chemistry* 280 (22), 20995-21003 (2005).
[131] Borbiev, T. *et al.*, p38 MAP kinase-dependent regulation of endothelial cell permeability. *American journal of physiology* 287 (5), L911-918 (2004).
[132] Gratton, J.P. *et al.*, Akt down-regulation of p38 signaling provides a novel mechanism of vascular endothelial growth factor-mediated cytoprotection in endothelial cells. *The Journal of biological chemistry* 276 (32), 30359-30365 (2001).
[133] Schieven, G.L., The biology of p38 kinase: a central role in inflammation. *Current topics in medicinal chemistry* 5 (10), 921-928 (2005).
[134] Smith, S.J. *et al.*, Inhibitory effect of p38 mitogen-activated protein kinase inhibitors on cytokine release from human macrophages. *British journal of pharmacology* 149 (4), 393-404 (2006).
[135] Ajizian, S.J., English, B.K., & Meals, E.A., Specific inhibitors of p38 and extracellular signal-regulated kinase mitogen-activated protein kinase pathways block inducible nitric oxide synthase and tumor necrosis factor accumulation in murine macrophages stimulated with lipopolysaccharide and interferon-gamma. *The Journal of infectious diseases* 179 (4), 939-944 (1999).
[136] Underwood, D.C. *et al.*, SB 239063, a p38 MAPK inhibitor, reduces neutrophilia, inflammatory cytokines, MMP-9, and fibrosis in lung. *American journal of physiology* 279 (5), L895-902 (2000).
[137] Sima, A.V., Stancu, C.S., & Simionescu, M., Vascular endothelium in atherosclerosis. *Cell Tissue Res* 335 (1), 191-203 (2009).
[138] Linton, M.F. & Fazio, S., Macrophages, inflammation, and atherosclerosis. *Int J Obes Relat Metab Disord* 27 Suppl 3, S35-40 (2003).
[139] Daugherty, A., Mouse models of atherosclerosis. *The American journal of the medical sciences* 323 (1), 3-10 (2002).
[140] Brill, J.A., Elion, E.A., & Fink, G.R., A role for autophosphorylation revealed by activated alleles of FUS3, the yeast MAP kinase homolog. *Mol Biol Cell* 5 (3), 297-312 (1994).
[141] Hall, J.P., Cherkasova, V., Elion, E., Gustin, M.C., & Winter, E., The osmoregulatory pathway represses mating pathway activity in Saccharomyces cerevisiae: isolation of a FUS3 mutant that is insensitive to the repression mechanism. *Mol Cell Biol* 16 (12), 6715-6723 (1996).
[142] Brunner, D. *et al.*, A gain-of-function mutation in Drosophila MAP kinase activates multiple receptor tyrosine kinase signaling pathways. *Cell* 76 (5), 875-888 (1994).
[143] Bott, C.M., Thorneycroft, S.G., & Marshall, C.J., The sevenmaker gain-of-function mutation in p42 MAP kinase leads to enhanced signalling and reduced sensitivity to dual specificity phosphatase action. *FEBS Lett* 352 (2), 201-205 (1994).
[144] Robinson, M.J., Stippec, S.A., Goldsmith, E., White, M.A., & Cobb, M.H., A constitutively active and nuclear form of the MAP kinase ERK2 is sufficient for neurite outgrowth and cell transformation. *Curr Biol* 8 (21), 1141-1150 (1998).
[145] Zheng, C., Xiang, J., Hunter, T., & Lin, A., The JNKK2-JNK1 fusion protein acts as a constitutively active c-Jun kinase that stimulates c-Jun transcription activity. *J Biol Chem* 274 (41), 28966-28971 (1999).

146 Bell, M., Capone, R., Pashtan, I., Levitzki, A., & Engelberg, D., Isolation of hyperactive mutants of the MAPK p38/Hog1 that are independent of MAPK kinase activation. *J Biol Chem* 276 (27), 25351-25358 (2001).
147 Clausen, B.E., Burkhardt, C., Reith, W., Renkawitz, R., & Forster, I., Conditional gene targeting in macrophages and granulocytes using LysMcre mice. *Transgenic research* 8 (4), 265-277 (1999).
148 Zhang, S.H., Reddick, R.L., Piedrahita, J.A., & Maeda, N., Spontaneous hypercholesterolemia and arterial lesions in mice lacking apolipoprotein E. *Science (New York, N.Y* 258 (5081), 468-471 (1992).
149 Seimon, T.A. *et al.*, Macrophage deficiency of p38alpha MAPK promotes apoptosis and plaque necrosis in advanced atherosclerotic lesions in mice. *The Journal of clinical investigation* 119 (4), 886-898 (2009).
150 Kotlyarov, A. *et al.*, MAPKAP kinase 2 is essential for LPS-induced TNF-alpha biosynthesis. *Nature cell biology* 1 (2), 94-97 (1999).
151 Westra, J. *et al.*, Strong inhibition of TNF-alpha production and inhibition of IL-8 and COX-2 mRNA expression in monocyte-derived macrophages by RWJ 67657, a p38 mitogen-activated protein kinase (MAPK) inhibitor. *Arthritis research & therapy* 6 (4), R384-392 (2004).
152 Kiermayer, C., Conrad, M., Schneider, M., Schmidt, J., & Brielmeier, M., Optimization of spatiotemporal gene inactivation in mouse heart by oral application of tamoxifen citrate. *Genesis* 45 (1), 11-16 (2007).
153 Nolden, L. *et al.*, Site-specific recombination in human embryonic stem cells induced by cell-permeant Cre recombinase. *Nature methods* 3 (6), 461-467 (2006).
154 Peitz, M., Pfannkuche, K., Rajewsky, K., & Edenhofer, F., Ability of the hydrophobic FGF and basic TAT peptides to promote cellular uptake of recombinant Cre recombinase: a tool for efficient genetic engineering of mammalian genomes. *Proc Natl Acad Sci U S A* 99 (7), 4489-4494 (2002).
155 Ricci, R. *et al.*, Requirement of JNK2 for scavenger receptor A-mediated foam cell formation in atherogenesis. *Science (New York, N.Y* 306 (5701), 1558-1561 (2004).
156 Yaakov, G., Bell, M., Hohmann, S., & Engelberg, D., Combination of two activating mutations in one HOG1 gene forms hyperactive enzymes that induce growth arrest. *Mol Cell Biol* 23 (14), 4826-4840 (2003).
157 Jiang, Y. *et al.*, Structure-function studies of p38 mitogen-activated protein kinase. Loop 12 influences substrate specificity and autophosphorylation, but not upstream kinase selection. *J Biol Chem* 272 (17), 11096-11102 (1997).
158 Fu, J., Yang, Z., Wei, J., Han, J., & Gu, J., Nuclear protein NP60 regulates p38 MAPK activity. *J Cell Sci* 119 (Pt 1), 115-123 (2006).
159 Zambrowicz, B.P. *et al.*, Disruption of overlapping transcripts in the ROSA beta geo 26 gene trap strain leads to widespread expression of beta-galactosidase in mouse embryos and hematopoietic cells. *Proc Natl Acad Sci U S A* 94 (8), 3789-3794 (1997).
160 Oberdoerffer, P., Otipoby, K.L., Maruyama, M., & Rajewsky, K., Unidirectional Cre-mediated genetic inversion in mice using the mutant loxP pair lox66/lox71. *Nucleic Acids Res* 31 (22), e140 (2003).
161 Salomonsson, L., Pettersson, S., Englund, M.C., Wiklund, O., & Ohlsson, B.G., Post-transcriptional regulation of VEGF expression by oxidised LDL in human macrophages. *European journal of clinical investigation* 32 (10), 767-774 (2002).
162 Sun, H.W. *et al.*, Involvement of integrins, MAPK, and NF-kappaB in regulation of the shear stress-induced MMP-9 expression in endothelial cells. *Biochemical and biophysical research communications* 353 (1), 152-158 (2007).
163 van Reyk, D.M. & Jessup, W., The macrophage in atherosclerosis: modulation of cell function by sterols. *J Leukoc Biol* 66 (4), 557-561 (1999).
164 Collot-Teixeira, S., Martin, J., McDermott-Roe, C., Poston, R., & McGregor, J.L., CD36 and macrophages in atherosclerosis. *Cardiovasc Res* 75 (3), 468-477 (2007).
165 Kuchibhotla, S. *et al.*, Absence of CD36 protects against atherosclerosis in ApoE knock-out mice with no additional protection provided by absence of scavenger receptor A I/II. *Cardiovasc Res* 78 (1), 185-196 (2008).
166 Tontonoz, P., Nagy, L., Alvarez, J.G., Thomazy, V.A., & Evans, R.M., PPARgamma promotes monocyte/macrophage differentiation and uptake of oxidized LDL. *Cell* 93 (2), 241-252 (1998).

[167] Janeway, C.A., Jr. & Medzhitov, R., Innate immune recognition. *Annu Rev Immunol* 20, 197-216 (2002).
[168] Edfeldt, K., Swedenborg, J., Hansson, G.K., & Yan, Z.Q., Expression of toll-like receptors in human atherosclerotic lesions: a possible pathway for plaque activation. *Circulation* 105 (10), 1158-1161 (2002).
[169] Kol, A., Lichtman, A.H., Finberg, R.W., Libby, P., & Kurt-Jones, E.A., Cutting edge: heat shock protein (HSP) 60 activates the innate immune response: CD14 is an essential receptor for HSP60 activation of mononuclear cells. *J Immunol* 164 (1), 13-17 (2000).
[170] Michelsen, K.S. *et al.*, Lack of Toll-like receptor 4 or myeloid differentiation factor 88 reduces atherosclerosis and alters plaque phenotype in mice deficient in apolipoprotein E. *Proc Natl Acad Sci U S A* 101 (29), 10679-10684 (2004).
[171] Bjorkbacka, H. *et al.*, Reduced atherosclerosis in MyD88-null mice links elevated serum cholesterol levels to activation of innate immunity signaling pathways. *Nat Med* 10 (4), 416-421 (2004).
[172] Kirii, H. *et al.*, Lack of interleukin-1beta decreases the severity of atherosclerosis in ApoE-deficient mice. *Arterioscler Thromb Vasc Biol* 23 (4), 656-660 (2003).
[173] Boisvert, W.A. *et al.*, Up-regulated expression of the CXCR2 ligand KC/GRO-alpha in atherosclerotic lesions plays a central role in macrophage accumulation and lesion progression. *Am J Pathol* 168 (4), 1385-1395 (2006).
[174] Murphy, N. *et al.*, Hypercholesterolaemia and circulating levels of CXC chemokines in apoE*3 Leiden mice. *Atherosclerosis* 163 (1), 69-77 (2002).
[175] Hastings, N.E., Feaver, R.E., Lee, M.Y., Wamhoff, B.R., & Blackman, B.R., Human IL-8 regulates smooth muscle cell VCAM-1 expression in response to endothelial cells exposed to atheroprone flow. *Arterioscler Thromb Vasc Biol* 29 (5), 725-731 (2009).
[176] Morris, J.B. *et al.*, p38 MAPK inhibition reduces aortic ultrasmall superparamagnetic iron oxide uptake in a mouse model of atherosclerosis: MRI assessment. *Arterioscler Thromb Vasc Biol* 28 (2), 265-271 (2008).
[177] Kang, Y.J. *et al.*, Macrophage deletion of p38alpha partially impairs lipopolysaccharide-induced cellular activation. *J Immunol* 180 (7), 5075-5082 (2008).
[178] Secchiero, P. *et al.*, Systemic tumor necrosis factor-related apoptosis-inducing ligand delivery shows antiatherosclerotic activity in apolipoprotein E-null diabetic mice. *Circulation* 114 (14), 1522-1530 (2006).
[179] Stoneman, V. *et al.*, Monocyte/macrophage suppression in CD11b diphtheria toxin receptor transgenic mice differentially affects atherogenesis and established plaques. *Circ Res* 100 (6), 884-893 (2007).
[180] Clarke, M.C. *et al.*, Apoptosis of vascular smooth muscle cells induces features of plaque vulnerability in atherosclerosis. *Nat Med* 12 (9), 1075-1080 (2006).
[181] Clarke, M.C. *et al.*, Chronic apoptosis of vascular smooth muscle cells accelerates atherosclerosis and promotes calcification and medial degeneration. *Circ Res* 102 (12), 1529-1538 (2008).
[182] Simon, C., Goepfert, H., & Boyd, D., Inhibition of the p38 mitogen-activated protein kinase by SB 203580 blocks PMA-induced Mr 92,000 type IV collagenase secretion and in vitro invasion. *Cancer research* 58 (6), 1135-1139 (1998).
[183] Westra, J., Kuldo, J.M., van Rijswijk, M.H., Molema, G., & Limburg, P.C., Chemokine production and E-selectin expression in activated endothelial cells are inhibited by p38 MAPK (mitogen activated protein kinase) inhibitor RWJ 67657. *Int Immunopharmacol* 5 (7-8), 1259-1269 (2005).
[184] Jersmann, H.P., Hii, C.S., Ferrante, J.V., & Ferrante, A., Bacterial lipopolysaccharide and tumor necrosis factor alpha synergistically increase expression of human endothelial adhesion molecules through activation of NF-kappaB and p38 mitogen-activated protein kinase signaling pathways. *Infect Immun* 69 (3), 1273-1279 (2001).
[185] Nihei, S., Yamashita, K., Tasaki, H., Ozumi, K., & Nakashima, Y., Oxidized low-density lipoprotein-induced apoptosis is attenuated by insulin-activated phosphatidylinositol 3-kinase/Akt through p38 mitogen-activated protein kinase. *Clin Exp Pharmacol Physiol* 32 (3), 224-229 (2005).
[186] Zhou, Z., Connell, M.C., & MacEwan, D.J., TNFR1-induced NF-kappaB, but not ERK, p38MAPK or JNK activation, mediates TNF-induced ICAM-1 and VCAM-1 expression on endothelial cells. *Cell Signal* 19 (6), 1238-1248 (2007).

187 Cybulsky, M.I. *et al.*, A major role for VCAM-1, but not ICAM-1, in early atherosclerosis. *J Clin Invest* 107 (10), 1255-1262 (2001).
188 Davies, M.J. *et al.*, The expression of the adhesion molecules ICAM-1, VCAM-1, PECAM, and E-selectin in human atherosclerosis. *J Pathol* 171 (3), 223-229 (1993).
189 Mach, F., The role of chemokines in atherosclerosis. *Curr Atheroscler Rep* 3 (3), 243-251 (2001).
190 Heller, E.A. *et al.*, Chemokine CXCL10 promotes atherogenesis by modulating the local balance of effector and regulatory T cells. *Circulation* 113 (19), 2301-2312 (2006).
191 Gu, L. *et al.*, Absence of monocyte chemoattractant protein-1 reduces atherosclerosis in low density lipoprotein receptor-deficient mice. *Mol Cell* 2 (2), 275-281 (1998).
192 Boring, L., Gosling, J., Cleary, M., & Charo, I.F., Decreased lesion formation in CCR2-/- mice reveals a role for chemokines in the initiation of atherosclerosis. *Nature* 394 (6696), 894-897 (1998).
193 Liu, J., Minemoto, Y., & Lin, A., c-Jun N-terminal protein kinase 1 (JNK1), but not JNK2, is essential for tumor necrosis factor alpha-induced c-Jun kinase activation and apoptosis. *Mol Cell Biol* 24 (24), 10844-10856 (2004).
194 Deng, Y., Ren, X., Yang, L., Lin, Y., & Wu, X., A JNK-dependent pathway is required for TNFalpha-induced apoptosis. *Cell* 115 (1), 61-70 (2003).
195 Kamata, H. *et al.*, Reactive oxygen species promote TNFalpha-induced death and sustained JNK activation by inhibiting MAP kinase phosphatases. *Cell* 120 (5), 649-661 (2005).
196 Min, W. & Pober, J.S., TNF initiates E-selectin transcription in human endothelial cells through parallel TRAF-NF-kappa B and TRAF-RAC/CDC42-JNK-c-Jun/ATF2 pathways. *J Immunol* 159 (7), 3508-3518 (1997).
197 Read, M.A. *et al.*, Tumor necrosis factor alpha-induced E-selectin expression is activated by the nuclear factor-kappaB and c-JUN N-terminal kinase/p38 mitogen-activated protein kinase pathways. *J Biol Chem* 272 (5), 2753-2761 (1997).
198 Ahmad, M., Theofanidis, P., & Medford, R.M., Role of activating protein-1 in the regulation of the vascular cell adhesion molecule-1 gene expression by tumor necrosis factor-alpha. *J Biol Chem* 273 (8), 4616-4621 (1998).
199 De Cesaris, P. *et al.*, Activation of Jun N-terminal kinase/stress-activated protein kinase pathway by tumor necrosis factor alpha leads to intercellular adhesion molecule-1 expression. *J Biol Chem* 274 (41), 28978-28982 (1999).
200 Sumara, G., Belwal, M., & Ricci, R., "Jnking" atherosclerosis. *Cell Mol Life Sci* 62 (21), 2487-2494 (2005).
201 Ju, H. *et al.*, p38 MAPK inhibitors ameliorate target organ damage in hypertension: Part 1. p38 MAPK-dependent endothelial dysfunction and hypertension. *J Pharmacol Exp Ther* 307 (3), 932-938 (2003).
202 Seeger, F.H. *et al.*, p38 mitogen-activated protein kinase downregulates endothelial progenitor cells. *Circulation* 111 (9), 1184-1191 (2005).
203 Qamirani, E., Ren, Y., Kuo, L., & Hein, T.W., C-reactive protein inhibits endothelium-dependent NO-mediated dilation in coronary arterioles by activating p38 kinase and NAD(P)H oxidase. *Arterioscler Thromb Vasc Biol* 25 (5), 995-1001 (2005).
204 Takahashi, M. *et al.*, Lysophosphatidylcholine induces apoptosis in human endothelial cells through a p38-mitogen-activated protein kinase-dependent mechanism. *Atherosclerosis* 161 (2), 387-394 (2002).
205 Harrison, D.G., The shear stress of keeping arteries clear. *Nat Med* 11 (4), 375-376 (2005).
206 Feaver, R.E., Hastings, N.E., Pryor, A., & Blackman, B.R., GRP78 upregulation by atheroprone shear stress via p38-, alpha2beta1-dependent mechanism in endothelial cells. *Arterioscler Thromb Vasc Biol* 28 (8), 1534-1541 (2008).
207 Orr, A.W. *et al.*, The subendothelial extracellular matrix modulates NF-kappaB activation by flow: a potential role in atherosclerosis. *J Cell Biol* 169 (1), 191-202 (2005).
208 Anter, E., Chen, K., Shapira, O.M., Karas, R.H., & Keaney, J.F., Jr., p38 mitogen-activated protein kinase activates eNOS in endothelial cells by an estrogen receptor alpha-dependent pathway in response to black tea polyphenols. *Circ Res* 96 (10), 1072-1078 (2005).
209 Thornton, T.M. & Rincon, M., Non-classical p38 map kinase functions: cell cycle checkpoints and survival. *Int J Biol Sci* 5 (1), 44-51 (2009).
210 Fan, L. *et al.*, A novel role of p38 alpha MAPK in mitotic progression independent of its kinase activity. *Cell Cycle* 4 (11), 1616-1624 (2005).

[211] Hanks, S.K., Quinn, A.M., & Hunter, T., The protein kinase family: conserved features and deduced phylogeny of the catalytic domains. *Science* 241 (4861), 42-52 (1988).

[212] Young, P.R. *et al.*, Pyridinyl imidazole inhibitors of p38 mitogen-activated protein kinase bind in the ATP site. *J Biol Chem* 272 (18), 12116-12121 (1997).

[213] Gareus, R. *et al.*, Endothelial cell-specific NF-kappaB inhibition protects mice from atherosclerosis. *Cell metabolism* 8 (5), 372-383 (2008).

[214] Holman, R.L., Mc, G.H., Jr., Strong, J.P., & Geer, J.C., Technics for studying atherosclerotic lesions. *Lab Invest* 7 (1), 42-47 (1958).

[215] Peiser, L., Gough, P.J., Kodama, T., & Gordon, S., Macrophage class A scavenger receptor-mediated phagocytosis of Escherichia coli: role of cell heterogeneity, microbial strain, and culture conditions in vitro. *Infection and immunity* 68 (4), 1953-1963 (2000).

[216] Hendriks, W.L., van der Boom, H., van Vark, L.C., & Havekes, L.M., Lipoprotein lipase stimulates the binding and uptake of moderately oxidized low-density lipoprotein by J774 macrophages. *The Biochemical journal* 314 (Pt 2), 563-568 (1996).

[217] Stephan, Z.F. & Yurachek, E.C., Rapid fluorometric assay of LDL receptor activity by DiI-labeled LDL. *Journal of lipid research* 34 (2), 325-330 (1993).

Appendix I

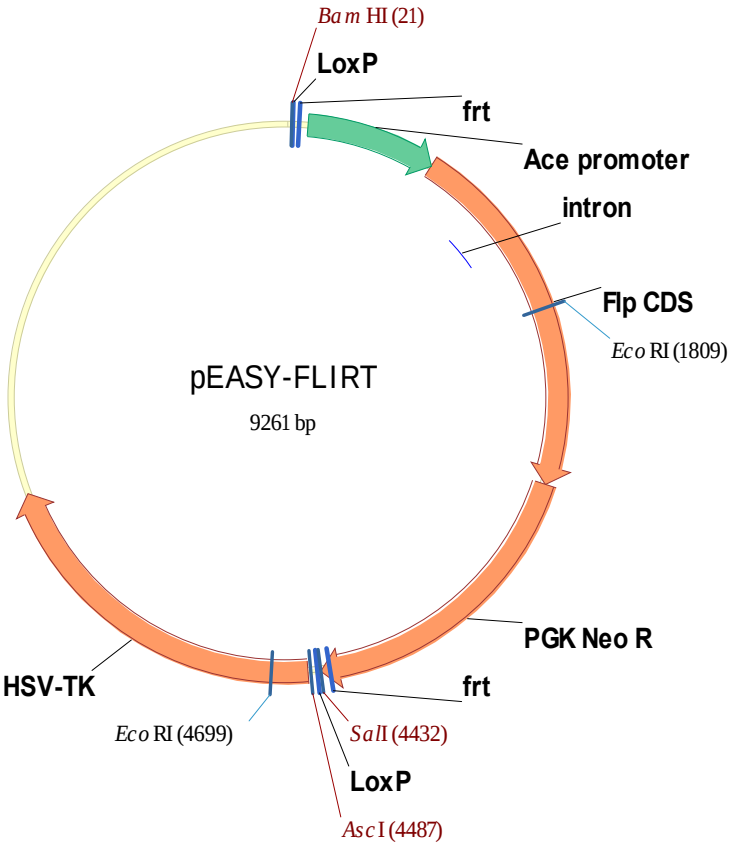
Bam HI (21)
LoxP
frt
Ace promoter
intron
Flp CDS
Eco RI (1809)
pEASY-FLIRT
9261 bp
PGK Neo R
HSV-TK
frt
Eco RI (4699)
SalI (4432)
LoxP
AscI (4487)

Appendix II

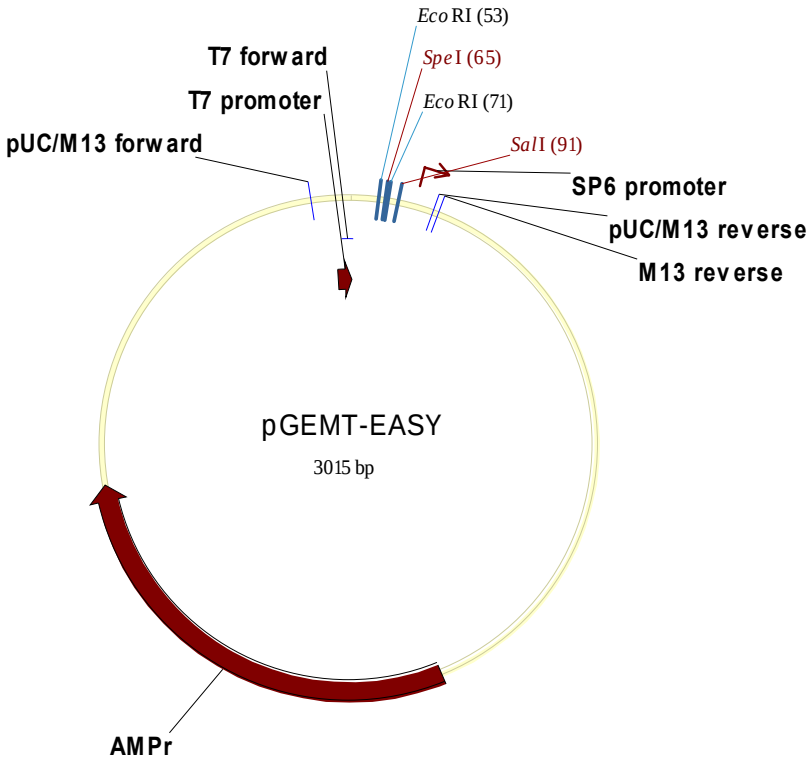
EcoRI (53)
SpeI (65)
EcoRI (71)
SalI (91)
T7 forward
T7 promoter
pUC/M13 forward
SP6 promoter
pUC/M13 reverse
M13 reverse
pGEMT-EASY
3015 bp
AMPr

Appendix III

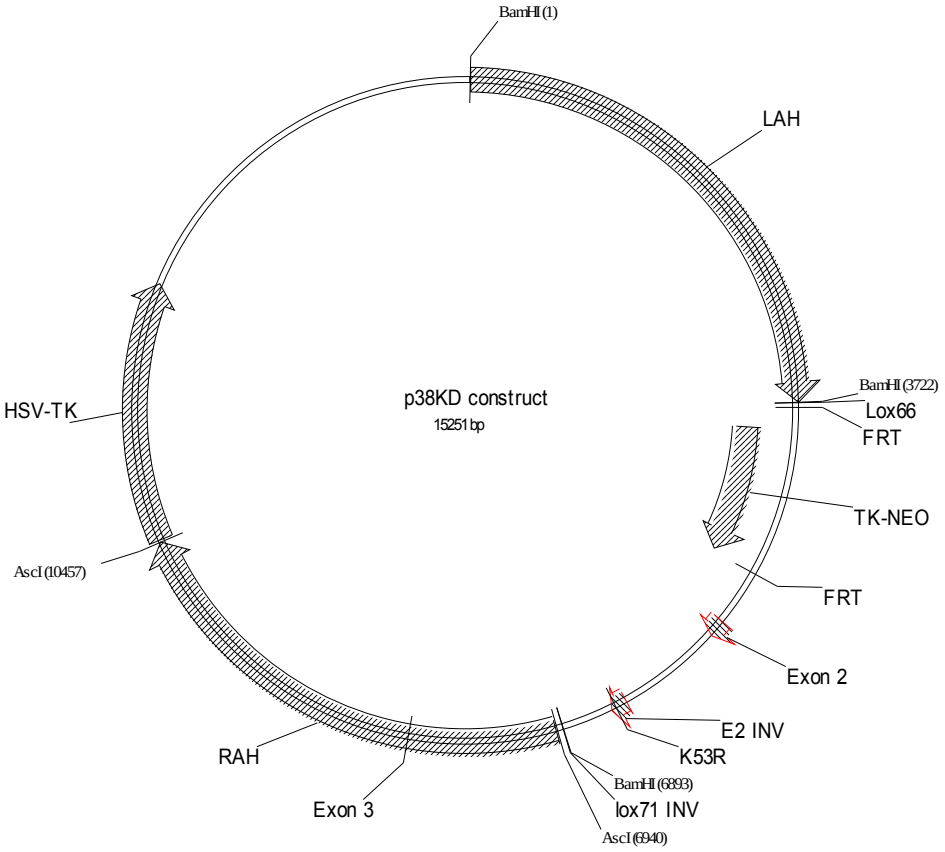

Appendix IV

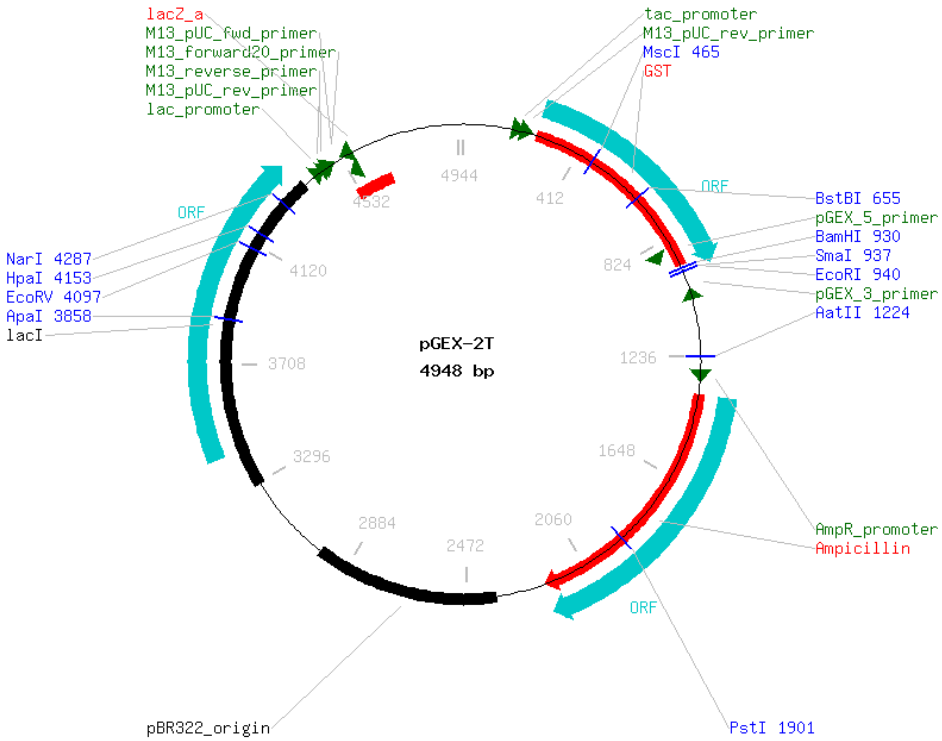
lacZ_a
M13_pUC_fwd_primer
M13_forward20_primer
M13_reverse_primer
M13_pUC_rev_primer
lac_promoter
tac_promoter
M13_pUC_rev_primer
MscI 465
GST
ORF
BstBI 655
pGEX_5_primer
BamHI 930
SmaI 937
EcoRI 940
pGEX_3_primer
AatII 1224
AmpR_promoter
Ampicillin
ORF
PstI 1901
pBR322_origin
ORF
NarI 4287
HpaI 4153
EcoRV 4097
ApaI 3858
lacI
4944
412
824
1236
1648
2060
2472
2884
3296
3708
4120
4532
pGEX-2T
4948 bp

Appendix V

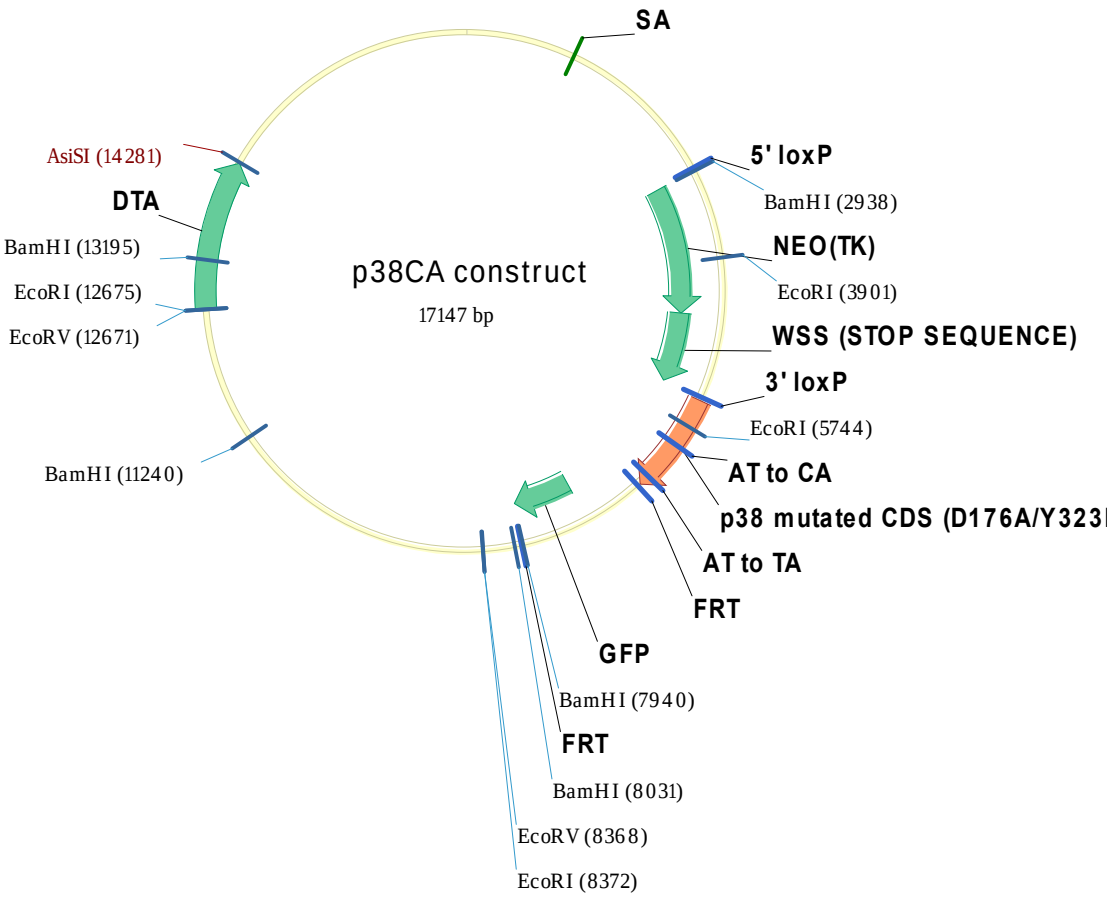
SA
5' loxP
BamHI (2938)
NEO(TK)
EcoRI (3901)
WSS (STOP SEQUENCE)
3' loxP
EcoRI (5744)
AT to CA
p38 mutated CDS (D176A/Y323
AT to TA
FRT
GFP
BamHI (7940)
FRT
BamHI (8031)
EcoRV (8368)
EcoRI (8372)
AsiSI (14281)
DTA
BamHI (13195)
EcoRI (12675)
EcoRV (12671)
BamHI (11240)
p38CA construct
17147 bp

Appendix VI

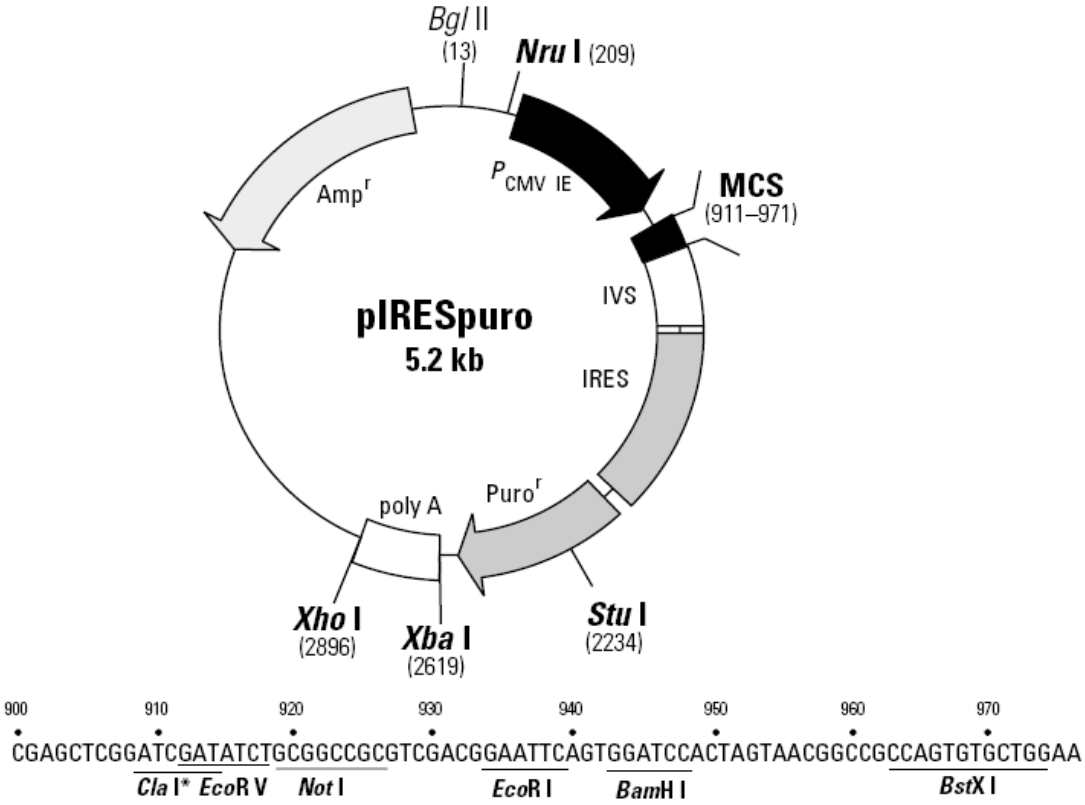

Restriction Map and Multiple Cloning Site (MCS) of pIRESpuro Vector. Unique restriction sites are in bold. The *Cla* I site in the MCS is methylated in the DNA provided by CLONTECH. If you wish to digest the vector with this enzyme, you will need to transform the vector into a *dam*⁻ host and make fresh DNA.